UNIVERSIDADE D
COIMBRA

Maria João Dias da Rocha Pereira

Exploring astrocyte-neuron mitochondrial transfer in Alzheimer's disease

VOLUME 1

Dissertação no âmbito do Mestrado em Investigação Biomédica, ramo de neurobiologia, orientada pelas Professoras Doutoras Ana Cristina Rego e Maria Ankarcrona e apresentada à Faculdade de Medicina da Universidade de Coimbra

Julho de 2021

ACKNOWLEDGEMENTS

This past year has been one of the most challenging, but rewarding, years I have had to date. The work here presented is the product of a long year of hard work that would not have been possible without the joint effort of so many people. Therefore, I would like to take the opportunity to thank everyone who accompanied me throughout this journey and contributed somehow to bring this thesis to life.

Firstly, I would like to thank my supervisors Professor Maria Ankarcrona, for the opportunity to integrate your research group, creating an amazing work environment and all the valuable insights given throughout the course of the project, and Professor Ana Cristina Rego for all the availability, support, and the help in reviewing this thesis.

To Luana, my non-official supervisor, I would not have made it without you. Thank you for being an amazing supervisor, for your unwavering support, all the trust, for everything that you have taught me, and for being such a joy to work with. Thank you for sharing your project with me and always including me in every decision. This is as much your work as it is mine.

To the remaining members of our group – thank you to Shubin for all the laughs, chats, and the valuable help in collecting the mitophagy data; to Laura and Giacomo, thank you for the relaxing moments, your advice and guidance. Thank you also to everyone working at BioClinicum for nice conversations and for providing help whenever I needed it.

To my friends at Jägargatan 20, many thanks for the movie/sitcom nights, Sunday brunches and dinners, all the amazing trips, and becoming family when I was so far away from home. Also thank you to my friends in Portugal, and France, for always being there for me, even from a distance.

Thank you to my amazing family, especially my mom, dad, and brother for your unconditional love and support, advice and all the sacrifices you have made over the years to get me here and shape me into who I am today. I love you very much and am forever grateful for everything.

Finally, I would like to thank the Erasmus+ Programme, for the opportunity to go abroad to develop my thesis and the Swedish Alzheimer Foundation (*Alzheimerfonden*, grant ref. no. AF-940103), The Swedish Research Council (*Vetenskapsrådet*, grant ref. no 2018–03102), the Loo and Hans Osterman Foundation (grant ref. no. 2020-01226) and the Foundation for Geriatric Diseases at Karolinska Institutet (grant ref. no. 2020-02310) for selecting and funding the project enclosed in this thesis.

ABSTRACT

Mitochondria play crucial roles in neuronal activity by providing adenosine triphosphate (ATP) and buffering calcium to power and regulate synaptic activity. Mitochondrial dysfunction contributes to synaptic deficits and has been shown to be an early event in neurodegenerative diseases, like Alzheimer's disease (AD). Recent evidence suggests astrocytes contribute to maintaining a healthy neuronal mitochondrial network by either degrading dysfunctional mitochondrial shed by neurons, and by donating healthy mitochondria. However, the relevance of these processes in AD is yet to be determined. Hence, using neuronal and astrocytic primary cultures isolated from the *App*$^{NL-G-F}$ AD mouse model, we investigated the mechanisms involved in astrocyte-neuron mitochondrial transfer. We found that *App*$^{NL-G-F}$ neurons have substantial deficits in mitochondrial anterograde transport, together with a reduced number of pre-synaptic mitochondria at the early stages of the disease, which likely reflects metabolic alterations at the synapse. On the other hand, astrocytes showed no bioenergetic nor movement impairments. However, we observed that WT, but not *App*$^{NL-G-F}$ astrocytes, increase the expression of mitochondria-associated genes when in co-culture with *App*$^{NL-G-F}$ neurons, suggesting *App*$^{NL-G-F}$ astrocytes might not be as efficient in providing support to affected neurons. To further assess this, we collected extracellular vesicles containing mitochondria (mito-EVs) from the conditioned media and observed that astrocytes engulf mitochondria released by neurons through actin-dependent mechanisms. Interestingly, the uptake of *App*$^{NL-G-F}$-derived mito-EVs by astrocytes was impaired, in comparison to WT-derived mito-EVs, leading to a higher accumulation of extracellular ATP. We also observed that, following engulfment, only a fraction of mitochondria integrated the astrocytic mitochondrial network, while another population appeared to undergo transmitophagy. However, this process might be impaired in *App*$^{NL-G-F}$ astrocytes, as shown by a decreased number of mitophagy events and downregulation of mitophagy-related genes. Altogether, these data indicate neuronal mitochondria are captured and directed to mitophagy in astrocytes and that this might be affected in the *App*$^{NL-G-F}$ model. Future experiments are still required to understand the dynamics between each neuronal and astrocytic phenotype and the possible implications of these outcomes for AD pathology.

KEY WORDS: Alzheimer's disease; mitochondrial transport and transfer; mito-EVs; mitophagy

RESUMO

As mitocôndrias desempenham um papel crucial para a atividade neuronal, através do fornecimento de adenosina trifosfato (ATP) e regulação da concentração de cálcio, potenciando e regulando a atividade sináptica. A disfunção mitocondrial resulta em défices sinápticos e é considerada um evento inicial em doenças neurodegenerativas, como a doença de Alzheimer (DA). Evidências recentes sugerem que os astrócitos ajudam a manter uma rede mitocondrial neuronal saudável, não só através da degradação de mitocôndria disfuncionais libertadas pelos neurónios, mas também pela doação de mitocôndrias saudáveis. No entanto, a relevância destes processos na DA ainda não foi determinada. Assim, usando culturas primárias de astrócitos e neurónios isolados de murganhos *App*$^{NL\text{-}G\text{-}F}$, um modelo da DA, investigámos os mecanismos envolvidos na transferência mitocondrial entre astrócitos e neurónios. Observou-se que os neurónios *App*$^{NL\text{-}G\text{-}F}$ apresentam défices substanciais no transporte mitocondrial anterógrado, juntamente com um número reduzido de mitocôndrias pré-sinápticas nos estadios iniciais da doença, o que provavelmente se reflete em alterações metabólicas na sinapse. Por outro lado, os astrócitos não apresentaram alterações bioenergéticas nem de movimento. No entanto, os astrócitos WT, ao contrário dos *App*$^{NL\text{-}G\text{-}F}$, aumentam a expressão de genes associados à mitocôndria quando em co-cultura com neurónios *App*$^{NL\text{-}G\text{-}F}$, sugerindo que os astrócitos *App*$^{NL\text{-}G\text{-}F}$ poderão não ser tão eficientes a ajudar neurónios disfuncionais. Para validar estas observações, recolhemos vesículas extracelulares contendo mitocôndrias (mito-EVs) do meio condicionado e observamos que os astrócitos internalizam mitocôndrias libertadas pelos neurónios através de mecanismos dependentes de actina. Curiosamente, a captação de mito-EVs derivadas das culturas *App*$^{NL\text{-}G\text{-}F}$ pelos astrócitos parece estar comprometida, em comparação com a captação de mito-EVs WT. Também verificamos que, após a internalização, apenas uma fração das mitocôndrias acabou por integrar a rede mitocondrial do astrócito, enquanto que a restante população parece ser direcionada para transmitofagia. Este processo parece estar comprometido em astrócitos *App*$^{NL\text{-}G\text{-}F}$, como evidenciado pela diminuição do número de eventos de mitofagia e da expressão de genes relacionados com mitofagia. Coletivamente, estes dados indicam que as mitocôndria neuronais são captadas e direcionadas para mitofagia e que isto poderá estar afetado no modelo *App*$^{NL\text{-}G\text{-}F}$. Experiências futuras são necessárias para entender como é que o fenótipo de cada tipo celular influência os resultados obtidos e as possíveis implicações para a patologia da DA.

PALAVRAS-CHAVE: Doença de Alzheimer; transferência e transporte mitocondrial; mito-EVs; mitofagia

TABLE OF CONTENTS

LIST OF ABBREVIATIONS

Aβ	Amyloid β-peptide
Acetyl-CoA	Acetyl coenzyme A
AD	Alzheimer's disease
AICD	APP intracellular cytoplasmic domain
AMBRA1	Autophagy and beclin 1 regulator 1
APOE	Apolipoprotein E
APP	Amyloid precursor protein
ATP	Adenosine triphosphate
BACE1	β-APP cleaving enzyme 1
Bnip3	BCL2/adenovirus E1B 19 kDa interacting protein 3
Ca^{2+}	Calcium
CM	Conditioned media
CNS	Central nervous system
CytoD	Cytochalasin D
Drp1	Dynamin-related protein 1
ECAR	Extracellular acidification rate
ER	Endoplasmic reticulum
ETC	Electron transport chain
EV	Extracellular vesicle
FAD	Familial AD
FUNDC1	FUN14 domain-containing protein 1
GABA	Gamma-Aminobutyric acid
GRP75	Glucose-regulated protein 75
IMM	Inner mitochondrial membrane
IMS	Intermembrane space
IP_3R	Inositol 1,4,5-triphosphate receptor
KIF5	Kinesin family member 5
LC3	Microtubule-associated protein light chain 3
LIR	LC3-interaction region
MAMs	Mitochondria-associated ER membranes
MAPT	Microtubule-associated protein tau
MCI	Mild cognitive impairment
MCU	Mitochondrial Ca^{2+} uniporter
MERCS	Mitochondria-ER contact sites
Mfn1 and Mfn2	Mitofusin 1 and 2

Miro1 and Miro2	Mitochondrial Rho GTPases 1 and 2
Mito-EVs	EVs-containing mitochondria
mPTP	Mitochondrial permeability transition pore
MSC	Mesenchymal stem cell
mtDNA	Mitochondrial DNA
NFTs	Neurofibrillary tangles
OCR	Oxygen consumption rate
OMM	Outer mitochondrial membrane
OPA1	Optic atrophy 1
OPTN	Optineurin
OXPHOS	Oxidative phosphorylation
PCN	Primary cortical neurons
PD	Parkinson's disease
PDH	Pyruvate dehydrogenase
PGC-1α	Peroxisome proliferator-activated receptor gamma coactivator 1-alpha
PINK1	PTEN-induced putative kinase 1
PMCA	Plasma membrane Ca^{2+}-ATPases
PS1 and PS2	Presenilin 1 and 2
PTP	Post-tetanic potentiation
p-ULK	Phosphorylated ULK1
ROS	Reactive oxygen species
SAD	Sporadic AD
SV	Synaptic vesicle
TCA	Tricarboxylic acid cycle
TFAM	Mitochondrial transcription factor A
TIM	Translocase of the inner membrane
TMRM	Tetramethylrhodamine, methyl ester
TNT	Tunnelling nanotube
TOM	Translocase of the outer membrane
Trak1 and Trak 2	Trafficking kinesin-binding proteins 1 and 2
ULK1	Unc-51-like autophagy activating kinase 1
VDAC1	Voltage-dependent anion-selective channel protein 1
VGCC	Voltage-gated Ca^{2+} channels
WT	Wild-type
$\Delta\psi_m$	Mitochondrial membrane potential

LIST OF FIGURES

LIST OF TABLES

1. INTRODUCTION

1.1. ALZHEIMER'S DISEASE

Alzheimer's disease (AD) is a multifactorial neurodegenerative disease mostly affecting the cerebral cortex and hippocampus, leading to progressive memory and cognitive decline (Kumar et al., 2015; Masters et al., 2015). With an overall mean incidence of 1-3% and a total prevalence of 10-30% in the elderly population, AD is one of the most common forms of dementia worldwide, accounting for 60-80% of all cases (Alzheimer's Association, 2020; Masters et al., 2015). AD was firstly reported by Alois Alzheimer, back in 1907, after he described the presence of extracellular neurotic plaques and intracellular fibrils in the brain of a 55-year-old woman (Stelzmann et al., 1995). Despite the advances made since then, leading to a deeper understanding of the mechanisms involved in the pathophysiology of the disease, development of better diagnostic techniques, and thousands of clinical trials conducted in the search for effective treatments, there is still a need for drugs that can prevent the progressive neurodegeneration observed in AD. Therefore, it is urgent to provide novel insights into the molecular mechanisms driving this disease and, with that, develop new diagnostic techniques and treatments that may have a positive impact on the lives of millions of people.

1.1.1. Pathophysiological hallmarks and aetiology

The efforts made throughout the years to unravel the mechanisms driving AD have provided valuable understanding about the pathophysiology of the disease. Pathophysiological hallmarks of AD include the accumulation of extracellular plaques and neurofibrillary tangles (NFTs) throughout the cortex and hippocampus, which are now known to be made up of amyloid β-peptide (Aβ) and tau protein, respectively (Glenner & Wong, 1984; Grundke-Iqbal et al., 1986; Masters et al., 1985). The disease is also characterized by neuronal death, particularly of cholinergic neurons of the forebrain and glutamatergic neurons in the cortex and hippocampus (Francis, 2005; Wenk, 2003). Cerebrovascular damage, synapse loss, activation of microglia and astrocytes, and mitochondrial dysfunction have also been more recently implicated in AD's pathophysiology (Querfurth & Laferla, 2010). However, and despite all the hypotheses proposed over the years, there is still some controversy regarding what is the initial event that triggers the disease. Currently, there are two main hypotheses accepted by the scientific community to explain AD's aetiology – the amyloid cascade hypothesis and the tau hypothesis.

1.1.1.1. The amyloid cascade hypothesis

Amyloid precursor protein (APP) is a transmembrane protein found at high levels in neuronal cells and thought to be involved in synaptic plasticity (Masters et al., 2015). APP can be metabolized through one of two different pathways – the amyloidogenic or the non-amyloidogenic pathway, as represented in Figure 1. In the non-amyloidogenic pathway, APP is first cleaved by α-secretase, yielding the sAPPα and C83/α-CTF peptides. α-CTF is subsequently cleaved by γ-secretase, which results in the production of other two peptides, APP intracellular cytoplasmic domain (AICD) and p3. On the other hand, in the amyloidogenic pathway, the first step is carried out by β-APP cleaving enzyme 1 (BACE1), also known as β-secretase, instead of α-secretase. This results in the production of the sAPPβ and C99/β-CTF peptides. Then, similarly to the non-amyloidogenic pathway, β-CTF is cleaved by γ-secretase, producing AICD and Aβ (Kumar et al., 2015; O'brien & Wong, 2011).

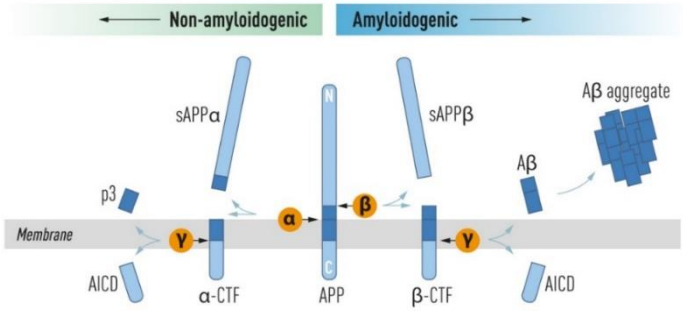

Figure 1 – APP processing pathways. In the non-amyloidogenic pathway, cleavage of APP within the Aβ sequence, shown in dark blue, by α-secretase yields sAPPα and α-CTF. The latter is further cleaved into p3 and AICD by γ-secretase. However, in the amyloidogenic pathway, β-secretase cleaves APP at the bond between Met671 and Asp672 (β-site), originating sAPPβ and β-CTF. Subsequent cleavage of β-CTF by γ-secretase forms Aβ and AICD. Aβ is a small peptide with propensity to aggregate and deposit, forming extracellular amyloid plaques. Adapted from Dentoni, 2021.

Aβ is a 38-43 amino acid peptide and, as a product of the normal metabolism of APP, it has physiological functions in the cell. Although not fully understood, it has been suggested that Aβ contributes to negatively control synaptic activity, as its absence can lead to excessive synaptic activity and, ultimately, excitotoxicity (Kamenetz et al., 2003; Pearson & Peers, 2006). However, at high concentrations, this peptide can become toxic since it can self-aggregate and deposit in the brain. So, it is crucial that a good balance between Aβ production and clearance exists to secure homeostasis. Accordingly, the amyloid cascade hypothesis postulates that AD results from an imbalance between Aβ production and clearance (Selkoe & Hardy, 2016). Polymorphisms in the apolipoprotein E (APOE) gene, particularly the APOE4 isoform, are considered major risk factors for AD, as it leads to an earlier age of onset (Corder et al., 1993; M. X. Tang et al., 1996). Studies indicate APOE4 promotes AD in a wide variety of ways. This protein appears to

not only enhance Aβ production by modulating the activity of γ-secretase but also impairs Aβ lysosomal degradation and proteolytic cleavage by neprilysin and the insulin-degrading enzyme, thus affecting Aβ clearance. Furthermore, APOE4 has been shown to promote Aβ aggregation and Aβ oligomers stabilization (Safieh et al., 2019).

Aβ exists in many different isoforms of which the most abundant ones are $A\beta_{40}$ and $A\beta_{42}$. Of the two, $A\beta_{42}$ has been shown to be more toxic and prone to aggregation than other isoforms. Unsurprisingly, the ratio $A\beta_{42}/A\beta_{40}$ is increased in AD (Hecimovic et al., 2004; Kumar-Singh et al., 2006). Toxic effects of $A\beta_{42}$ include induction of oxidative damage, and synaptic and mitochondrial dysfunction (Kumar et al., 2015). Also, the observation that Aβ seems to promote tau protein phosphorylation provides strong evidence to support the amyloid cascade hypothesis (De Felice et al., 2008).

While sporadic AD (SAD) may be the most common type of AD among patients, it has been the study of familial cases of AD (FAD) that have brought some of the strongest lines of evidence supporting the idea that Aβ is the causative effect of this disease. In this small subgroup of patients, which represents <1% of all cases, the various mutations detected so far affect genes coding for APP, presenilin 1 and 2 (PS1 and PS2, respectively) (Bekris et al., 2011).

As of today, about 32 APP mutations have been reported (Bekris et al., 2011). Some of the most relevant ones for this thesis include the Swedish double mutation (KM670/671NL), near BACE1's cleavage site, the Iberian mutation (I716F), close to the γ-secretase's cleavage site, and the Arctic mutation (E693G), found within the protein sequence. The Swedish and Iberian mutations modify APP processing. This favours the production of Aβ, especially the more toxic and less soluble $A\beta_{42}$ isoform, increasing the ratio of $A\beta_{42}/A\beta_{40}$. In its turn, the Arctic mutation promotes Aβ aggregation and deposition (Saito et al., 2014). Another important mutation found in the *App* gene is the A673T mutation located close to the β-secretase cleavage site. This variant was shown to be protective, and carriers do not develop the disease. This was linked to the decrease in APP cleavage by BACE of approximately 40%, reducing the production of Aβ *in vitro*. This suggests that reducing the frequency of APP processing through the amyloidogenic pathway would probably have protective effects (Jonsson et al., 2012).

PS1 or PS2 are components of the γ-secretase complex and, just like most mutations known for APP, mutations in these proteins predominantly lead to a rise in the $A\beta_{42}/A\beta_{40}$ ratio (Bekris et al., 2011). Also, the discovery that people with Down's syndrome, who possess a third copy of the chromosome 21 where the *APP* gene is located, have a high increase in the production of Aβ and develop AD-like symptoms, including dementia and cognitive deterioration, and pathological hallmarks such as the

presence of amyloid plaques, NFTs, and mitochondrial dysfunction, early in life further supports this hypothesis (Head et al., 2012; Wisniewski et al., 1985).

Nonetheless, this hypothesis fails to explain relevant aspects such as why are amyloid plaques also found in healthy non-demented patients or why do some AD patients present only very few plaques (Edison et al., 2007; Fagan et al., 2009; Li et al., 2008; Price et al., 2009)? Importantly, the distribution of Aβ plaques in the brain of AD patients does not seem to correlate with their degree of cognitive impairment, further questioning the validity of this hypothesis (Terry et al., 1991).

1.1.1.2. The tau hypothesis

Tau protein is a microtubule-associated protein (MAPT) involved in the assembly and stabilization of microtubules (Drubin & Kirschner, 1986). The function of this protein is dependent on its phosphorylation state. When phosphorylated, tau loses its ability to bind to microtubules, which leads to their disorganization and disintegration (Mandelkow et al., 1995; Rodríguez-Martín et al., 2013). As one of the main components of the cytoskeleton and due to its involvement in axonal transport, the collapse of the microtubule network affects both cellular structure and axonal transport of various cellular organelles. Consequently, this compromises cellular function and may lead to cell death (Kolarova et al., 2012). This, together with the discovery that the main component of NFTs is hyperphosphorylated tau protein, led to the establishment of the tau hypothesis for AD postulating that the cause of the disease is the accumulation of hyperphosphorylated forms of tau (Kosik et al., 1986).

Over the last years, this hypothesis has gained momentum after the observation that, unlike what happens with Aβ pathology, the distribution and the increasing accumulation of NFTs highly correlates with the severity and progression of cognitive impairment and clinical symptoms in AD patients (Bejanin et al., 2017; Ghoshal et al., 2002; Okamura & Yanai, 2017). However, the fact that Aβ has been shown to induce tau hyperphosphorylation has challenged this hypothesis, as it suggests that Aβ rather than tau could be the trigger for AD (M. Jin et al., 2011; Kametani & Hasegawa, 2018).

1.1.2. Mouse models in AD

Over the years, many experimental models have been developed in order to study AD. Most of what is known today about AD's pathophysiology comes from studies carried out using these models, which are also extremely relevant to the initial testing of novel therapeutical strategies for this disease.

To date, transgenic mice remain the most widely used animal models in AD research. These include models based on Aβ pathology, such as the PDAPP, which

carries the APP Indiana mutation (V717F) (Games et al., 1995), the Tg2576, expressing the Swedish double mutation (K670N/M671L) (Hsiao et al., 1996), and various APP/PS1 mouse models containing different sets of mutations in *App* and *Psen1*, detailed in Table 1. Overall, these models present amyloid plaque formation in the cortex and hippocampus, gliosis, synaptic dysfunction, and cognitive impairment, but they lack other AD hallmarks, namely the presence of NFTs, general neurodegeneration, and brain atrophy (Drummond & Wisniewski, 2017). Accordingly, tau pathology-based transgenic mouse models, with or without Aβ pathology, were developed in an attempt to create more representative models of AD pathophysiology. Among these, the 3xTg mouse model (Table 1), carrying mutations in the genes coding for APP, PS1 and MAPT, is considered to be the most complete model of AD. This model presents Aβ accumulation in neurons and plaque formation in the cortex and hippocampus, followed by NFTs formation. Cognitive and synaptic impairments are also evident, together with astrogliosis and localized neurodegeneration (Drummond & Wisniewski, 2017; Oddo, Caccamo, Kitazawa, et al., 2003; Oddo, Caccamo, Shepherd, et al., 2003).

Table 1 – Mouse models commonly used in AD research.

Model	Mutation	AD pathology	Reference
PDAPP	Indiana (App^{V717F})	Extracellular Aβ plaques in cortex and hippocampus, gliosis, and cognitive and synaptic impairment	(Games et al., 1995)
Tg2576	Swedish ($App^{K670N/M671L}$)	Aβ plaques in the cortex, hippocampus and cerebellum, gliosis, synaptic loss, and memory and learning impairment	(Hsiao et al., 1996)
3xTg	Swedish ($App^{K670N/M671L}$), $PS1^{M146V}$, Tau^{P301L}	Intraneuronal Aβ, plaques in cortex and hippocampus, NFTs, synaptic dysfunction	(Oddo et al., 2003)
***App*$^{NL-F}$**	Swedish ($App^{K670N/M671L}$), Iberian (App^{I716F})	Aβ plaque formation, gliosis, synaptic dysfunction, and memory impairment	(Saito et al., 2014)
***App*$^{NL-G-F}$**	Swedish ($App^{K670N/M671L}$), Iberian (App^{I716F}), Arctic (App^{E693G})	Aβ plaques, neuroinflammation, synaptic loss, and memory impairment	(Saito et al., 2014)

Despite all the valuable insights these models have provided so far, they present two major challenges. Transgenic mouse models are based on mutations found in FAD patients, which reflect only a very small percentage of total AD cases and present quite a different pathology from SAD (Drummond & Wisniewski, 2017; Colin L. Masters et al., 2015). This may compromise the translatability of results to humans and may account for the high number of failed clinical trials in AD. Moreover, overexpression of APP and

tau at non-physiological levels may account for some of the pathologic changes seen in these mice, resulting in confounding effects regarding AD's pathophysiology and associated cellular and molecular mechanisms (Drummond & Wisniewski, 2017; Hall & Roberson, 2012).

The most recently developed knock-in (KI) mouse models (Table 1) aim at preventing the non-physiological expression of APP. In these models, APP FAD mutations are inserted in the humanized mouse Aβ sequence (Saito et al., 2014). Since the protein is not being overexpressed, APP and Aβ are expressed at normal levels in the correct cell types and brain regions, which avoids possible confounding effects due to protein overexpression. However, the problem regarding the translatability of findings to SAD patients persists in these models (Drummond & Wisniewski, 2017). Also, these models are only representative of amyloid pathology, as they do not present increase tau phosphorylation nor brain atrophy (Saito et al., 2014). Two of the most relevant APP KI mouse models include the App^{NL-F} and App^{NL-G-F} mice. The App^{NL-F} mouse model has the Swedish double mutation and the Iberian mutation. Amyloid plaque formation and gliosis start around 6 months, followed by synaptic dysfunction at 9 months and memory impairment at 18 months. The App^{NL-G-F} mouse model has an additional mutation – the Arctic mutation. This results in a much more aggressive phenotype with Aβ plaques first appearing at 2 months, followed by neuroinflammation at 3 months, synaptic loss at 4-5 months and, finally, memory impairment at around 6 months old (Saito et al., 2014).

1.2. MITOCHONDRIA

Over the years, several organelles have been shown to be highly affected in AD, leading to dysfunction of many cellular functions. Among these, mitochondria have increasingly been implicated in AD pathology, as accumulating studies show pronounced mitochondrial dysfunction in this disease. Mitochondria are cellular organelles believed to have been originated circa 2 billion years ago when an α-proteobacterium was engulfed and incorporated into a pre-eukaryotic cell in a process known as endosymbiosis (Dyall et al., 2004). Mitochondria are very curious organelles in the sense that, unlike the remaining cellular compartments found in animal cells, they possess their own genomic material. In fact, some of the most robust lines of evidence supporting the endosymbiotic theory derive from phylogenetic studies tracking the origin of mitochondrial-encoded genes to α-proteobacteria (Andersson et al., 2003). However, mitochondrial DNA (mtDNA) underwent many mutations throughout the ages, and several of its genes were even transferred to the nuclear genome. Currently, the human mitochondrial genome consists of a small, circular DNA molecule coding for 13 proteins. Mitochondria are now recognized as crucial cellular organelles that evolved, adapted

and gained a myriad of new functions besides their original role as adenosine triphosphate (ATP) producers (Friedman & Nunnari, 2014; Gabaldón & Huynen, 2004).

1.2.1. Mitochondrial structure

Structurally, mitochondria pose as unusual organelles since they are comprised of two different membranes – the outer mitochondrial membrane (OMM) and inner mitochondrial membrane (IMM) – separated by the intermembrane space (IMS), as illustrated in Figure 2 (Alberts et al., 2017; Freya & Mannellab, 2000). The OMM is permeable to several metabolites and ions, like calcium (Ca^{2+}), that can passively diffuse through porin molecules. On the other hand, the IMM is impermeable to most molecules and possesses transporters through which only very specific molecules can be exchanged (Alberts et al., 2017). Additionally, protein transport complexes, such as the translocase of the outer membrane (TOM) and the translocase of the inner membrane (TIM), are present at the OMM and IMM, respectively. As most mitochondrial proteins are nucleus-encoded, these complexes are crucial to ensure mitochondrial proteins are imported into the organelle (Newmeyer & Ferguson-Miller, 2003). The IMM has yet another particular characteristic. This membrane is folded into cristae that protrude into the mitochondrial matrix and highly increase the IMM's surface area, contributing to a more efficient rate of respiration and redox reactions. The mitochondrial matrix is enclosed within the IMM and contains several copies of mtDNA as well as enzymes and constituents of the tricarboxylic acid (TCA) cycle (Alberts et al., 2017; Freya & Mannellab, 2000).

1.2.2. Mitochondria, bioenergetic hubs and beyond

Mitochondria are indispensable for eukaryotic cells. These organelles are mainly acknowledged by their involvement in ATP production, which fuels virtually all cellular functions. Nonetheless, mitochondria are much more than simple energy suppliers and participate in a wide variety of cellular mechanisms controlling cell survival and death, as described ahead.

Bioenergetics – mitochondria are the major source of energy in the cell. It is at its heart that the final steps of amino acids, fatty acids, and sugars' metabolism takes place. In most cells, glucose firstly undergoes glycolysis, a process through which it is broken down into pyruvate. Pyruvate is then transported into the mitochondrial matrix where it is converted into acetyl coenzyme A (acetyl-CoA) by the action of the enzyme pyruvate dehydrogenase (PDH). Similarly, fatty acids and amino acids can also be converted into acetyl-CoA. As shown in Figure 2, this molecule then enters the TCA cycle being further metabolized, while electron donors – NADH and $FADH_2$ – are generated. NADH and

$FADH_2$ donate their electrons to the complexes I-IV of the electron transport chain (ETC) embedded in the mitochondrial cristae. The electrons travel along the chain until they are finally accepted by O_2, at complex IV, producing H_2O. During this process, known as oxidative phosphorylation (OXPHOS), protons are also pumped into the IMS, which generates a proton gradient across the IMM and helps to establish a negative mitochondrial membrane potential ($\Delta\psi_m$). This potential gradient is ultimately used to power complex V, also known as ATP synthase, to produce ATP. Furthermore, $\Delta\psi_m$ is also involved in promoting ion and metabolite exchange and protein import (Osellame et al., 2012).

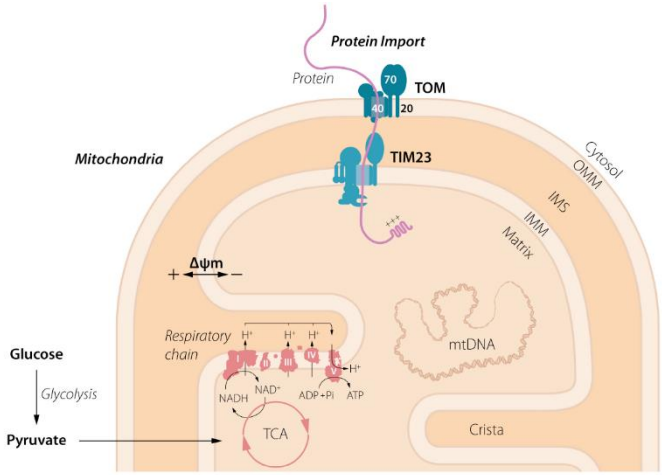

Figure 2 – Mitochondrial structure and function. Mitochondria are comprised of an OMM and an IMM, separated by the IMS. In the innermost mitochondrial compartment – the matrix – several copies of mtDNA can be found. Even so, most mitochondrial genes are nucleus-encoded, which implicates these proteins must be imported into the organelle through the TOM and TIM complexes. Some of these proteins integrate the complexes of the ETC, also known as the respiratory chain. The ETC uses the energy provided by the flux of electrons donated by NADH and $FADH_2$, electron donors formed during the TCA cycle, to generate mitochondrial membrane potential ($\Delta\psi_m$) and drive ATP synthesis. Adapted from Dentoni, 2021.

Reactive oxygen species (ROS) production – as previously mentioned, the final acceptor of the electrons transferred along the ETC is O_2, at complex IV. However, in some cases, electrons leak from the complexes prematurely. These unpaired electrons are thereby directly taken up by O_2, forming superoxide and other ROS (Osellame et al., 2012). At physiological levels, ROS are fundamental for many cellular functions since they act as signalling molecules. On the contrary, if present at high concentrations, ROS become highly toxic. Thus, a fine balance between ROS production and clearance must be achieved to prevent ROS negative effects, which might include DNA damage, protein oxidation, and lipid peroxidation, a process collectively known as oxidative stress (Mittler, 2017).

Ca^{2+} signalling – Ca^{2+} plays important roles in mitochondria, as it helps maintain $\Delta\psi_m$ and is involved in mitochondrial metabolism and apoptosis (Duchen, 2000). Hence, mitochondria also contribute to Ca^{2+} signalling by storing and exchanging Ca^{2+} with the

cytosol and the endoplasmic reticulum (ER) to meet their own requirements. Part of the Ca^{2+} transferred from ER to mitochondria occurs at mitochondria-ER contact sites (MERCS) through a complex constituted by the inositol 1,4,5-triphosphate receptor (IP_3R) at the ER, and the voltage-dependent anion-selective channel protein 1 (VDAC1) at the OMM, both chaperoned by the glucose-regulated protein 75 (GRP75). Ca^{2+} is then imported into the matrix through the mitochondrial Ca^{2+} uniporter (MCU) complex (Rowland & Voeltz, 2012). The crucial role MERCS play in Ca^{2+} signalling is related to the fact that the MCU is a low-affinity transporter. The release of high amounts of Ca^{2+} at the contact sites creates local regions of extremely high Ca^{2+} concentrations, thus enabling efficient transfer of this ion into mitochondria (Rizzuto et al., 1998). However, it is important to tightly control Ca^{2+} uptake by mitochondria as high concentrations may result in mitochondrial permeability transitional pore (mPTP) opening and, consequently, apoptosis (Hajnóczky et al., 2006).

Cell death – another crucial role mitochondria play in cells is promoting cell death through apoptosis. Upon certain stimuli, the mPTP opens, increasing the permeability of the OMM. As a consequence, $\Delta\psi_m$ is lost, production of ATP ceases and many proteins normally located in the IMS are suddenly released to the cytosol. Among these, cytochrome *c* is of most importance as, once in the cytosol, it activates the caspase cascade, leading to apoptosis (Newmeyer & Ferguson-Miller, 2003; Zamzami & Kroemer, 2001).

1.2.3. Neuronal mitochondria

Neurons have extremely high metabolic needs as they must constantly maintain transmembrane ionic gradients and sustain the activity of millions of synapses (Rangaraju et al., 2019). In fact, it is estimated that, at rest, a single cortical neuron spends about 4.7 billion ATP molecules per second (Zhu et al., 2012). While it is true that, before differentiating, neurons mainly rely on glycolysis to meet their metabolic requirements, they gradually switch to OXPHOS, becoming increasingly dependent on mitochondria (X. Zheng et al., 2016). Even so, glycolysis is still necessary after maturation for certain activities, such as vesicular fast axonal transport (Zala et al., 2013). It is also important to recognize that neurons are differentiated cells consisting of diverse regions engaging in quite different activities. This reflects unique metabolic requirements from each neuronal segment.

In mature neurons, most ATP is consumed by the activity of Na^+/K^+-ATPases and plasma membrane Ca^{2+}-ATPases (PMCA) scattered throughout the cell to maintain ionic gradients across the membrane and, consequently, neuronal excitability (Ames, 2000). Also, the synapse is undoubtedly one of the most energetically demanding neuronal

regions (Lennie, 2003). Here, mitochondria contribute with ATP not only to maintain ionic gradients but also to regulate neurotransmission, as represented in Figure 3. Variations in the mitochondrial pool at the synapse have been shown to largely affect the probability of synaptic vesicle (SV) exocytosis due to differences in ATP availability and Ca^{2+} signals (T. Sun et al., 2013). Accordingly, mutations in the dynamin-related protein 1 (Drp1) gene, involved in mitochondrial fission, as it will be described further ahead, seem to decrease the number of synaptic mitochondria, which leads to deficits in SV replenishment close to the release sites, impairing neurotransmission (Verstreken et al., 2005). ATP has further been shown to power myosin ATPase during vesicle mobilization (Bi et al., 1997). Despite all this, it is SV recycling which appears to be the most energetically demanding process during neurotransmission (Pathak et al., 2015; Rangaraju et al., 2014). Altogether, these studies elucidate how fundamental mitochondrial ATP is to enable appropriate SV dynamics and, hence, synaptic transmission.

Ca^{2+} buffering by mitochondria is also crucial during neurotransmission, as depicted in Figure 3. Upon the arrival of an action potential to the presynaptic terminal, voltage-gated Ca^{2+} channels (VGCC) open, which results in a fast influx of this ion and, consequently, SV exocytosis (Jahn & Fasshauer, 2012). Mitochondria intervene in this process by buffering large amounts of Ca^{2+} to later gradually release it back to the cytosol. These two effects seem to be rather contradictory at first but they work together to tightly regulate neuronal response to stimuli. Initial Ca^{2+} buffering attenuates transients in Ca^{2+} levels, decreasing the probability of SV release and allowing a faster recovery following stimulation (Billups & Forsythe, 2002). It also keeps Ca^{2+} concentration within a certain range to prevent spontaneous SV release (Alnaes & Rahamimoff, 1975). During post-tetanic potentiation (PTP), a short period following high-frequency action potentials, mitochondria slowly release the previously sequestred Ca^{2+}. This increases SV release probability, which is critical for synaptic plasticity mechanisms (Y. G. Tang & Zucker, 1997; Yang et al., 2021). Furthermore, a study has suggested that mitochondrial contribution for Ca^{2+} homeostasis at the synapse is more indirect as they provide ATP to power the activity of the PMCA, thus decreasing intracellular Ca^{2+} (Zenisek & Matthews, 2000). Similarly, Ca^{2+} may also have secondary roles in synaptic transmission as it activates several enzymes of the TCA cycle and complexes of the ETC, increasing mitochondrial-derived ATP production (Llorente-Folch et al., 2015).

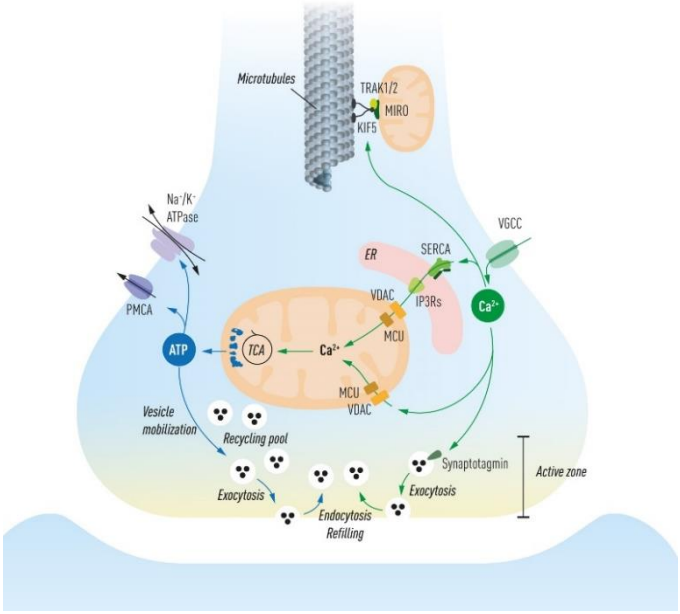

Figure 3 – Mitochondrial function at the pre-synapse. Mitochondria are transported to active synapses through the Miro-Trak-KIF5 transport complex where they are arrested upon Ca^{2+} binding to Miro. As shown in green, once at the presynaptic terminal, these organelles, in coordination with the ER, buffer Ca^{2+}, which activates enzymes of the TCA and complexes of the ETC to power ATP synthesis in mitochondria. Mitochondrial-mediated Ca^{2+} sequestration regulates exocytosis, endocytosis and SV refilling as Ca^{2+} activates all three processes. The pathways highlighted in blue showcase how mitochondrial-derived ATP is involved in maintaining ionic gradients by activating Na^{+}/K^{+} ATPases and PMCA and driving vesicle mobilization to the active zone, exocytosis, endocytosis, and neurotransmission reload into SV. Adapted from Dentoni, 2021.

1.2.4. Mitochondrial dynamics

For a long time, mitochondria were thought to be static and isolated organelles. However, it is now known that mitochondria are actually extremely dynamic structures. In response to cellular demands and depending on their own integrity and health, mitochondria can fuse with one another, divide, move throughout the cell and undergo turnover. These processes further regulate one another and are of high importance to maintain a healthy and well-distributed mitochondrial network capable of meeting cellular metabolic demands.

1.2.4.1. Mitochondrial network, a balance between fusion and fission

Mitochondrial morphology, number, function, and distribution throughout the cell are tightly regulated by a balance between mitochondrial fusion and fission (Tilokani et al., 2018). Mitochondrial fusion involves merging two or more mitochondria into one through the coordinated action of three dynamin-related GTPases. First, mitofusin 1 and 2 (Mfn1 and Mfn2) work together to enable OMM fusion (H. Chen et al., 2003), followed by optic atrophy 1 (OPA1), which mediates IMM fusion (H. Chen et al., 2005; Cipolat et al., 2004). This process generates tubular mitochondria and allows the exchange of

mitochondrial content, such as metabolites, proteins, and mtDNA, between different mitochondria, which promotes mitochondrial function while preventing the accumulation of damaged mitochondria (X. Zhu et al., 2013). In its turn, mitochondrial fission is crucial for mitochondrial movement, degradation, and during cell division as it ensures equal distribution of mitochondria to daughter cells (Otera et al., 2013). Fission is mainly mediated by the cytosolic GTPase Drp1 which, upon being recruited to the OMM and attached to its adaptors Fis1 (Mozdy et al., 2000), Mdv1 (Tieu & Nunnari, 2000), and Caf4 (Griffin et al., 2005), forms a ring-like structure that constricts the membrane until division occurs, forming smaller rounded mitochondria (Smirnova et al., 2001). ER was also observed to mediate constriction of mitochondria and facilitate the formation of Drp1 coils and subsequent fission (Friedman et al., 2011).

1.2.4.2. Mitochondrial transport

Mitochondrial biogenesis is thought to mainly occur close to the nucleus where most mitochondrial proteins are encoded (A. F. Davis & Clayton, 1996). This, allied to the limited diffusion capacity of ATP in the cytosol (Hubley et al., 1996), requires mitochondria to constantly move between cellular regions to meet local metabolic requirements. Even though this occurs in all cell types, intracellular mitochondrial transport is of particular relevance in long and polarized cells such as neurons (Z. H. Sheng, 2014). Neuronal mitochondria can be seen constantly travelling throughout the cell, both towards and away from the soma – retrograde and anterograde directions, respectively –, at velocities that can range from 0.2-2 μm/sec (Chen & Sheng, 2013; Kang et al., 2008). Interestingly, it has been reported that mitochondria with high $\Delta\psi_m$, hence considered healthy and active, normally undergo anterograde transport to reach distal cellular regions, like the synapse, which has higher metabolic demands. On the other hand, low $\Delta\psi_m$ mitochondria are regarded as damaged and preferentially travel in the opposite direction, probably to be degraded in the soma (Miller & Sheetz, 2004). Mature neurons, however, appear to have higher expression of syntaphilin (Zhou et al., 2016), an axonal mitochondria docking protein (Kang et al., 2008). This may account for the decreased percentage of motile mitochondria seen in mature neurons as they tend to spend more time at the presynapse (Lewis et al., 2016; Smit-Rigter et al., 2016).

Long-distance transport depends on microtubules, polarized structures formed by the assembly of α- and β-tubulin heterodimeric subunits (Conde & Cáceres, 2009). To travel along microtubules, cargoes must associate with motor proteins that use energy generated by ATP hydrolysis to drive mitochondrial transport. Movement towards the plus end of the microtubule is generally mediated by members of the kinesin superfamily proteins (KIF), while dynein mediates transport directed towards the minus

extremity. Since the plus end of axonal microtubules is always directed distally and the minus end faces the soma, KIF and dynein drive axonal anterograde and retrograde mitochondrial transport, respectively (Hirokawa et al., 2010).

In neurons, the kinesin family member 5 (KIF5) is essential for mitochondria axonal anterograde transport (Pilling et al., 2006; Tanaka et al., 1998). Three isoforms of KIF5 proteins are known in mammals – KIF5A, KIF5B, and KIF5C. KIF5B is expressed across all cell types, whilst KIF5A and KIF5C are neuron-specific (Kanai et al., 2000). Interestingly, KIF5 does not directly attach to mitochondria, but instead uses adaptor proteins – the trafficking kinesin-binding proteins 1 and 2 (Trak1 and 2) (van Spronsen et al., 2013). The importance of these proteins in mitochondrial transport is highlighted by studies showing that knock out or expressing mutants of Trak1 impairs mitochondrial motility in axons of hippocampal neurons (Brickley & Stephenson, 2011), whereas increasing Trak2 expression improves movement of axonal mitochondria (Yanmin Chen & Sheng, 2013). Trak1 and Trak2 further bind the mitochondrial Rho GTPases 1 and 2 (Miro1 and 2). Miro are OMM proteins possessing two EF-hand Ca^{2+}-binding motifs and two GTPase domains shown to be critical during mitochondrial trafficking (Fransson et al., 2006). Recently, it was reported that increasing the expression of Miro1 improves mitochondrial transport, probably by enhancing the recruitment of Trak2 to mitochondria, hinting at the importance of the Miro1-Trak2 complex for mitochondrial movement, particularly in hippocampal neurons (MacAskill, Brickley, et al., 2009). Miro involvement in mitochondrial motility seems to be related to its role as a Ca^{2+} sensor. When intracellular Ca^{2+} levels are elevated, this ion links to Miro's EF-hand motifs, changing its conformation. The exact effects of this conformational change are not fully understood yet, but this interaction certainly halts mitochondrial transport (Saotome et al., 2008; Xinnan Wang & Schwarz, 2009). Thus, whenever mitochondria pass by an active synapse, where Ca^{2+} levels are high, mitochondria are arrested at these sites producing ATP and regulating Ca^{2+} concentration to enable synaptic transmission (MacAskill, Rinholm, et al., 2009). Therefore, as shown in Figure 3, the Miro-Trak-KIF5 complex forms the transport machinery responsible for modulating axonal mitochondria anterograde transport.

Dynein motor proteins mediate mitochondrial retrograde movement in axons (Pilling et al., 2006). Whether dynein attaches directly or indirectly to mitochondria is still not very well established, although some adaptor proteins have been suggested to mediate dynein-mitochondria binding. Evidence suggests that Trak has dynein-binding sites, indicating that it can also participate in dynein-dependent transport (van Spronsen et al., 2013). Additionally, Miro may also be involved in axonal mitochondria retrograde transport as deletion of *Miro* in *Drosophila* compromises kinesin- and dynein-mediated

mitochondrial transport alike (Russo et al., 2009). In fact, mitochondria appear to simultaneously associate with both dynein and KIF5, as suggested by studies demonstrating dynein and kinesin co-localization with mitochondria moving in both directions (N. Hirokawa et al., 1990; Xinnan Wang & Schwarz, 2009). However, this does not seem to lead to a competitive mechanism to determine the direction of movement as inhibition of kinesin-mediated transport does not necessarily favour dynein-mediated transport (MacAskill, Rinholm, et al., 2009; Wang & Schwarz, 2009). Thus, kinesin and dynein seem to act together to tightly regulate mitochondrial transport upon variations in cellular needs.

It is also important to address that moving a mitochondrion for such long distances comes with its obstacles. As previously stated, most mitochondrial proteins are nucleus-encoded. So how can mitochondria maintain their protein composition to remain functional when they are located so far away from the soma? Recent studies have demonstrated mRNAs encoding mitochondrial proteins are locally translated at axons and synapses, contributing to mitochondrial integrity and neuronal health (Cioni et al., 2019; Kuzniewska et al., 2020). Alternatively, healthy mitochondria could also be transferred from neighbouring cells, such as astrocytes, to quickly replenish defective mitochondria with functional ones, as it has been reported (Hayakawa et al., 2016). Furthermore, the cell's degradation machinery is predominantly found in the soma, and studies show that damaged mitochondria undergo retrograde transport to be eliminated (Y. Zheng et al., 2019). Following the same line of thought, this poses as a challenging process since high amounts of energy are required to drive mitochondrial transport and dysfunctional mitochondria typically showcase loss of $\Delta\psi_m$ and impairment of ATP production. Indeed, it is yet to be unravelled how damaged mitochondria might obtain sufficient ATP to travel back to the soma.

1.2.4.3. Mitophagy

When damaged, mitochondria produce a myriad of stress molecules, such as ROS, which compromise a series of vital cellular mechanisms and promote apoptosis (Hamacher-Brady & Brady, 2016). In fact, accumulation of dysfunctional mitochondria has been shown to be involved in ageing, inflammation, and many diseases, such as neurodegenerative disease (Chan, 2006; Green et al., 2011). Thus, to prevent cellular dysfunction, cells rely on quality control mechanisms responsible for removing aged or dysfunctional mitochondria.

Autophagy is a quality control process mainly involved in the degradation of proteins and dysfunctional or unnecessary organelles. During this process, autophagosomes, double-membrane structures that enclose the material to be

degraded, are formed (Mizushima, 2007). Autophagosome elongation is dependent on proteins belonging to the microtubule-associated protein light chain 3 (LC3) family. In normal conditions, LC3 exists in the cytosol in the form of LC3-I. Upon autophagy induction, LC3-I is conjugated with phosphatidylethanolamine, forming LC3-II, which can then be integrated into the autophagosome, enabling its elongation. The gamma-aminobutyric acid receptor associated-protein family is involved in autophagosome maturation and closure (Hamacher-Brady & Brady, 2016; Weidberg et al., 2010). The autophagosome then fuses with lysosomes, forming the autophagolysosomes where the content transported in the autophagosomes will be degraded by hydrolases (Mizushima, 2007).

Autophagy can be selective or non-selective. Mitophagy involves the selective degradation of mitochondria through autophagy and is normally induced by hypoxia or loss of $\Delta\psi_m$ (Hamacher-Brady & Brady, 2016). Mitophagy can occur through two main mechanisms – the PINK1/Parkin pathway or receptor-mediated mitophagy (Figure 4).

In healthy conditions, the serine/threonine kinase PTEN-induced putative kinase 1 (PINK1) is readily imported into the IMS where it is cleaved by the presenilin-associated rhomboid-like protein. However, as depicted in Figure 4a, upon mitochondrial uncoupling, mitochondrial import of PINK1 ceases and it accumulates in the OMM (S. M. Jin et al., 2010). PINK1 exerts its kinase activity at the OMM by phosphorylating Mfn2, ubiquitin, and Parkin. Consequently, the E3 ubiquitin ligase Parkin is recruited to the OMM where it ubiquitylates several proteins anchored to the OMM (Yu Chen & Dorn II, 2013; Kane et al., 2014; Shiba-Fukushima et al., 2012). Then, p62, optineurin (OPTN) and other autophagy receptors are recruited to the OMM, where they bind to both the ubiquitylated proteins of the OMM through their ubiquitin-binding domain, and to LC3-II in the autophagosome via their LC3-interacting region (LIR) domain, leading to mitochondrial enclosure in the autophagosome (Geisler et al., 2010; Wong & Holzbaur, 2014).

Additionally, autophagic stimuli result in phosphorylation and consequent activation of Unc-51-like autophagy activating kinase 1 (ULK1), a serine/threonine kinase involved in autophagy regulation (Wani et al., 2015). The autophagy and beclin 1 regulator 1 (AMBRA1) is a substrate of phosphorylated ULK1 (p-ULK1) (Di Bartolomeo et al., 2010) and, once phosphorylated by this enzyme, translocates to the OMM where it interacts with Parkin and stimulates autophagosome formation (van Humbeeck et al., 2011).

On the other hand, receptor-mediated autophagy, shown in Figure 4b, is dependent on the phosphorylation state of the LIR motifs of mitophagy receptors located at the OMM. Some of these receptors include BCL2/adenovirus E1B 19 kDa interacting

protei n 3 (Bnip3), its homologue Bnip3/Nix, and FUN14 domain-containing protein 1 (FUNDC1). Similarly to AMBRA1, FUNDC1 activity and binding to LC3-II is promoted by its phosphorylation by p-ULK1 (Wu et al., 2014). Furthermore, AMBRA1 too possesses a LIR domain which directly binds to LC3-II mediating Parkin-independent mitophagy (Strappazzon et al., 2015).

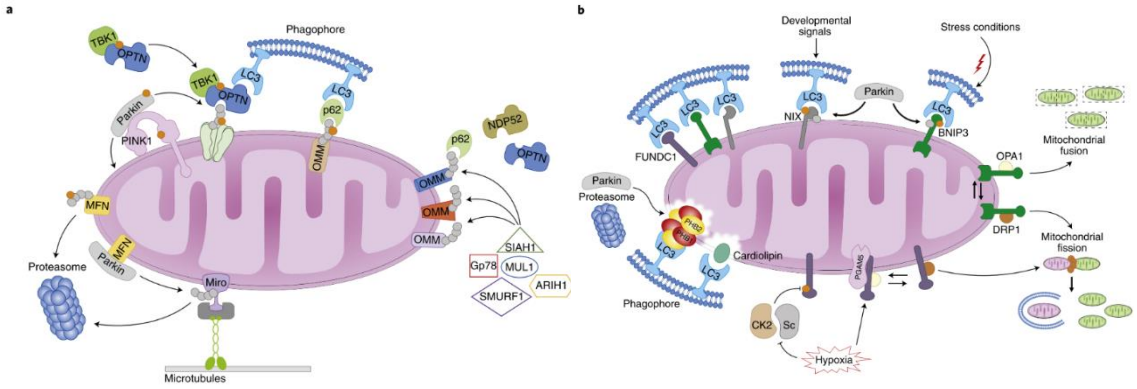

Figure 4 – Mitophagy mechanisms. (a) PINK1/Parkin-dependent mitophagy. Following mitochondrial damage, PINK1 accumulates in the OMM and recruits Parkin to mitochondria. PINK1 and Parkin phosphorylate and ubiquitinate several OMM components, respectively, targeting them for autophagy. Alternatively, SIAH1, Gp78, MUL1, ARIH1, and SMURF1 may also act as E3 ubiquitin ligases. The adaptor proteins OPTN, p62, and NDP52 then simultaneously bind the ubiquitinated proteins and LC3-II, initiating the mitophagy process. The PINK1/Parkin pathway both influences and is influenced by mitochondrial fusion-fission and transport. **(b) Receptor-mediated mitophagy.** FUNDC1, BNIP3, and NIX localize to the OMM and directly bind LC3 depending on their phosphorylation state, whereas other molecules like PHB2 and cardiolipin are exposed at the OMM upon mitochondrial impairment where they interact with LC3 to mediate mitochondrial clearance. Parkin may also ubiquitinate BNIP3/NIX showcasing the crosstalk between both mitophagy pathways. The phosphorylation state of FUNDC1 is regulated by the CK2/Sc kinases and PGAM5 phosphatase, which modulates mitochondrial network under hypoxic conditions. During mitophagy, Drp1 is recruited to the OMM while Opa1 is liberated, resulting in the generation of small mitochondria, which are more easily captured by the autophagosome. Adapted from Palikaras et al., 2018.

Importantly, mitochondrial transport has been associated with mitophagy as dynein is involved in transporting autophagosomes towards the lysosomes. The dynein complex also appears to regulate the availability of AMBRA1 to participate in autophagy (Di Bartolomeo et al., 2010). Recent evidence further suggests that, in migrating cells, KIF5B, myosin19, and Drp1 contribute to mitochondrial quality control maintenance by regulating the traffic of small, damaged mitochondria to the periphery of the cell where they are packed into mitosomes. These vesicular structures then dispose of the dysfunctional mitochondria enabling faster recovery of mitochondrial health following mitochondrial stress (Jiao et al., 2021).

1.2.5. Mitochondrial dysfunction in AD

Mounting evidence supports that mitochondria play central roles in AD's pathology. Positron emission tomography studies have revealed that, compared to

healthy subjects, cerebral glucose metabolism in AD patients is highly decreased. Activity levels of enzymes involved in mitochondrial ATP production, including cytochrome c oxidase, ATP synthase, and PDH are reduced in AD brains, which impairs $\Delta\psi_m$ and ATP synthesis. Accordingly, ROS production and consequent lipid peroxidation and protein and DNA oxidative damage are also increased in AD post-mortem brains (Perez Ortiz & Swerdlow, 2019). More recently, a large-scale proteomic analysis of AD brain and cerebrospinal fluid also revealed that protein network modules linked to sugar metabolism and mitochondrial function emerged as one of the most significant modules associated with AD pathology and cognitive impairment (Johnson et al., 2020). Indeed, introducing mtDNA from AD or mild cognitive impairment (MCI) patients in mtDNA deprived cells results in decreased ATP production, enhanced oxidative stress and apoptosis, impairment of Ca^{2+} buffering, depolarization and fragmentation of mitochondria, and increased Aβ production, supporting Swerdlow and Khan's theory that mitochondrial dysfunction might be the trigger for AD (Swerdlow & Khan, 2004). Data collected from 3xTg-AD mice further indicates that mitochondrial bioenergetics impairment precedes Aβ plaque formation (Yao et al., 2009). Furthermore, our group has shown that Aβ peptide localizes at mitochondria cristae and is imported into mitochondria via the TOM import machinery (Hansson Petersen et al., 2008). At mitochondria, Aβ interacts with several enzymes, including mitochondrial complex IV and the mPTP-integrating protein Cyclophilin D, causing mitochondrial dysfunction and oxidative damage (Manczak et al., 2006).

Mitochondrial biogenesis also seems to be impaired in AD as shown by a reduced number of mitochondria as well as lower levels of peroxisome proliferator-activated receptor gamma coactivator 1-alpha (PGC-1α), mitochondrial transcription factor A (TFAM), and nuclear respiratory factor 1 and 2, proteins involved in generating new mitochondria, in human AD hippocampus and *App*^{Swe} models (Qin et al., 2009; B. Sheng et al., 2012). Reduced mitochondrial biogenesis in AD may further relate to fusion and fission deregulation. Wang et al. described the presence of fragmented mitochondria, which accumulated in the perinuclear region, in an APP overexpression model (Xinglong Wang et al., 2008). Later, fragmented mitochondria were also observed in AD brains accompanied by upregulation of Fis1 and downregulation of Drp1, Mfn1 and 2, and Opa1 (Xinglong Wang et al., 2009). Interestingly, both Aβ and hyperphosphorylated tau seem to promote excessive mitochondrial fragmentation by associating with Drp1 and increasing its GTPase activity (Manczak et al., 2011; Manczak & Reddy, 2012).

Mitochondrial distribution to the synapses is also deficient in AD models. Aβ has been reported to decrease the number of motile mitochondria, anterograde transport, and the mean velocity of mitochondrial movement in hippocampal neurons *in vitro*.

Importantly, this is concomitant with increased mitochondrial fission and synaptic mRNA and protein levels downregulation (Calkins et al., 2011). Tau hyperphosphorylation compromises microtubule assembly and stabilization, leading to increased inter-microtubule distance and defects in mitochondria trafficking (Kopeikina et al., 2011). Remarkably, the ability of tau to impair axonal transport does not necessarily involve microtubule dysfunction as in many models retrograde transport is not affected (LaPointe et al., 2009). Altogether, these data suggest that Aβ and tau alter mitochondrial fusion-fission dynamics and movement towards the synapse, which may account for the synaptic degeneration and consequent cognitive decline characteristic of AD. Synaptic mitochondria seem to be more susceptible to age-dependent accumulation of Aβ (Du et al., 2010). Indeed, synaptic mitochondrial are more dysfunctional than non-synaptic mitochondria and the degree of mitochondrial impairment correlates with both Aβ accumulation and degree of cognitive decline, further highlighting the importance of synaptic mitochondria in AD pathology (Dragicevic et al., 2010).

Mitophagy mitigates cognitive impairment and Aβ and tau pathology in AD models (Fang et al., 2019). However, dysfunctional mitochondria build up in AD, suggesting mitophagy is vastly compromised. Deficiency in autophagosome fusion with lysosomes (Boland et al., 2008; Coffey et al., 2014) and downregulation of PINK1 and Parkin protein levels due to Aβ and hyperphosphorylated tau-induced toxicity (Oliver & Reddy, 2019) have been appointed as likely causes of mitophagy impairment in AD.

Communication between the ER and mitochondria is also important in AD. Our group and others have shown that APP, Aβ and C99, and PS1 and PS2 locate at mitochondria-associated ER membranes (MAMs) (Area-Gomez et al., 2012; Del Prete et al., 2017). Furthermore, APP and APP-derived fragments, including AICD and C83, localize with the OMM, which indicates APP processing might occur at these sites, contributing to mitochondrial dysfunction (Pavlov et al., 2011). Indeed, Aβ has been shown to be generated in MAMs (Schreiner et al., 2015). Increased number of MERCS and MAM-associated proteins have been reported in fibroblasts from both SAD and FAD subjects (Area-Gomez et al., 2012) and AD models (Del Prete et al., 2017; Hedskog et al., 2013; Leal et al., 2020), an event observed before the appearance of plaques. This is consistent with the idea that Aβ may be produced at MAMs where it can associate with mitochondria leading to mitochondrial dysfunction. On the other hand, Mfn2 knockdown also increases MERCS number while decreasing Aβ production, hinting that this protein could be a potential target for AD prevention and treatment (Leal et al., 2016).

Collectively, these data denote mitochondria's pivotal roles in AD, making them appealing therapeutical targets. To date, drugs targeting mitochondria have largely focused on modulating oxidative stress. For instance, MitoQ is an antioxidant able to

prevent oxidative damage, reduce Aβ production, astrogliosis, synaptic loss, and improve cognition (Mcmanus et al., 2011). *In vitro* studies have shown the positive impact of SS31 mitochondrial-target peptide on mitochondrial function and transport, and synaptic function (Calkins et al., 2011). Besides antioxidants, oxaloacetate, an intermediate of the TCA cycle, seems to be beneficial to mitochondrial function and biogenesis, neuroinflammation, and neurogenesis (Wilkins et al., 2014). Recently, luteolin has also emerged as a mitochondrial function enhancer by increasing the number of MERCS and Ca^{2+} shuttling to mitochondria, mitigating mitochondrial and locomotor deficits in Huntington disease models, hinting that this molecule could also be promising for AD (Naia et al., 2021).

1.3. ASTROCYTES

In the central nervous system (CNS), neurons are found in the midst of glial cells, including microglia, astrocytes, oligodendrocytes and NG2 glia. Among these, astrocytes, so-called due to their star-shaped morphology, are the most abundant ones. Through their numerous and ramified processes, astrocytes connect not only with neighbouring astrocytes via gap junctions, but also with neurons, both at the axonal and synaptic level, and blood vessels (Sofroniew & Vinters, 2010). This intricate network astrocytes establish with other neural components put them at the heart of the CNS and enables them to regulate many cerebral functions.

1.3.1. Physiological roles of astrocytes

Initially regarded as simple supportive cells, throughout the years, astrocytes have been shown to be involved in a wide variety of vital functions in the CNS, ranging from neurotransmission, regulation of blood flow and metabolism, to neuroinflammation.

Regulation of blood flow – neuronal activity requires high O_2 and nutrient supply to generate energy. As they contact both blood vessels and the synapse, astrocytes are the main regulators of blood flow in response to oscillations in synaptic activity. In fact, these cells produce and release molecules such as prostaglandins, nitric oxide, and arachidonic acid, thus controlling vasoconstriction and dilatation (Iadecola & Nedergaard, 2007; Koehler et al., 2009). Interestingly, MERCS localized in astrocytic endfeet were shown to be important for vascular remodelling (Göbel et al., 2020).

Brain homeostasis – astrocytes modulate various aspects of the extracellular environment including fluid, ion, and neurotransmitter homeostasis. These cells express a myriad of ionic channels, such as K^+ channels, Na^+/H^+ exchangers, and bicarbonate transporters (Sofroniew & Vinters, 2010). Particularly important during neuronal activity is K^+ buffering by astrocytes. Triggering of action potentials involves efflux of K^+ from

neurons, which results in extracellular accumulation of this ion and neuronal depolarization. Astrocytes uptake large quantities of K^+, thus controlling neuronal excitability and preventing excitotoxicity (Kofuji & Newman, 2004). This is coupled to water movements across astrocytes' membranes due to activation of water channels known as aquaporins that densely populate perisynaptic and endfeet processes contacting blood vessels (Nagelhus et al., 2004). Astrocytes also express neurotransmitter transporters involved in removing these molecules from the synapse to modulate synaptic activity, as it will be discussed further ahead.

Metabolic support – astrocytes are the primary storage site of glycogen in the CNS. Importantly, glycogen reserves in these cells appear to be strategically located near synapses (Phelps, 1972). During sustained neuronal activity, glutamate release activates Na^+-dependent glutamate transporters in astrocytes. This increases Na^+ concentration in astrocytes and induces break down of the glycogen reserves into lactate, which is then transported into and used by active neurons (Magistretti, 2006). Also, astrocytes endfeet can easily uptake glucose from blood vessels to rapidly meet changes in metabolic requirements (Sofroniew & Vinters, 2010). Astrocytes further uptake apoE-positive lipid particles containing toxic fatty acids produced and released by neurons during periods of intense activity. Once inside the astrocytes, these toxic fatty acids are loaded into lipid droplets and detoxified, thus protecting neurons during neuronal activity (Ioannou et al., 2019b).

Synaptic transmission – the idea that synaptic transmission exclusively depends on communication between pre- and post-synaptic neurons has long been surpassed. In reality, accumulating evidence reveals that astrocytes also respond to and modulate synaptic activity. These observations led to the establishment of the tripartite synapse concept, postulating that synaptic transmission results from bidirectional communication between astrocytes and neurons (Perea et al., 2009). Contrarily to neurons, astrocytes are incapable of generating action potentials. Instead, the excitability of these glial cells relies on variations in cytosolic Ca^{2+} concentration that can either occur spontaneously or be induced by neurotransmitter release, like glutamate, from the pre-synaptic neuron (Charles et al., 1991; Cornell-Bell et al., 1990). Indeed, astrocytes express many different neurotransmitter receptors which, upon activation, induce Ca^{2+} release from the ER (Perea et al., 2009). Rises in intracellular Ca^{2+} concentration in astrocytes stimulates the release of gliotransmitters like glutamate, D-serine, and gamma-Aminobutyric acid (GABA), influencing neuronal activity and may underlie mechanisms of PTP (Angulo et al., 2008; Fellin et al., 2004; Jourdain et al., 2007; Oliet & Mothet, 2009). Neuronal activity further induces Miro1-driven mitochondrial confinement within astrocytic processes close to synapses. These mitochondria might control astrocyte excitability by buffering

Ca^{2+}, modulating gliotransmission and, consequently, neuronal activity (T. Stephen et al., 2015).

Astrocytes further ensure neurotransmitter homeostasis and prevent excitotoxicity by removing neurotransmitters, such as glutamate and GABA, from the synaptic cleft following an action potential. Once inside the astrocytes, these neurotransmitters are recycled into their precursor, glutamine. The inactive molecule can then be released to the synaptic space to be taken up by neurons where they are packed into SV after being reconverted back into their active forms (Bak et al., 2006).

Neuroinflammation and glial scar formation – astrocytes respond to CNS injury by undergoing a series of morphological, molecular and functional changes collectively known as reactive astrogliosis. Depending on the nature, severity, and time after the stimuli, astroglia might present either pro- or anti-inflammatory phenotypes (Liddelow & Barres, 2017; Sofroniew & Vinters, 2010). In their reactive state, astrocytes also extend their processes to form a tissue lining – the glial scar – that envelops the lesion site. Astrogliosis and scar formation have been shown to be beneficial and improve CNS recovery by promoting wound closure, blood-brain barrier repair, providing neuronal protection, and restricting the spread of inflammation (Sofroniew, 2015). Nonetheless, a fine balance between pro- and anti-inflammatory functions must be maintained to guarantee that the inflammatory response is sufficient to eliminate the danger, but not too excessive that it becomes harmful.

1.3.2. Astrocytes involvement in AD

Early evidence indicating that astrocytes may play a role in AD came from Alois Alzheimer who described the presence of astroglia surrounding neurotic plaques (Alzheimer, 1910). Since then, this has also been reported in the brain of AD mouse models (Matsuoka et al., 2001) as well as in AD patients (Nagele et al., 2003). These reactive astrocytes are thought to participate in Aβ clearance. Indeed, astrocytes located in the vicinity of amyloid plaques were found to have higher expression levels of enzymes involved in Aβ degradation, like neprilysin and metalloproteinases 2 and 9 (Apelt et al., n.d.; Yin et al., 2006). Astrocytes are the main producers of ApoE in the CNS (Mahley, 2016). *ApoE* knockout astrocytes fail to engulf Aβ deposits compared to WT mice (Koistinaho et al., 2004) and astrocytes expressing ApoE4 are less efficient than ApoE3 astrocytes in removing Aβ plaques (Simonovitch et al., 2016), thus suggesting the crucial role of astrocytes in the elimination of this peptide. Importantly, ApoE4 astrocytes are also less efficient in mobilizing neuronal lipid droplets, decreasing fatty acid oxidation and contributing to lipid dysregulation and bioenergetic deficits (Qi et al., 2021). Conversely, AD-like pathology induces Aβ production by astrocytes. AD and stressed

astrocytes express high levels of BACE1 (Roßner et al., 2005) as do astrocytes surrounding Aβ deposits in AD mice models (Heneka et al., 2005; Roßner et al., 2001). Importantly, the degree of astrogliosis seems to correlate with the degree of cognitive decline further suggesting that astrocytes might play a central role in disease progression (Simpson et al., 2010).

Gliotransmission is also affected in AD. Exposure of cultured astrocytes to Aβ increases cytosolic Ca^{2+} concentration altering gliotransmitter release (Lee et al., 2014). Neuronal-astrocyte communication is further impaired due to Aβ-induced release of glutamate from astrocytes (Talantova et al., 2013) and dysfunction of glutamate receptors (Mota et al., 2014). Similarly, the synthesis of the inhibitory neurotransmitter GABA has been suggested to be increased in astrocytes from APP/PS1 mice (Mitew et al., 2013). Interestingly, preventing GABA production and release from astrocytes restores cognitive functions and impairments in synaptic plasticity (Jo et al., 2014). Neurotransmitter turnover also appears to be altered as shown by reduced levels of glutamine, the precursor molecule of glutamate and GABA, in an AD rat model (Nilsen et al., 2014) and glutamine synthase, which converts glutamate and GABA into glutamine, in post-mortem AD brains (Robinson, 2000). Altogether, these findings indicate that impairment in gliotransmission may underlie mechanisms of neurotoxicity and contribute to AD pathology.

Finally, accumulating evidence reports that Aβ compromises astrocyte use of glucose (Schubert et al., 2009; Soucek et al., 2003), and affects mitochondrial function and mitochondria-ER coupling (Dematteis et al., 2020). On top of that, glucose and lactate transporters have been found to be decreased in cultured astrocytes from AD mice (Merlini et al., 2011), suggesting that these cells fail to provide neurons with adequate metabolic support. In agreement, neurons co-cultured with astrocytes pre-treated with Aβ had a worse survival rate than the ones co-cultured with non-treated astrocytes (Allaman et al., 2010).

1.4. INTERCELLULAR MITOCHONDRIAL TRANSFER

Normal cell physiology, tissue homeostasis, and cell survival largely depend on intercellular communication. It has long been recognized that cells communicate through hormones, growth factors, cytokines, and many other molecules to assemble appropriate responses to a myriad of stimuli (Murray & Krasnodembskaya, 2019). Lately, a new mode of communication between cells related to the transfer of cellular organelles, including mitochondria, has gained some attention. Spees and colleagues provided the first evidence of functional mitochondrial intercellular transport by showing that human stem cells donate healthy mitochondria to mtDNA-deprived cells, rescuing aerobic

respiration in the recipient cells. However, at the time, they were unable to ascertain exactly how this occurred (Spees et al., 2006). Since then, many studies have emerged demonstrating the beneficial effects of this process, while elucidating the possible underlying mechanisms.

1.4.1. Mechanisms of intercellular mitochondrial transfer

Mitochondrial transfer is likely triggered by the release of damage signals from the cells carrying dysfunctional mitochondria. The signalling and regulatory mechanisms involved in this exchange remain unclear, but it is now well established that, as depicted in Figure 5, mitochondrial transfer occurs via three main ways – formation of tunnelling nanotubes (TNTs), release and capture of extracellular vesicles (EVs), and cellular fusion.

Tunnelling nanotubes – TNTs consist of cytoplasmic protrusions that form open channels allowing direct communication between two cells. These structures range from 50-200 nm in width and can extend for several cell diameters (Rustom et al., 2004). Rustom et al. were the first ones demonstrating cellular organelles may be transferred between cells via TNTs (Rustom et al., 2004). Following this, Liu and colleagues showed that TNT-mediated mitochondrial transfer occurs from mesenchymal stem cells (MSCs) to damaged human umbilical vein epithelial cells (HUVECs), leading to restoration of aerobic respiration in HUVECS. Interestingly, mitochondrial exchange was ablated upon inhibition of nanotube formation (Liu et al., 2014). Accordingly, mitochondrial transfer rescues UV-injured PC12 cells from apoptosis, but this is prevented by either disruption of TNT development or co-culturing the UV-damaged PC12 cells with unhealthy cells (X. Wang & Gerdes, 2015). The fundamental role of TNTs in mitochondrial transfer is further highlighted by the observation that impairment of TNT formation largely affects this process, whereas inhibition of mechanisms like phagocytosis, endocytosis, or exocytosis has almost no impact (Bukoreshtliev et al., 2009). TNTs also allow, on the other hand, the spread of seeds as pathological tau protein assemblies and Aβ can be transported (Abounit et al., 2016).

TNT formation appears to depend on the detection of stress signals since shielding phosphatidylserines at the surface of apoptotic cells hinders TNT-mediated intercellular contacts (Liu et al., 2014). Furthermore, serum starvation and hydrogen peroxide (Y. Wang et al., 2011), as well as treatment with stress agents like ethidium bromide (Cho et al., 2012) or rotenone (Ahmad et al., 2014), induce TNT generation. TNTs have been shown to emerge from the cells accepting mitochondria (X. Wang & Gerdes, 2015; Y. Wang et al., 2011). However, further studies are still required to determine whether this could be generalized to other cell types or not.

Nanotubes are commonly actin-based, but certain cell types, such as astrocytes and primary neurons, might present thicker TNTs made up of microtubules (Xiang Wang et al., 2012). These cytoskeleton filaments provide the highways through which cellular organelles and membrane vesicles are transported from one cell to the other. Therefore, motor proteins, particularly Miro1, seem to have key roles in promoting intercellular mitochondrial transport through TNTs (Ahmad et al., 2014; Babenko et al., 2018). Interestingly, it was also recently shown that the transfer of mitochondria within the dendritic network rely on contact between the ER and mitochondria (Gao et al., 2019).

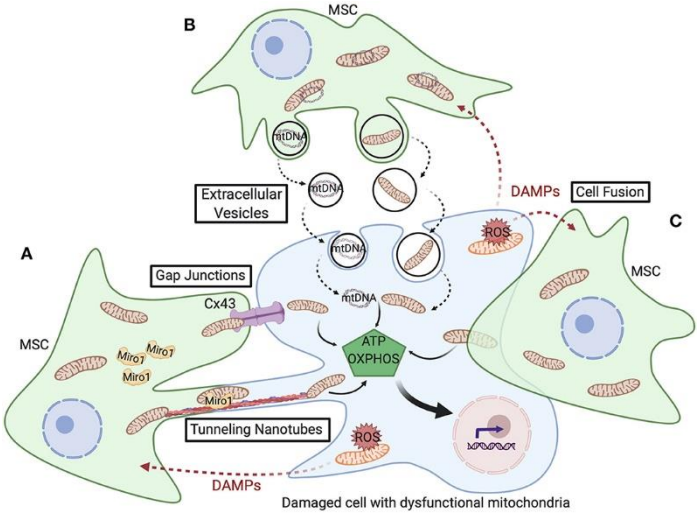

Figure 5 – Mechanisms mediating intercellular mitochondrial transfer. Mitochondrial transfer is likely triggered by the detection of danger signals released by cells containing dysfunctional mitochondria. Mitochondrial donation can occur via **(A)** transport through TNTs, **(B)** EVs-containing mitochondria (mito-EVs), or **(C)** cell fusion. This process appears to be regulated by connexin 43, which promotes cell-cell attachment via gap junction, and Miro1. Mitochondrial integration into the stressed cell's mitochondrial network results in restoration of mitochondrial and, consequently, cellular function. Adapted from Mohammadalipour et al., 2020.

Extracellular vesicles – virtually all cell types release vesicles to the extracellular space. These are then captured by neighbouring or distant cells, unloading their cargo in their cytoplasm. Therefore, EVs are important mediators of several physiological and pathological processes in the organism (Torralba et al., 2016). EVs are a heterogeneous group of vesicles and, depending on size and biogenesis, they can be further classified into exosomes, microvesicles, and apoptotic bodies. Exosomes are formed during endosome maturation and comprise the smallest EVs, ranging between 30-100 nm in diameter, whereas microvesicles may vary between 50-1000 nm in diameter and are formed through the sequential protrusion, budding and fission of the plasma membrane. Apoptotic bodies are generated during apoptosis and can be smaller, 50-1000 nm wide, or larger, one to several µm, vesicles (Murray & Krasnodembskaya, 2019).

Even though exosomes are likely too small to carry whole mitochondria, evidence suggests these structures may transport mtDNA (Guescini et al., 2010). On the other

hand, larger EVs have been consistently reported to contain entire mitochondria (mito-EVs), which are captured by cells with defective mitochondria resulting in improvement of mitochondrial and cellular function. A recent report from the Efrat Levy lab showed that mito-EVs contain a specific subset of mitochondrial constituents. OXPHOS complexes and PDH complex subunits were almost fully represented, as well as other energy production pathways, such as TCA cycle, fatty acid β-oxidation, and membrane transporters of metabolites directly linked to energy production. In contrast, cytosol-to-mitochondria peptide import machinery was scarcely found (D'Acunzo et al., 2021). Notably, authors reported that mito-EVs cargo alter during pathophysiological processes where mitochondrial dysfunction is present. In the pioneering study developed by Islam et al. EV-mediated mitochondrial transfer from MSCs to lung alveolar epithelial cells improved the recipient cells´ ATP levels and protected against acute lung injury. Interestingly, connexin 43 seems to regulate this mitochondrial exchange by promoting the attachment of the donor and recipient cell via the establishment of gap junctions, leading to the formation of TNTs and EVs (Islam et al., 2012). Oxidative phosphorylation was found to be enhanced in macrophages after internalizing MSCs-derived mito-EVs (Phinney et al., 2015), while neural stem cells too release intact, healthy mitochondria inside EVs to restore mitochondrial function in target cells (Peruzzotti-Jametti et al., 2021).

Cell fusion – this is a rare form of intercellular communication involving the permanent or transient fusion of the plasma membrane of two independent cells, while the nuclei remain unaffected. Cell fusion enables cytosolic components and organelles, like mitochondria, to be shared between the merging cells (Murray & Krasnodembskaya, 2019). Both embryonic and adult stem cells were found to fuse with cardiomyocytes, hepatocytes, and neurons, probably contributing to their differentiation, plasticity and survival (Alvarez-Dolado et al., 2003). However, as most investigations on this topic use pluripotent or multipotent stem cells as one of the fusion cells, the physiological relevance of this process has been highly challenged (Torralba et al., 2016).

1.4.2. Astrocyte-neuron mitochondrial transfer

As reviewed in section **1.3.1. Physiological roles of astrocytes**, astrocytes support neurons in a wide variety of functions. Mounting evidence now links mitochondria to astrocytes' neuroprotective roles. Indeed, inhibiting astrocytic mitochondria fails to protect neurons against toxicity (Volobouéva et al., 2007) and they further appear to aid neuronal cells in maintaining their mitochondrial network healthy. Neurons release damaged mitochondria to be degraded and recycled in astrocytes, in a process known as transmitophagy (C. H. O. Davis et al., 2014; Morales et al., 2020). On the other hand,

the groundbreaking study carried out by Hayakawa and colleagues revealed that, following uptake of extracellular mitochondrial particles released by astrocytes in a process dependent on CD38 signalling, ATP levels and neuronal viability were restored in neurons subjected to ischaemia (Hayakawa et al., 2016). Co-culturing cisplatin-treated neurons with astrocytes protected against neuronal death, neuronal mitochondria depolarization and Ca^{2+} abnormalities caused by the cisplatin treatment. These beneficial effects were associated with Miro1-dependent mitochondrial transfer from astrocytes to the treated neurons (English et al., 2020). These observations further extend to neurodegeneration models since, in a rotenone-induced *in vitro* Parkinson's disease (PD) model, iPSC-derived astrocytes donated functional mitochondria to dopaminergic neurons halting their degeneration (Cheng et al., 2020).

Taken together, these studies suggest astrocyte-neuron mitochondrial transport underlies important rescue mechanisms to preserve neuronal function and survival, hinting that this could become a promising therapeutical strategy for CNS diseases. In a rat model of PD, xenogeneic/allogeneic mitochondrial transplantation enhanced the survival of dopaminergic neurons and improved neuronal function (Chang et al., 2016), while systemic intravenous mitochondrial injection in a PD mouse model blocked PD progression (Shi et al., 2017). Following ischaemia, autologous mitochondrial injection in the heart's affected area improved post-ischemia recovery (Masuzawa et al., 2013). Nonetheless, very few clinical trials have been launched so far to treat neurodegenerative diseases, stroke and traumatic brain injury recurring to this technique.

2. RESEARCH AIMS

Moving mitochondria along neuronal arborizations consumes high amounts of energy. In AD, mitochondrial function and transport to the synapse are severely compromised. Under these circumstances, it would be more energetically favourable for neurons if mitochondria could reach the synapse from closer locations, such as astrocytic processes at the tripartite synapse, and be eliminated from there when damaged. Indeed, astrocytes can not only transfer healthy mitochondria to stressed neighbouring neurons, improving their function and survival but also receive neuronal mitochondria for degradation. However, the relevance of these processes in neurodegenerative diseases and, particularly, in AD is still widely unknown. Therefore, we hypothesize that intercellular mitochondrial transfer occurs between astrocytes and neurons and that this process is impaired in AD, contributing to the loss of the pre-synaptic mitochondrial pool and deficient mitochondrial elimination, leading to synaptic dysfunction and neuronal death. Furthermore, we propose that to do so, astrocytes undergo transcriptomic changes to acquire the necessary machinery to carry out these processes.

Therefore, the overall goal of the thesis herein presented was to further elucidate the mechanisms underlying intercellular mitochondrial transfer between neural cells in AD. To this end, experiments were carried out in neuronal and astrocytic WT and *App*$^{NL-G-F}$ primary cultures. We established astrocyte-neuron co-cultures and used a combination of biochemical, functional and imaging techniques to determine whether mitochondrial transfer occurred. Furthermore, several techniques, including ATP assays, western blotting, and flow cytometry were implemented to evaluate the health of the mitochondria being transferred. More specifically, the aims of this thesis included:

- Characterization of bioenergetics and mitochondrial trafficking and elimination in neuronal and astrocytic primary *App*$^{NL-G-F}$ cultures.
- Assessment of transcriptomic remodelling of astrocytes co-cultured with neurons.
- Exploring the specific mechanisms underlying mitochondrial exchange between astrocytes and neurons *in vitro* and how this is affected in *App*$^{NL-G-F}$ co-cultures.

3. METHODS AND MATERIALS

3.1. Animal models and ethical considerations

In order to study the hypothesis herein proposed, the C57B6/J A*pp* knock-in (KI) mouse model containing the Swedish (K670N/M671L), Iberian (I716F) and Arctic (E693G) mutations (*App*$^{NL-G-F}$), previously described by Saito *et al.* (2014), was used. Additionally, C57B6/J wild-type (WT) mice were used as controls. The animals were housed at Comparative Medicine´s Annex (KM-A) at Karolinska Institutet under 12:12h light/dark cycles, controlled temperature (22-23°C) and *ad libitum* access to food and water. Ethical approval to all studies was given by the "Regionala Etikprövningsnämnden" (Regional Ethics Review Board, ref no. 12779/2019). All experiments were performed taking into account the guidelines given by the Institutional Animal Care and Use of Committee and the European Community directive (2010/63/EU).

3.2. Primary cell cultures

Primary cortical neurons (PCN) and primary cortico-hippocampal astrocytes were isolated from 17 days old C57B6/J WT and *App*$^{NL-G-F}$ mouse embryos. Dissection was performed in ice-cold Hank's balanced salt solution (HBSS) (ThermoFisher, Cat. no. 14025092). Cortices were incubated for 10 minutes (min) in Accutase solution (Sigma Aldrich, Cat. no. A6964). Digestion was stopped by diluting Accutase 1:4 in unsupplemented neurobasal medium (ThermoFisher, Cat. no. 21103049), followed by centrifugation at 170 *xg* for 3 min. Tissue was then mechanically dissociated in neurobasal medium supplemented with 2 mM L-Glutamine (ThermoFisher, Cat. no. A2916801) and 1x B27 (Gibco, Cat. no. 17504044). For astrocytes culture, only mechanical dissociation was performed in DMEM/F12 medium (Sigma Aldrich, Cat. no. D5030) supplemented with 10% of heat-inactivated Fetal Bovine Serum (HI-FBS) (Gibco, Cat. no. 10270106) and 0.5% N2 (ThermoFisher, Cat. no. 17502048). The cell homogenates were filtered using 40 µm cell strainers (Corning, Cat. no. 352340). Following that, neurons were plated in supplemented neurobasal medium in 0.1 mg/mL poly-D-coated plates (Sigma Aldrich, Cat. no. P7280) at a density of 45-53 x 10^3 cells/cm^2. Every six days the medium was changed by replacing only half of the medium with fresh neurobasal supplemented medium. Astrocytes were plated in non-coated T75 flasks (Sarstedt, Cat. no. 83.3911.002) and kept in supplemented DMEM/F12 medium. The medium was changed every three-four days. At this stage, both astrocytes and microglia are present.

To obtain pure astrocytic cultures, astrocytes were passaged, and microglia removed following a previously published protocol (Saura et al., 2003) with minor modifications. At DIV13-14, or once astrocytes reached confluence, the media was removed and 5 mL Dubelco's Phosphate Buffered Saline (PBS) buffer (Gibco, Cat. no. 14190-094) was added to wash the cells. Then, 3 mL of 0.08% Trypsin-EDTA (0.25% Trypsin-EDTA (ThermoFisher, Cat. no. 25200056) diluted in DMEM/F12 without FBS, was added. The cells were placed in the incubator at 37 °C for 25-30 min. This allowed the astrocytes to detach as a single layer, while microglia remained attached to the flask. Afterwards, 5 mL of supplemented DMEM/F12 was added to the flask to stop trypsinization. The cells were centrifuged for 3 min at 170 *xg* and the supernatant was removed. To dissociate astrocytes in single cells, 1 mL of 0.25% Trypsin-EDTA was added to the astrocytes and the cells were incubated at 37 °C for 1 min. After the incubation period, the cells were homogenized 2-3 times with a pipette to finalize astrocyte dissociation and a washing step was performed by adding 4 mL of supplemented DMEM/F12. A 3 min centrifugation at 170 *xg* followed, and the supernatant was discarded. Finally, 1-2 mL of fresh supplemented DMEM/F12 was added and the cells were plated at a density of 20 x 10^3 cell/cm^2. Both neurons and astrocytes were kept in a humified incubator at a temperature of 37 °C and 5% CO_2/95% air.

The purity of both neuronal and astrocytic cultures was accessed. Neuronal cultures displayed a purity of 86% (Figure S1a), while astrocytic cultures presented a purity of 94%, with 6% contamination by $Iba1^+$ microglia (Figure S1b).

3.3. Astrocyte-neurons co-cultures

Two different types of co-cultures were established depending on the experiments to be performed. To study astrocytes-neuron mitochondrial transfer and gene expression in astrocytes, the two cell types were co-cultured in two different layers in 6-well plates. To achieve this, paraffin wax (Sigma Aldrich, Cat. no. 327204-1KG) was melted and 4 paraffin dots were made in each well. The plates were sterilized under UV light for 20 min, coated with 0.1 mg/mL poly-D-lysine, and the astrocytes plated in supplemented DMEM/F12 medium. Co-cultures were performed when astrocytes reached confluence. For that, conditioned media (CM) was recovered from the neuronal cultures and filtered with 0.2 µm filters (VWR, Cat. no. 28145-501) to remove cell debris and any mitochondria that might have been released to the CM until the moment of co-culture. Then, neurons at DIV12 plated in coverslips were placed on top of the paraffin dots. The co-cultures were maintained in 3 mL of supplemented neurobasal medium, in a proportion of 1:1 of filtered CM media and fresh supplemented neurobasal media. To

evaluate mitophagy in astrocytes, co-cultures were established in 10 mm MatTek dishes (MatTek Life Sciences, Cat. no. P35G-1.5-10-C). Prior to co-culture, astrocytes were plated in 12-well plates and transfected with either MitoDsRed or mt-Keima plasmid, as described below, while neurons were plated at the periphery of MatTek dishes. Co-cultures were performed at neuronal DIV12 and 48 hours (h) after astrocytes transfection. Astrocytes were detached with 0.25% Trypsin-EDTA and trypsinization was blocked after 5 min with DMEM/F12 with FBS (1:4). Cells were centrifuged at 170 *xg* for 3 min. The supernatant was discarded, and the astrocytes were diluted in supplemented neurobasal media. The cells were added dropwise in the 10 mm glass centre of the MatTek dishes with neurons plated in the periphery.

Astrocytic cellular and mitochondrial morphology were evaluated to make sure media change from DMEM/F12 to neurobasal did not affect these parameters (Figure S2). Experiments were performed 48 h after co-culture.

3.4. Cell transfection

To identify mitochondrial network in neurons and astrocytes in living cells, the pLV-mitoDsRed vector, kindly given by Pantelis Tsoulfas, was used (Addgene, Cat. no. 44386; http://n2t.net/addgene:44386; RRID: Addgene_44386) (Kitay et al., 2013). This plasmid contains the sequence for a fusion protein constituted by the P1 isoform of F_1F_0-ATP synthase, which targets the protein to the IMM, and DsRed, a red fluorescent protein. Mitophagy in live astrocytes was assessed recurring to the mKeima-Red-Mito-7, a gift from Michael Davidson (Addgene, Cat. no. 56018; http://n2t.net/addgene:56018; RRID: Addgene_56018). The mt-Keima plasmid codes for a fusion protein consisting of the sequence for COX8, a subunit of the cytochrome c oxidase complex of the ETC, and Keima. Keima is a pH-dependent fluorescence protein that has a single emission wavelength at 620 nm. However, depending on the pH properties of the environment, its excitation spectrum changes. In neutral pH, excitation occurs at around 440 nm (green), while in acidic environments, like the one present within lysosomes, the excitation spectrum changes to 586 nm (red). Therefore, and since Keima is resistant to degradation in the lysosome, this plasmid is highly suitable to study mitophagy (N. Sun et al., 2017).

Both plasmids were amplified in bacteria growth in LB media (Sigma Aldrich, Cat. no. L3022.) supplemented with 100 µg/mL ampicillin (ThermoFisher, Cat. no. 11593027) and extracted and purified using the EndoFree® Plasmid Maxi Kit (Qiagen, Cat. no. 12362), according to the manufacturer's protocol. Cells were transfected with Lipofectamine 2000 reagent (ThermoFisher, Cat. no. 11668019) following the manufacturer's instructions. Briefly, liposomes were obtained in opti-MEM media

(ThermoFisher, Cat. no. 31985062) and 1.6 µg of DNA was used for 12-well plates and 0.2 µg of the plasmids were used for MatTek dishes. Neurons were transfected for 1.5 h in half-volume of neurobasal CM, while astrocytes were transfected for 2 h in opti-MEM medium. Once the transfection period ended, the transfection solution was removed and fresh supplemented DMEM/F12 was added to the astrocytes; for neurons, half of supplemented neurobasal medium and half of the CM previously saved was used.

3.5. Evaluation of mitochondrial function in neurons

Mitochondrial membrane potential measurement – tetramethylrhodamine, methyl ester (TMRM) is a cell-permeant cationic dye that accumulates in healthy mitochondria with intact $\Delta\psi_m$, emitting bright fluorescence. Mitochondria depolarization leads to TMRM extrusion from mitochondria and, consequently, a decrease in the signal. Therefore, to assess $\Delta\psi_m$ integrity in neurons, cells were incubated with 10 nM TMRM (ThermoFisher, Cat. no. T668) in 1 x artificial cerebrospinal fluid (ACSF) with $NaHCO_3$, prepared by diluting 10 x ACSF (NaCl 124 mM, KCl 2.5 mM, NaH_2PO_4 1.25 mM, glucose 10 mM) + 26 mM $NaHCO_3$ in H_2O, and supplemented with 1.5 mM $CaCl_2$ and 1.5 mM $MgCl_2$ for 30 min at 37 ºC. After the incubation period, neurons were washed and imaged in supplemented 1 x ACSF without $NaHCO_3$. The experiment was carried out at 37 ºC and the z-stack images were acquired using a 63x objective with NA=1.4 in the LSM980-Airy confocal microscope (Zeiss). The Fiji software was used to process the z-stack images into a 3D reconstruction. ROIs were drawn using the segmented line, a threshold was applied to the obtained image and fluorescence intensity was measured.

ATP measurement – the CellTiter-Glo® Luminescent Cell Viability Assay (Promega, Cat. no. G7570) was used to measure ATP levels. This assay can induce cell lysis and takes advantage of the properties of luciferase to catalyze a reaction that produces a luminescence signal directly proportional to the amount of ATP present in the sample. Therefore, at DIV12, media from neurons plated in 96-well plates was removed and replaced by 100 µL of unbuffered DMEM 5030 media (Sigma Aldrich, Cat. no. 5030) supplemented with 10 mM sodium pyruvate (ThermoFisher, Cat. no. 11360070) and 2 mM L-Glutamine (pH 7.2-7.4). Cells were incubated at 37 ºC for 1 h. After incubation, 100 µL of the CellTiter-Glo® reagent was added to the cells, which were then placed in the shaker for about 2 min. Incubation of 10 min at RT followed and luminescence levels were measured in a plate reader. Results were normalized to protein content.

3.6. Seahorse analysis

Seahorse is a technique widely used to study cellular metabolic function. This technique allows the measurement of oxygen consumption rate (OCR) and extracellular acidification rate (ECAR) in live cells, thus providing information on key cellular functions, such as mitochondrial respiration and glycolysis, respectively. Therefore, to assess metabolic function in astrocytes, cells were grown in poly-D-coated 96-well Seahorse XF96 microplates (Agilent). The day before the experiment, the sensor cartridge (Seahorse Bioscience) was calibrated by placing it on a 96-well calibration plate (Seahorse Bioscience) filled with sterile ddH_2O in a humified CO_2-free incubator at 37 °C, overnight. The next day, the ddH_2O was replaced by XF calibrant solution (Seahorse Bioscience), previously warmed up overnight in the CO_2-free incubator. The cartridge sensor was left in the incubator with the calibrant solution for 1 h. For OCR measurements, cell media was replaced by unbuffered DMEM supplemented with 17.5 mM glucose, 0.5 mM pyruvate and 2.5 mM L-glutamine, pH = 7.2-7.4. OCR was measured using the Seahorse® XF96 analyzer (Agilent) at baseline, and after sequential stimulation with 1 µM oligomycin A (Sigma Aldrich, Cat. no. 75351), 1 µM carbonyl cyanide-4-(trifluoromethoxy)phenylhydrazone (FCCP) (Sigma Aldrich, Cat. no. C2920), and 0.5 µM of both antimycin A (Ant A) (Sigma Aldrich, Cat. no. A8674) and rotenone (Rot) (Sigma Aldrich, Cat. no. R8875). Accordingly, mitochondrial basal respiration, maximal respiration, ATP production and spare respiratory capacity (SRC) were automatically calculated using the Seahorse XF Cell Mito Stress test report generator from Wave 2.6.1 software (Agilent). Data were given in pmol O_2/min and normalized for protein content.

ECAR was also measured to determine the glycolytic function of the cells. This was carried out in unbuffered DMEM medium supplemented with 2.5 mM L-glutamine. ECAR values were sequentially obtained at baseline and following sequential stimulation with 15 mM glucose, 1 µM oligomycin A, and 50 mM 2-Deoxy-D-glucose. Glycolysis, glycolytic capacity, glycolytic reserve values were obtained using the Seahorse XF Glycolytic Stress Test Summary Report from Wave 2.6.1 software. Data were presented in mpH/min/µg protein.

3.7. Mitochondrial movement and displacement

MitoDsRed-transfected astrocytes or PCN were washed and incubated in 1 x ACSF, prepared by diluting 10 x ACSF in H_2O, supplemented with 1.5 mM $CaCl_2$ and 1.5 mM $MgCl_2$, and mitochondrial movement studies were carried out at 37 °C. Live imaging was performed using a 63x objective with NA=1.4 in the LSM980-Airy confocal microscope (Zeiss). Acquisitions were done with a pinhole aperture of 150 µm and

images taken every 5 sec for a total of 120 frames or every 10 sec for a total of 30 frames, for neurons or astrocytes, respectively. All images were corrected to fluorescence variations using Bleach Correction plugin developed by Miura and Rietdorf, and time lapse-dependent x-y drift applying the TurboReg plugin. In neurons, mitochondrial movement analysis was done using the Kymograph Macro in Fiji (Rietdorf and Seitz, 2004). ROIs were drawn using segmented line following mitochondria trajectory across projections. Kymographs were generated in an x-y dimension (distance, time) (López-Doménech et al., 2018) with minor modifications: mitochondrial network was thresholded and the area subtracted with the mitochondrial area of the previous timepoint (- 10 sec). The resultant area is the mitochondrial fraction that moved during the time between frames. This process was repeated for ten pairs of frames and averaged as a single displacement value.

3.8. Mitophagy events assessment in astrocytes

After 48 h of co-culture with neurons, astrocytes transfected with mt-Keima were washed and incubated in 1 x ACSF supplemented with 1.5 mM $CaCl_2$ and 1.5 mM $MgCl_2$. Then, live imaging was performed at 37 ºC to assess the number of mitophagy events in astrocytes. The z-stack images were taken on the LSM980-Airy confocal microscope using a 63x lens with NA=1.4%. Fluorescence was detected by using two different excitation wavelengths – 458 nm (green) and 561 nm (red) – and emission at 620 nm. The Fiji software was used to analyze the obtained images. Z-stack images were processed, and ROIs were designed in the resultant 3D reconstructions. A threshold was applied, and fluorescence was measured in both green and red channels. The ratio of the % area of red to green signal indicates the % of mitochondria localizing within the lysosome.

3.9. Evaluation of mitochondria in the CM

Astrocyte-neuron co-cultures were performed in 6-well plates, as described above. To evaluate the presence and health of mitochondria in the CM, 9 mL of CM, per condition, were collected 48 h after co-culture. The CM was centrifuged at 1,000 *xg* for 10 min to remove cell debris. Then, one of the following experiments were performed:

ATP measurement – after the first centrifugation of the CM, the supernatant was collected and centrifuged once again at 13,000 *xg* for 25 min, followed by a washing step with 1 mL of PBS. The resultant mitochondrial pellet was resuspended in 50 µL of PBS and added to an equal amount of the Cell Titer-Glo® reagent in a 96-well white plate.

Following incubation of 30 min at RT, the luminescence levels were measured in a plate reader (Tecan). ATP levels are normalized for the number of cells.

Mitochondria membrane potential measurement – following removal of cell debris, the supernatant was incubated with 1 µM JC-1 dye (ThermoFisher, Cat. no. T3168) for 30 min at 37 ºC. JC-1 is a commonly used dye to evaluate $\Delta\psi_m$ as it accumulates in mitochondria with healthy membrane potential. Accumulation inside the mitochondria results in the formation of JC-1 aggregates, which shifts the dye's fluorescence emission spectrum from 529 nm (green) to 590 nm (red). Thus, at the end of the incubation period, the CM was analyzed on a flow cytometer (BD Biosciences). To determine $\Delta\psi_m$ integrity, 488 nm excitation was applied to the sample using a PE-A filter, and the number of red fluorescent particles was counted. Carbonyl cyanide m-chlorophenyl hydrazone (CCCP) (Sigma Aldrich, Cat. no. C2920-10MG), which induces mitochondrial depolarization, was used as control.

Protein analysis – after the first centrifugation, the supernatant was centrifuged again at 13,000 *xg* for 25 min to pellet the mitochondria. The supernatant was then discarded, and the pellet was resuspended in 15 µL of RIPA buffer (150 mM NaCl, 50 mM Tris pH 7.5, 1 % Triton X-100, 0.5 % sodium deoxycholate, 0.1 % SDS) supplemented with 1:100 protease inhibitor cocktail (GBiosciences, Cat. no. 786-433) and phosphatase inhibitors (Promega, Cat. no. G8000). Samples were incubated on ice for 30 min and denatured with sample buffer (Li-Cor, Cat. no. 928-40004) for 5 min at 95 ºC. Western blotting was performed as described in section **3.13. Protein extracts and Western Blotting** and the membranes incubated with primary antibodies against TOM20, PDH and OxPHOS proteins (Table 2).

3.10. Mitochondrial endocytosis/phagocytosis

Astrocytes and PCN were plated separately in 6-well plates. At neuronal DIV13, the media from astrocytes was removed and the cells were incubated at 37 ºC for 30 min, with DMSO, 20 µM PitStop2 (Sigma Aldrich, Cat. no. SML1169-5MG), a clathrin-mediated endocytosis inhibitor, or 10 µM Cytochalasin D (CytoD) (Sigma Aldrich, Cat. no. C8273-1MG), an actin-mediated phagocytosis and endocytosis inhibitor, diluted in 500 µL neurobasal media as previously described (Peruzzotti-Jametti et al., 2021). During the incubation period, the CM from neurons was centrifuged at 1,000 *xg* for 10 min at RT to remove cell debris. The supernatant was recovered and treated with either DMSO or with the inhibitors at the previously indicated concentrations. 1.5 mL of the treated neuronal CM was added to the astrocytes and another incubation of 30 min at 37 ºC followed. 6 mL of CM were collected per condition, and ATP levels were measured as described in section **3.9. Evaluation of mitochondria in the CM**.

3.11. Assessment of mitochondrial engulfment by astrocytes and inclusion in the mitochondrial network or lysosomes

Astrocytes were plated in 10 mm MatTek dishes, while PCN were plated in 6-well plates. At DIV6, 6 mL of neuronal CM per condition was recovered and centrifuged at 1,000 *xg* for 10 min at RT. Then, the supernatant was incubated for 30 min at 37 ºC with 250 nM MitoTracker Orange (ThermoFisher, Cat. no. M7510) Following the incubation, the CM treated with MitoTracker Orange was centrifuged at 13,000 *xg* for 25 min at RT. The supernatant was then discarded and the mito-EVs pellet was resuspended in the appropriate volume of supplemented DMEM/F12 and added on top of the astrocytes. As a positive control, astrocytes were incubated for 30 min with CytoD (10 µM) to block endocytosis/phagocytosis of mito-EVs. Cells were incubated at 37 ºC for 1 h. Astrocytes were fixed with 4% PFA (Sigma Aldrich, Cat. no. 158127) for 15 min at RT. Immunocytochemistry and image analysis and acquisition proceed as described in **3.12. Immunocytochemistry** section. Anti-TOM20 or anti-LAMP1 primary antibodies were used to label mitochondrial network or lysosomes, respectively (Table 2).

3.12. Immunocytochemistry and image analysis

Cells were fixed using 4 % PFA in PBS for 15 min at RT. Then, 0.2% Triton X-100 (Sigma Aldrich, Cat. no. X100-1L) in PBS was added for 2 min to permeabilize the cells, followed by 1 h blocking period with 3 % Bovine Serum Albumin (BSA)/PBS (Sigma Aldrich, Cat. no. A6003). The cells were incubated overnight at 4 °C with primaries antibodies (Table 2) diluted in 3 % BSA/PBS solution. After three washing steps, the cells were incubated for 1 h at RT with the appropriate Alexa Fluor secondary antibodies (Table 2) diluted in 3 % BSA/PBS. Nuclei were stained using a 4 µg/mL Hoechst solution, prepared in PBS, and incubated for 15 min at RT. Lastly, the Antifade mounting media (VectaShield Plus, Cat. no. H-1900) was used to mount the coverslips. The z-stack images were acquired using a Plan-Apochromat/1.4NA 63x lens on Zeiss LSM880 or LSM980 confocal microscopes. Z-stack images were processed, and a 3D reconstruction was performed in the Fiji software. To evaluate mitochondrial morphology, a selected face of the 3D was thresholded to create a binary image that was further used to analyze mitochondrial area and aspect ratio. For evaluation of mitochondrial engulfment and integration in the astrocytic mitochondrial network, 3D reconstructions of the z-stack images acquired from the samples labelled for TOM20 were performed. Then, the total number of MitoTracker^{+} particles detected in astrocytes was counted and classified into three different subgroups – TOM20^{+}, TOM20^{-}, and surrounded by TOM20^{+} doughnut. For co-localization analysis, Mander's M2 coefficient was applied in z-stacked images.

Table 2 – List of primary and secondary antibodies.

Antibody	Species	Dilution	Category number	Brand
GFAP	Mouse	1:1 000	MAB360	Millipore
Iba1	Rabbit	1:150	09-19741	Wako
Kif5β	Rabbit	1:1000	ab167429	Abcam
LAMP1	Rat	1:200	ab25245	Abcam
LC3I/II	Rabbit	1:1000	38685	Cell Signaling Technology
MAP2	Chicken	1:1 000	ab5392	Abcam
Miro1	Rabbit	1:750	HPA010687	Sigma Aldrich
OxPHOS	Mouse	1:1000	ab110413	Abcam
Parkin	Mouse	1:200 (ICC) 1:1000 (WB)	sc-32282	Santa Cruz Biotechnology
PDH-E1α	Mouse	1:1000	sc-377092	Santa Cruz Biotechnology
p(Ser555)-ULK1	Rabbit	1:500	5869S	Cell Signaling Technology
p62	Rabbit	1:300	5114	Cell Signaling Technology
TOM20	Rabbit	1:200 (ICC) 1:1000 (WB)	sc-11415	Santa Cruz Biotechnology
Trak1	Rabbit	1:500	HPA005853	Sigma Aldrich
Trak2	Rabbit	1:500	HPA015827	Sigma Aldrich
β3-tubulin	Mouse	1:2500	80016	Santa Cruz Biotechnology
Alexa Fluor 488 anti-mouse	Mouse	1:500	A11001	Molecular Probes
Alexa Fluor 488 anti-rat	Rat	1:500	A21208	Invitrogen
Alexa Fluor 594 anti-chicken	Chicken	1:500	A32759	Invitrogen
Alexa Flour 594 anti-rabbit	Rabbit	1:500	A11012	Life Technologies
Alexa Fluor 633 anti-rabbit	Rabbit	1:500	A21071	Invitrogen
IRDye 800CW anti-mouse	Mouse	1:20 000	926-32212	Invitrogen
IRDye 800CW anti-rabbit	Rabbit	1:20 000	926-32213	Invitrogen

3.13. Protein extracts and western blotting

Cells were lysed using RIPA buffer supplemented with protease and phosphatase inhibitors to obtain total cellular extracts. Subsequentially, a benzonase solution (1 M Tris pH = 8.0, 0.5 M $MgSO_4$ and 1x benzonase (Millipore, Cat. no. 70664-10KUN)) was used to degrade nucleic acids. The cell lysate was incubated on ice for 30 min, followed by centrifugation of 5 min at 20,200 *xg* at 4 °C and the pellet, containing cell debris, was discarded. Protein concentration was determined by using the Pierce BCA Protein Assay Kit (ThermoFisher, Cat. no. 23225). Samples were denatured in sample buffer for 5 min at 95 ºC. 15-20 µg of protein were loaded into and separated on NuPAGE 4-12 % Bis-Tris gels (Invitrogen, Cat. no. NP0321BOX) in NuPAGE MES SDS running buffer (ThermoFisher, Cat. no. NP0002). For LC3I/II detection, NuPAGE 12% Bis-Tris gels were used (Invitrogen, Cat. no. NP0321BOX) in NuPAGE MOPS SDS running buffer (Invitrogen, Cat. no. NP0001). The ECL™ Rainbow™ Marker – Full Range (GE HealthCare, Cat. no. RPN800E) was used as the molecular marker. The proteins were transferred for 2 h to 0.45 µm nitrocellulose membranes (GE Healthcare, Cat. no. 10600002) and blocked for 1 h at RT with 5% BSA/TBS-T. Afterwards, the membranes were incubated overnight at 4 °C with the following primary antibodies (Table 2) diluted in 5% BSA/TBS-T: Kif5β, Trak1, Trak2, Miro1, OXPHOS, TOM20, PDH-E1α, p62, LC3I/II, Parkin, and p(Ser555)-ULK1. b3-tubulin was used as the loading control. The membranes were washed and then, incubated with the appropriate secondary antibodies (Table 2) diluted in 1 % BSA/TBS-T for 1 h at RT. The Odyssey CLx Imaging System (LI-COR Biosciences) was used to develop the membranes and the Image Studio software (LI-COR Biosciences) was used for protein levels quantification.

3.14. RNA extraction and real-time PCR (qPCR)

Astrocyte-neurons co-cultures were established as described above and, after 48h of co-culture, RNA was extracted from astrocytes using the RNeasy® Mini Kit (Qiagen, Cat. no. 74104) by following the manufacturer's instructions. RNA concentration was determined using the Nanodrop 2000 spectrophotometer (Thermo Scientific) and the RNA integrity was confirmed by A260/280 > 1.9. Then, RNA was diluted to a final concentration of 10 ng/µL and converted into cDNA using the High-Capacity cDNA Reverse Transcription Kit (Applied Biosystems, Cat. no. 4368814). The reaction was carried out in the S1000 thermocycler (Bio-Rad) with the following steps: 10 min at 25°C, 120 min at 37°C and 5 min at 85°C. qPCR was performed using the TaqMan™ Fast Advanced Master Mix (Applied Biosystems, Cat. no. 4444557) with the

primers listed in table 3 and run in the Applied Biosystems™ 7500 fast qPCR system. Actin was used as the housekeeping gene. Results are expressed as double delta Ct values (ΔΔCt) using WT astrocytes as control.

3.15. Lactate Dehydrogenase (LDH) release assay

LDH assay is commonly used to study cellular cytotoxicity. When the plasma membrane is disrupted, such as during necrosis, the cytosolic enzyme LDH is released into the cell culture medium. LDH release was assessed using a commercially available colourimetric assay (Promega, Cat. no. G1780) according to the manufacturer's instructions. Neurons and astrocytes were plated in 96-well plates. As a positive control, a few wells were incubated with 10 µL of lysis buffer 1 h prior to assay, to induce maximum LDH release. Cell media was collected to a clean 96-well plate and each well was further incubated with 50 µl of the CytoTox 96 reagent for 30 min at room temperature and protected from light. Absorbance was recorded at 492 nm and data normalized to protein levels.

3.16. Synaptic mitochondria quantification by transmission electron microcopy (TEM)

Three to four months-old animals were anaesthetized and perfused with 2% glutaraldehyde and 1% formaldehyde in 0.1 phosphate buffer solution through intracardial perfusion. Brains were stored in fixing solution until hemispheres were cut in a brain slicer matrix and coronal slices collected for sectioning. Leica Ultracut UCT was used to create ultrathin sections, and uranyl acetate and lead citrate were used as contrasting agents. Sections were examined at 100 kV using a Tecnai 12 BioTWIN transmission electron microscope. Digital images were acquired from the hippocampus *Cornu Ammonis* area 1 (CA1) at a primary magnification of 30,000 x. Ten different cells were snapped per brain and 30 to 40 synapses were analyzed per condition. A synapse was considered when the presence of both synaptic vesicles and post-synaptic density were detected.

3.17. Statistical analysis

Data were analyzed using GraphPad Prism 8.00 (GraphPad software). Data did not follow a normal distribution, hence a non-parametric independent test (Mann-Whitney U-test) was used to compare pairs of samples. For multiple sample comparisons, the Kruskal-Wallis test was applied. The existence of outliers was evaluated using the ROUT (Q=1%) method and excluded when identified. All values are shown as mean ± standard error of the mean (SEM), n = corresponds to number of

independent experiments or number of individual cells/animals, ns = non-significant, * $p \leq 0.05$, ** $p \leq 0.01$, *** $p \leq 0.001$, **** $p \leq 0.0001$. Statistical significance was considered when $p \leq 0.05$.

Table 3 – List of primers.

Gene	Description	Species	Category number	Brand
Actb	Actin beta	Mouse	Mm02619580_g1	Applied Biosystems
Ambra1	Autophagy and Beclin 1 Regulator 1	Mouse	Mm00554370_m1	Applied Biosystems
Atp5k	ATP synthase, H+ transporting, mitochondrial F1F0 complex, subunit E	Mouse	Mm00833200_g1	Applied Biosystems
ATP8	ATP synthase F0 subunit 8	Mouse	Mm04225236_g1	Applied Biosystems
Atp5k	ATP synthase, H+ transporting, mitochondrial F1F0 complex, subunit E	Mouse	Mm00833200_g1	Applied Biosystems
Fundc1	FUN14 Domain Containing 1	Mouse	Mm00511132_m1	Applied Biosystems
Kif5b	Kinesin Family Member 5 beta	Mouse	Mm00515276_m1	Applied Biosystems
Park2	Parkinson disease (autosomal recessive, juvenile) 2, parkin	Mouse	Mm00450186_m1	Applied Biosystems
Pink1	PTEN induced putative kinase 1	Mouse	Mm00550827_m1	Applied Biosystems
Ppargc1a	Peroxisome proliferator-activated receptor gamma coactivator 1-alpha (PGC-1α)	Mouse	Mm01208835_m1	Applied Biosystems
Rhot1	ras homolog gene family, member T1; Miro1	Mouse	Mm01304158_m1	Applied Biosystems
Rhot2	ras homolog gene family, member T2; Miro2	Mouse	Mm00524478_m1	Applied Biosystems
Tfam	Mitochondrial transcription factor A	Mouse	Mm00447485_m1	Applied Biosystems

4. RESULTS

4.1. Bioenergetic parameters are unaffected in *App*$^{NL-G-F}$ cultures

Mitochondrial dysfunction is a common feature of AD (Cenini & Voos, 2019). The use of *App* KI models for AD research has been gaining supporters, however, bioenergetic alterations have not been characterized so far. Therefore, we isolated PCN and astrocytes from *App*$^{NL-G-F}$ mouse embryos and age-matched WT controls to evaluate the presence of bioenergetic impairment.

Firstly, we assessed $\Delta\psi_m$ integrity in WT and *App*$^{NL-G-F}$ PCN using $TMRM^+$, a positively charged probe, which accumulates in mitochondria depending on its membrane potential. The more negative $\Delta\psi_m$ is, the more the probe accumulates, and the brighter the fluorescence will be when in non-quenching conditions. Confocal images revealed the presence of healthy mitochondria, as indicated by intense TMRM fluorescence, in the soma and neurites of WT and *App*$^{NL-G-F}$ neurons alike (Figure 6a). TMRM fluorescence quantification further indicated that WT and *App*$^{NL-G-F}$ PCN have no differences in $\Delta\psi_m$ ($p = 0.4824$) (Figure 6b). Neuronal mitochondrial function was also evaluated by measuring ATP levels in cells cultured in pyruvate-based media to favour OXPHOS-derived ATP, rather than from glycolysis. Consistently with TMRM data, mitochondrial ATP levels did not seem to be affected in PCN obtained from *App*$^{NL-G-F}$ mice, when compared to WT ($p = 0.4841$) (Figure 6c).

Bioenergetics in astrocytes was evaluated recurring to the Seahorse XF Analyzer. Mitochondrial respiration in these cells was evaluated by measuring OCR (Figure 6d). We found that WT and *App*$^{NL-G-F}$ astrocytes had no differences in basal and maximal respiration, mitochondrial complex V-derived ATP production, and spare respiratory capacity (SRC) (Figure 6e-f). Additionally, ECAR measurements provided data on glycolytic function (Figure 6g). Glycolysis, glycolytic capacity, and glycolytic reserve also remained unchanged in *App*$^{NL-G-F}$ astrocytes, relatively to WT (Figure 6h-i).

This data indicates that both neuronal and astrocytic *App*$^{NL-G-F}$ cultures preserve bioenergetic function, unlike what has been described for other AD models (Dematteis et al., 2020b; Hauptmann et al., 2009).

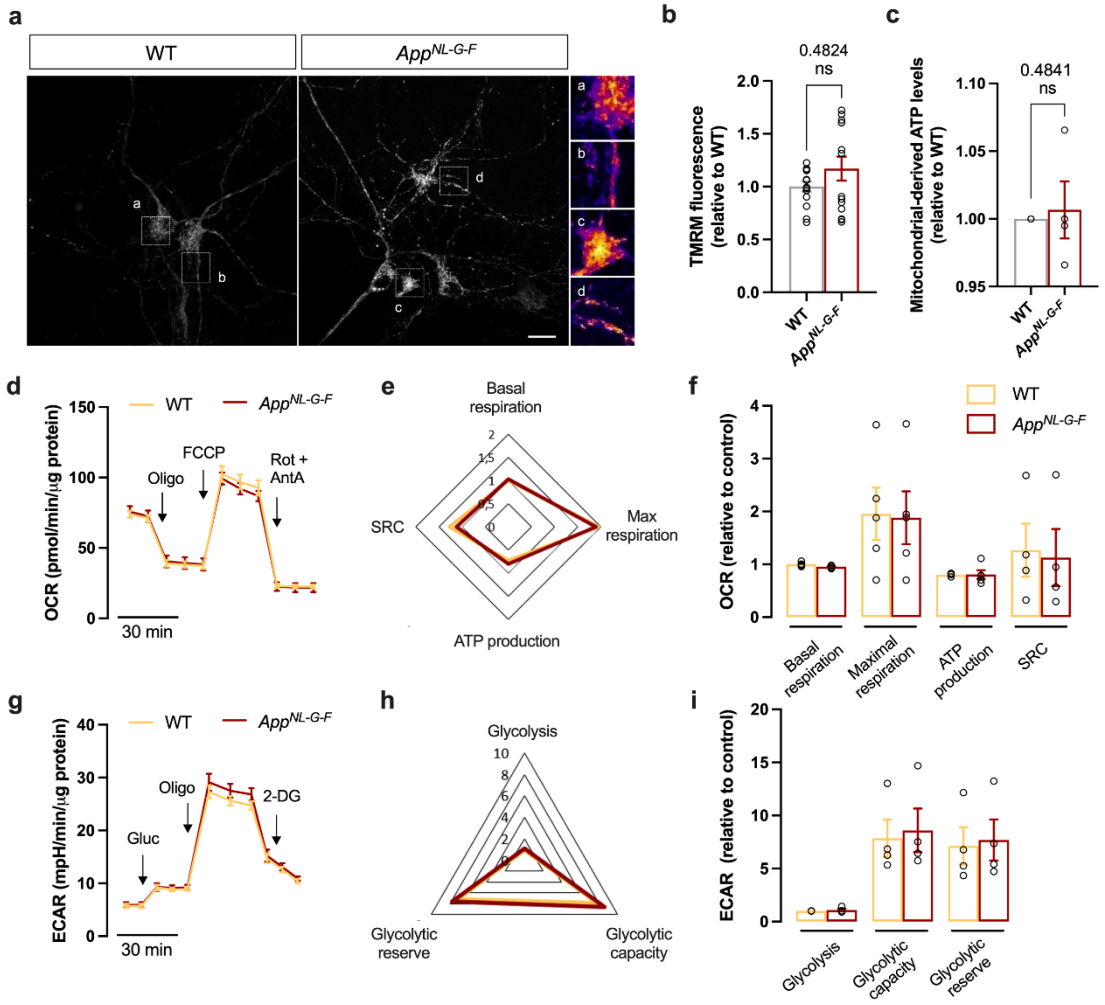

Figure 6 – Bioenergetic profile of App^{NL-G-F} PCN and astrocytes. (a) Representative confocal images showing TMRM fluorescence in WT and App^{NL-G-F} PCN. Neurons were incubated with 10 nM TMRM for 30 min at 37 °C. Scale bar=40 µm. **(b)** TMRM fluorescence quantification standardized to WT (n=14 cells from 3 independent cultures). **(c)** Quantification of mitochondrial ATP levels in neurons incubated, for 1 h, in pyruvate supplemented medium without glucose. Results are normalized to WT (n=5). **(d)** Mitochondrial respiration in WT and App^{NL-G-F} primary astrocytes following sequential injection of oligomycin (Oligo, 1 µM), FCCP (1 µM), and rotenone + antimycin A (Rot + Ant A, 0.5 µM each), as shown by representative traces of OCR. **(e)** Radar chart represents the fold-increase of OCR parameters relatively to basal respiration of WT astrocytes. **(f)** Quantification of OCR parameters retrieved from the Seahorse XF Cell Mito Stress Test and normalized to WT (n=4-6). **(g)** ECAR traces representing glycolytic activity in WT and App^{NL-G-F} astrocytes after sequential injection of glucose (15 mM), Oligo (1 µM), and 2-deoxy-D-glucose (2-DG, 50 mM). **(h)** Spider chart exhibiting variations in ECAR parameters relatively to glycolysis of WT astrocytes. **(i)** Quantification of ECAR parameters retrieved from the Seahorse XF Glycolytic Stress Test and normalized to WT (n=4). Data presented as mean ± SEM. ns = non-significant

4.2. Dysfunction of mitochondrial movement in *App^{NL-G-F}* neurons

Mounting evidence indicates mitochondrial transport is highly compromised in AD (Reddy et al., 2012). Adequate mitochondrial transport is vital to meet variations in metabolic demands and maintain cellular homeostasis. Hence, we sought to determine

whether mitochondrial distribution is altered in neurons and astrocytes from the *App*$^{NL-G-F}$ KI mouse model.

First, we recorded the movement of mitoDsRed-labelled mitochondria in neurites from WT and *App*$^{NL-G-F}$ PCN, for 10 minutes. Analysis of the obtained kymographs (Figure 7a) revealed a significant decrease in the number of motile mitochondria in the KI neurons, relatively to WT ($p = 0.0049$) (Figure 7b). Further analysis of the motile mitochondria showed that mitochondrial anterograde transport was severely decreased and significantly slower in *App*$^{NL-G-F}$ neurons, compared to WT cells ($p = 0.0003$ and $p \leq 0.0001$, respectively), while retrograde transport remained unchanged (Figure 7c-d). We then asked whether compromised mitochondrial anterograde transport would reflect alterations of the pre-synaptic mitochondrial pool. To investigate this, we imaged brain slices from 4 months old early-symptomatic *App*$^{NL-G-F}$ mice. Indeed, we found a significant reduction in the number of mitochondria at the pre-synaptic terminal of *App*$^{NL-G-F}$ mice ($p = 0.0137$) (Figure 7e-f).

We then assessed mitochondrial movement in astrocytes, as little is known about mitochondrial dynamics in this cell type. WT and *App*$^{NL-G-F}$ astrocytes were transfected with mitoDsRed to label mitochondria and sequential images were obtained to quantify mitochondrial displacement, i.e., the percentage of mitochondria that changed their position over 30 seconds, represented in cyan in Figure 7g. In contrast to neurons, astrocytes showed no changes in mitochondrial movement ($p = 0.8467$) (Figure 7h).

Finally, we investigated if changes in the protein expression of mitochondrial transport machinery could be underlying the alterations observed in mitochondrial movement in *App*$^{NL-G-F}$ neurons. Remarkably, immunoblots of WT and *App*$^{NL-G-F}$ extracts revealed no differences in the levels of mitochondrial transport proteins in both neurons and astrocytes (Figure 7i-j).

Altogether, this data indicates mitochondrial anterograde transport is highly defective in *App*$^{NL-G-F}$ neurons, possibly resulting in a decrease of the pool of pre-synaptic mitochondria at the early stages of the disease. Mitochondria are indispensable organelles at the pre-synapse, performing crucial roles during synaptic activity (Devine & Kittler, 2018). These findings may account for the early synaptic dysfunction that originates in pre-synaptic terminals observed in this AD model (Hark et al., 2021). However, further investigation would be needed to sustain this hypothesis.

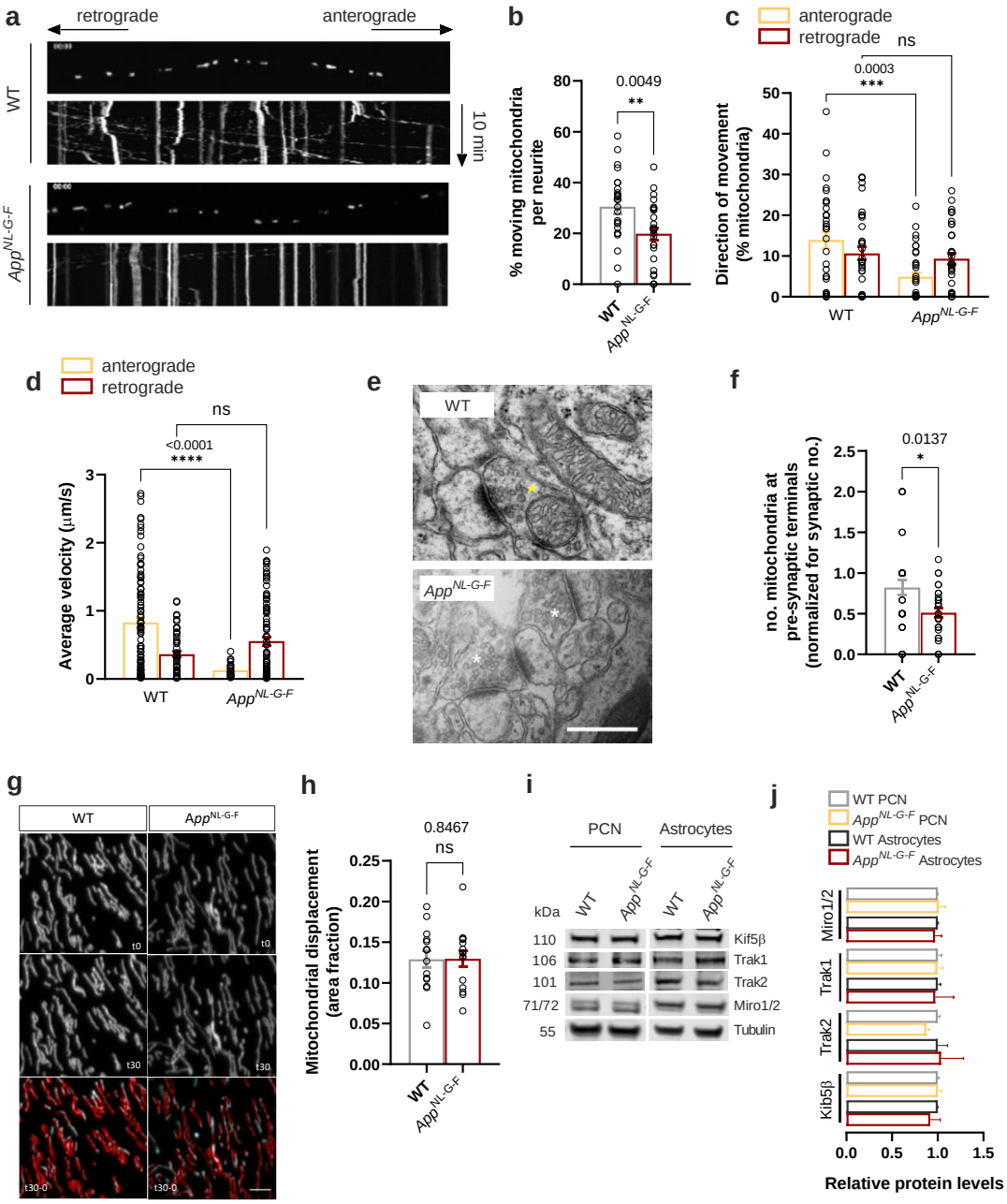

Figure 7 – Mitochondrial movement is impaired in App^{NL-G-F} neurons, but not in astrocytes. (a) Representative kymographs (xx, distance vs yy, time) of mitochondrial transport in mitoDsRed-transfected WT and App^{NL-G-F} neurons were recorded over a period of 10 min. **(b)** % of motile mitochondria per neurite, **(c)** % of mitochondria moving anterogradely or retrogradely, and **(d)** average velocity (µm/s) of movement obtained through the analysis of kymographs (n=26-27 neurites from 4 independent cultures). **(e)** Representative TEM images showing mitochondria at the pre-synaptic terminal in the brain of 4 months old WT and App^{NL-G-F} mice. * indicates pre-synaptic terminals containing SV; yellow: with mitochondria, white: without mitochondria. Scale bar=500 nm. **(f)** The bar graph shows quantification of the number of mitochondria at the pre-synapse standardized to the number of synapses (n=27-40 analysed synapses from 4 mice). **(g)** Confocal images depicting mitochondrial displacement in MitoDsRed-transfected WT and App^{NL-G-F} astrocytes. Scale bar=8 µm **(h)** Quantification of the average area of mitochondrial displacement (n=14-15 cells from 4 independent cultures). **(i)** Representative immunoblots of whole-cell extracts from WT and App^{NL-G-F} neurons and astrocytes. Blots were incubated with antibodies against the indicated mitochondrial transport proteins and β-tubulin was used as the loading control. **(j)** Bar graph showing mitochondrial transport machinery protein levels normalized to β3-tubulin (n=5-7). Data presented as mean ± SEM. * $p \leq 0.05$, ** $p \leq 0.01$, *** $p \leq 0.001$, **** $p \leq 0.0001$. ns=non-significant.

4.3. Altered transcriptomic profile in astrocytes co-cultured with neurons

Despite normal levels of ATP in *App*$^{NL-G-F}$ PCN, the observations that mitochondrial anterograde transport is impaired and that the number of pre-synaptic mitochondria is decreased at early stages of the disease, suggest that ATP deficiency may occur at specific cellular compartments where energy requirements are higher, as the synapse, leading to neuronal stress. Astrocytes, in turn, support several neuronal functions by exchanging metabolites, neurotransmitters and even mitochondria, as recently described (Hayakawa et al., 2016; Sofroniew & Vinters, 2010). Although the signals that trigger mitochondrial transfer between these cells are not understood, we theorized that transcriptomic remodelling would be necessary to support neuronal functions.

We established different co-culture conditions, as depicted in Figure 8a, and performed real-time PCR (qPCR) to look at differential gene expression of mitochondria-related genes in WT and *App*$^{NL-G-F}$ astrocytes across the different conditions. Astrocyte treatment with rotenone, an inhibitor of complex I of the ETC, was used to induce mitochondrial stress and, thus, ensure AD phenotype specificity of the obtained results. We found that WT astrocytes in co-culture with either WT or *App*$^{NL-G-F}$ neurons upregulate the gene coding for KIF5β, an important regulator of the mitochondrial anterograde transport. On the other hand, *App*$^{NL-G-F}$ astrocytes cultured alone showed severe downregulation of all the genes involved in mitochondrial transport, despite no changes in mitochondrial displacement. The most remarkable transcriptional alteration was observed in *App* KI astrocytes co-cultured with WT PCN, with an upregulation of all mitochondrial movement and biogenesis genes analysed, while co-culture with *App*$^{NL-G-F}$ PCN maintained gene expression at low levels (Figure 8b). The mitochondrial-encoded *mt-Atp8* gene was downregulated across all conditions (Figure 8b), indicating a possible effect on mtDNA, that is not specifically induced by Aβ since rotenone itself induces *mt-Atp8* downregulation without affecting ATP production or cellular viability (Figure S3). Mitochondrial biogenesis-related genes were highly downregulated in WT astrocytes-WT PCN co-cultures. Interestingly, in *App*$^{NL-G-F}$ astrocytes co-cultured with neurons an upregulation of the major mitochondrial transcription factor *Tfam* was observed, when compared to *App*$^{NL-G-F}$ astrocytes cultured alone (Figure 8b). Furthermore, no differences were observed in *Ppargc1a* expression levels in *App*$^{NL-G-F}$ astrocytes co-cultured with WT astrocytes, relatively to *App*$^{NL-G-F}$ cultured alone, while co-culture with *App*$^{NL-G-F}$ PCN resulted in downregulation of this gene (Figure 8b).

Collectively, these findings suggest that astrocytes in co-culture with neurons can shape their mitochondrial-related transcriptome to assist neighbouring neurons.

However, *App*$^{NL-G-F}$ astrocytes co-cultured with *App*$^{NL-G-F}$ neurons presented gene downregulation suggesting that neuron-astrocyte communication can be impaired.

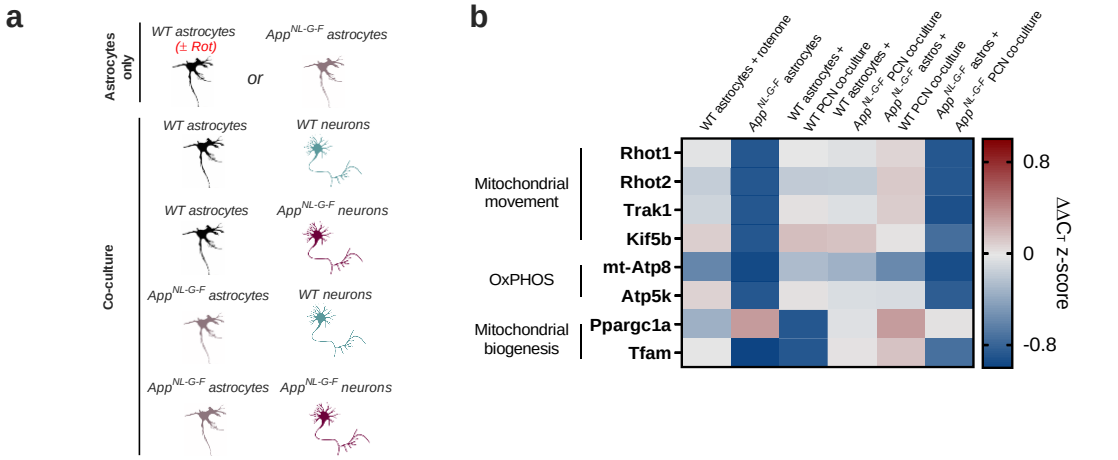

Figure 8 – Transcriptomic changes in astrocytes when in co-culture with neurons. (a) Schematic representation of the study conditions. **(b)** Heatmap presents the expression levels of mitochondrial transport, oxidative phosphorylation (OxPHOS), and mitochondrial biogenesis-related genes in astrocytes from the indicated conditions. Results are normalized to the WT astrocytes only condition. Red indicates upregulation, while blue indicates downregulation. β-actin was used as the housekeeping gene. Rotenone (10 nM) treatment was performed for 24 h (n=2-9). Data presented as mean ± SEM.

4.4. EVs containing functionally intact mitochondria are released from PCN and captured by astrocytes through actin-dependent mechanisms

It has been previously reported that astrocytes can improve neuronal function by transferring healthy mitochondria to stressed neurons (Hayakawa et al., 2016). Here we have shown deficits in mitochondrial transport in *App*$^{NL-G-F}$ PCN, which could underlie synaptic deficits, and increased expression of mitochondrial transport-related genes in astrocytes co-cultured with neurons. Hence, we next studied if, in our model, mitochondrial transfer occurs between neurons and astrocytes.

Both TNTs and EVs have been described as mediators of intercellular mitochondrial transfer (Torralba et al., 2016). Here, we decided to explore mitochondrial transfer via release of mito-EVs to the CM. Mito-EVs were isolated from the CM of astrocytes, PCN and astrocytes-PCN co-cultures by following the experimental setup depicted in Figure 9a. Then, mitochondrial presence in the CM and their structural and functional integrity were determined by analysis of protein content, $\Delta\psi_m$ and ATP levels measurement.

Immunoblots revealed the presence of OMM, IMM and mitochondrial matrix proteins in EVs collected from the CM (Figure 9b). Since the samples were heated at 95 °C before gel running, the heat-sensitive complex IV of the ETC is not visible. This data, particularly the presence of the matrix proteins PDH and SDHB, a protein that links glycolysis to the TCA cycle and a subunit of complex II of the ETC, respectively, suggests

that cells may release structurally intact mitochondria to the CM. Further analysis of mito-EVs using electron microscopy will be needed to confirm this assumption. Interestingly, protein levels were the highest in CM derived from PCN cultures, decreasing in CM recovered from the co-cultures, while in WT astrocytes' CM no proteins were detected (Figure 9b).

To evaluate if released mitochondria retained functionality, CM recovered from co-cultures was incubated with JC-1 for 30 min, and then analysed by flow cytometry. JC-1 is a fluorescent cationic dye that accumulates in mitochondria with high $\Delta\psi_m$, forming aggregates that emit red fluorescence. Upon loss of $\Delta\psi_m$, JC-1 exits the mitochondria, and its fluorescence shifts from red to green. Flow cytometry results indicate that the released mitochondria maintain a healthy membrane potential, as shown by the number of red fluorescent particles detected in the study condition (green trace) (Figure 9c). CCCP-induced mitochondrial depolarization (red trace) reduced the number of red particles detected, while no red particles were identified in fresh media incubated with the dye (black trace), thus ensuring the specificity of the signal.

We further evaluated ATP levels using a luminescence-based assay in mitochondrial-enriched pellets isolated from the CM. Accordingly, with the results obtained from western blotting (Figure 9b), we observed very low ATP levels in both WT and *App*$^{NL-G-F}$ astrocyte-derived CM, while WT and *App*$^{NL-G-F}$ neuronal CM exhibited similar high ATP levels (Figure 9d). ATP levels were significantly decreased when WT PCN were co-cultured with WT astrocytes, as compared to WT neurons cultured alone ($p = 0.0282$). The same tendency was observed between the conditions WT PCN only and *App*$^{NL-G-F}$ astrocytes co-culture with WT PCN, although not significant ($p = 0.0658$) (Figure 9d). Decreased ATP levels were further observed in WT or *App*$^{NL-G-F}$ astrocytes co-cultured with *App*$^{NL-G-F}$ PCN, when compared to *App*$^{NL-G-F}$ PCN cultured alone, however, these differences were also not significant ($p = 0.2536$ and $p = 0.3276$, respectively). Another interesting finding relates to the fact that ATP levels were significantly increased in WT and *App*$^{NL-G-F}$ astrocyte co-cultures with *App*$^{NL-G-F}$ neurons, in comparison with astrocytes from both phenotypes in co-culture with WT neurons ($p = 0.0145$ and $p = 0.0423$, respectively) (Figure 9d). Hence, the aforementioned results collectively suggest that neurons, instead of astrocytes, release high amounts of functionally intact mitochondria in EVs, which might be captured by astrocytes in co-culture as lower extracellular ATP is detected. Additionally, astrocytes appear to have decreased ability to uptake *App*$^{NL-G-F}$ PCN-derived mito-EVs, in comparison with WT mito-EVs.

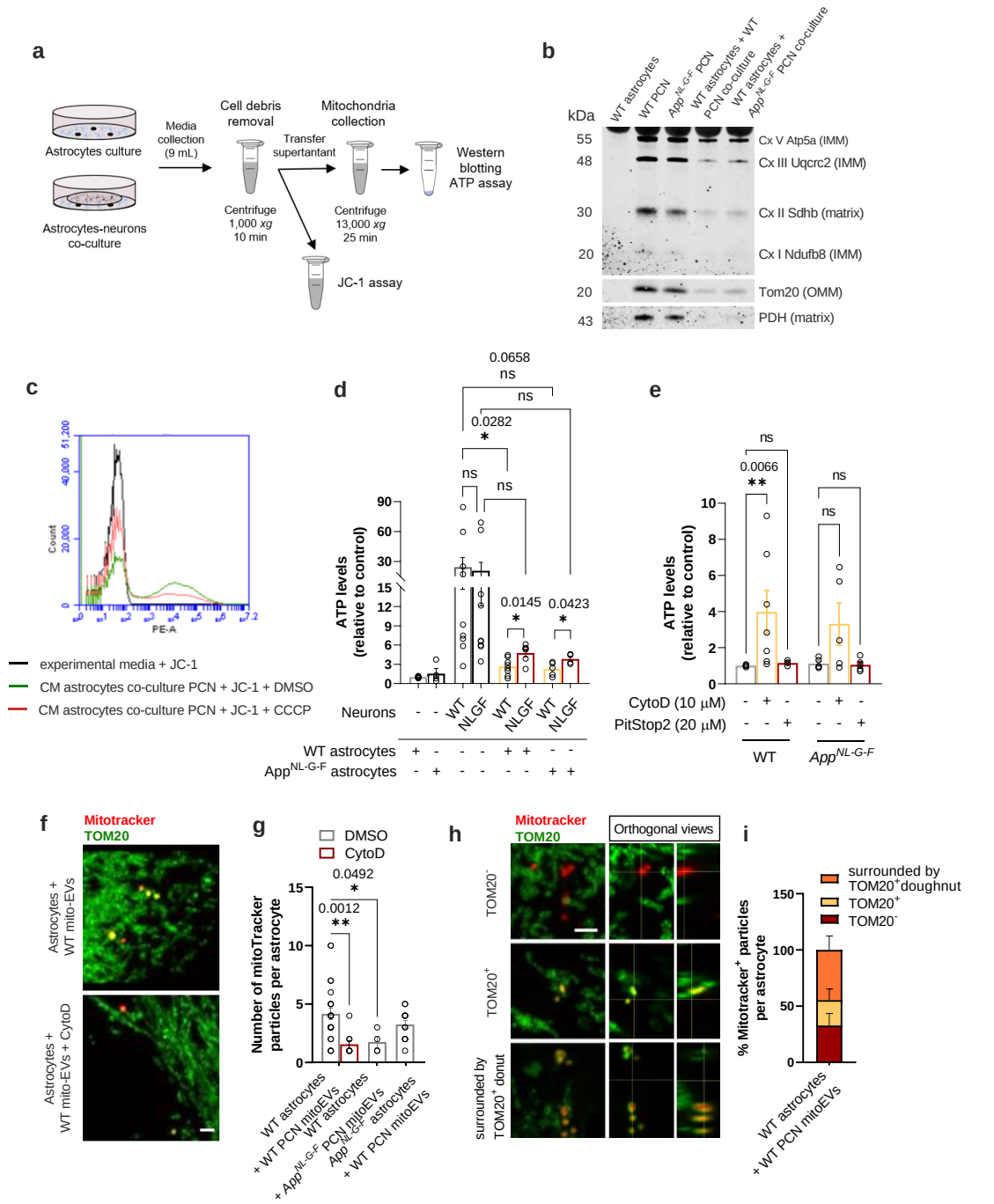

Figure 9 – Astrocytes in co-culture uptake neuronal-derived mito-EVs. (a) Experimental setup for mito-EVs isolation from the conditioned media (CM). **(b)** Representative immunoblots of mitochondrial-enriched pellets obtained from CM recovered from the indicated conditions. Blots were incubated with antibodies against ETC complexes subunits, TOM20, and PDH. **(c)** Flow cytometry results showcase the number of particles positive for JC-1 red fluorescence as a measure of $\Delta\psi_m$ of mitochondria in the CM. **(d)** The bar graph shows ATP levels quantification of mitochondrial-enriched pellets isolated from CM collected from the indicated conditions. Results are standardized to WT astrocytes (n=3-12). **(e)** Quantification of extracellular ATP levels in CM from WT or App^{NL-G-F} PCN previously added to astrocytes for 30 min. Cytochalasin D (cytoD, 10 µM) and PitStop2 (20 µM) were used as actin and clathrin-mediated endocytosis/phagocytosis inhibitors, respectively. Results are standardized to WT controls (n=4-8). **(f)** Representative confocal images showing MitoTracker$^+$ particles (in red) in astrocytes. TOM20 (in green) was used to label mitochondrial network. Scale bar=2.6 µm. **(g)** The bar graph indicates the number of MitoTracker$^+$ particles per astrocyte (n=9-24 cells from 2-3 independent cultures). **(h)** Representative confocal images showing three different populations of MitoTracker-labelled particles captured by astrocytes. Scale bar=2 µm. **(i)** Bar graph indicates

the percentage of each population of MitoTracker^{+} particle per astrocyte (n=12 cells from 2 independent cultures). Data presented as mean ± SEM. * $p \leq 0.05$, ** $p \leq 0.01$.

To test the hypothesis that astrocytes are indeed taking up mito-EVs released by neurons, we incubated WT astrocytes with either WT or *App*$^{NL-G-F}$ PCN-derived CM and used two mechanistically different compounds – cytoD, which inhibits actin polymerization (MacLean-Fletcher & Pollard, 1980), and PitStop2, a clathrin inhibitor (Von Kleist et al., 2011) – to block endocytosis/phagocytosis in astrocytes. We found that WT astrocytes incubated with WT PCN CM treated with cytoD had significantly increased ATP levels in the CM, relatively to the untreated condition ($p = 0.0066$) (Figure 9e), revealing that actin-dependent mechanisms mediate mito-EVs engulfment by astrocytes. A tendency for ATP levels to increase upon cytoD treatment of WT astrocytes incubated with *App*$^{NL-G-F}$ neurons CM, compared to the untreated condition, was also observed, even though this was not significant. Additionally, PitStop2 treatment showed no effects in the amount of ATP levels found in the CM, compared to the controls (Figure 9e).

We then looked for visual confirmation of neuronal mitochondria engulfment by astrocytes. For this, we collected CM from PCN and incubated it with MitoTracker Orange to label mitochondria. MitoTracker-labelled mitochondria were further isolated from the CM and added to astrocytes for 1 h. Preliminary data revealed the presence of MitoTracker labelled particles inside astrocytes (Figure 9f). Treatment with cytoD considerably decreased the number of detected particles (Figure 9g). No changes were observed in the number of engulfed WT PCN-derived particles between WT or *App*$^{NL-G-F}$ astrocytes, however, decreased number of *App*$^{NL-G-F}$ PCN-derived particles were engulfed (Figure 9g), confirming previous data (Figure 9d). Furthermore, we observed that while some of these particles were TOM20^{-} and did not seem to integrate the astrocytic mitochondrial network, other particles were TOM20^{+}, presenting yellow fluorescence, and appeared to be integrated within the host's mitochondrial network, as observed in the depicted z-stack orthogonal views (Figure 9h, i). A third population of MitoTracker-labelled particles, representing about half of the detected particles, was found surrounded by TOM20^{+} doughnuts (Figure 9g, i). We hypothesize these particles were in the process of integrating the mitochondria network when the samples were fixed, although additional time-dependent experiments would be needed to confirm this finding. Taken together, these results provide evidence that astrocytes uptake mitochondria released by PCN in an actin-dependent mechanism and only a portion of these mitochondria integrate their mitochondrial network. On the other hand, under our

experimental setup is unlikely that astrocytes transfer mitochondria to neurons through mito-EVs.

4.5. A fraction of the neuronal mitochondria are targeted to mitophagy following engulfment by WT astrocytes

So far, we have observed that astrocytes engulf neuronal-derived mitochondria, but only a part of these seems to integrate the host's mitochondrial network. Different reports have indicated that astrocytes degrade mitochondria released by neurons (C. H. O. Davis et al., 2014; Morales et al., 2020). Therefore, we hypothesized that a population of neuronal mitochondria taken up by astrocytes might undergo transmitophagy and that this process could be impaired in this AD model, contributing to the pathology.

Firstly, we used mt-Keima to determine alterations in the number of mitophagy events in astrocytes in the presence or absence of neurons (Figure 10a). This pH-sensitive mitochondria-targeted construct is ideal to study mitophagy as it gradually shifts its excitation wavelength from green to red, upon sensing the acidic environment of the lysosome. Despite no alterations in bioenergetic parameters, we observed *App*$^{NL-G-F}$ astrocytes display decreased mitophagy ($p = 0.0535$). Interestingly, preliminary data indicates that both WT and *App*$^{NL-G-F}$ astrocytes in co-culture show a tendency to increase mitophagy, in comparison with astrocytes cultured alone (Figure 10a, b). A significant increase in mitophagy events was also observed with the mitochondrial uncoupler FCCP ($p = 0.0122$), as loss of $\Delta\psi_m$ triggers mitochondria elimination, validating the assay.

Considering the previous results, we then sought out to specifically determine if captured mitochondria would undergo degradation. We used MitoTracker Orange to label mitochondria in CM from WT and *App*$^{NL-G-F}$ PCN. Then, labelled mito-EVs were added to astrocytes culture and co-localization analysis between MitoTracker and LAMP1, a lysosomal protein, was performed in astrocytes (Figure 10c). Interestingly, we observed higher immunoreactivity of LAMP1 surrounding mito-EVs, clearly depicted in the inserts in Figure 10c. Using Mander´s overlap coefficient we found that in WT astrocytes, similar amounts of the engulfed WT and *App*$^{NL-G-F}$ mitochondria co-localized with the lysosome. Furthermore, WT and *App*$^{NL-G-F}$ astrocytes showed no differences in WT PCN-derived mitochondria co-localization with the lysosomes (Figure 10c, d).

We further enquired which mitophagy-related cascade would be involved in the observed increase of transmitophagy events. Therefore, we started by assessing alterations in mRNA levels of mitophagy-related genes. qPCR data revealed an upregulation of *Fundc1* and *Ambra1*, involved in receptor-mediated mitophagy, in WT

astrocytes co-cultured with WT or *App*$^{NL\text{-}G\text{-}F}$ neurons, as well as in *App*$^{NL\text{-}G\text{-}F}$ astrocytes-WT neurons co-cultures, relatively to control (Figure 10e).

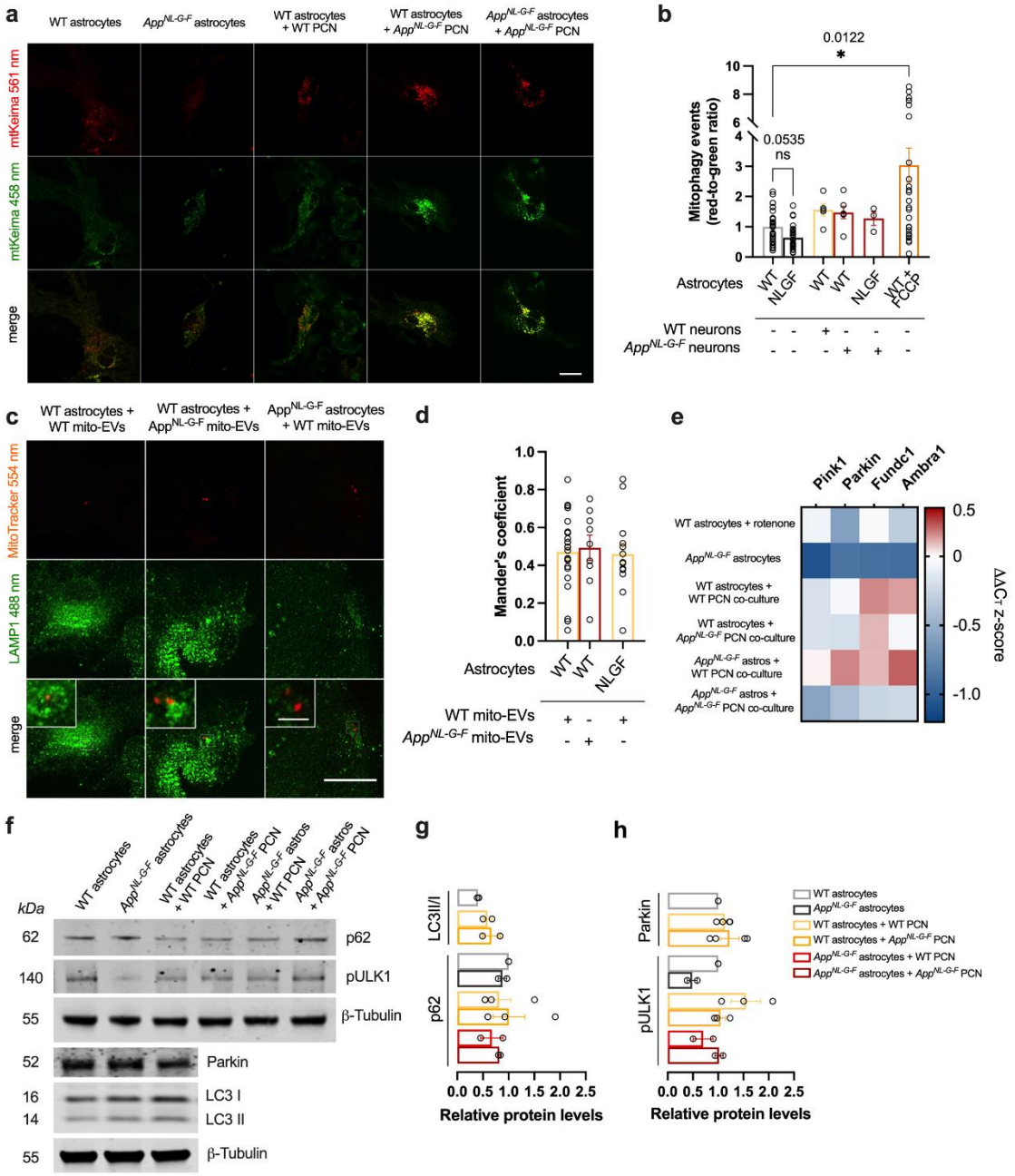

Figure 10 – Neuronal mitochondria undergo mitophagy in WT astrocytes. (a) Representative confocal images showing mt-Keima transfected WT and App$^{NL\text{-}G\text{-}F}$ astrocytes in the presence or absence of neurons. Scale bar=20 µm. **(b)** The bar graph indicates the number of mitophagy events in astrocytes from the indicated conditions as determined by red-to-green ratio quantification (n=26-30 cells from no co-culture conditions; n=5-6 cells from co-culture conditions, 2-4 independent cultures). **(c)** Representative confocal images of MitoTracker (red) and LAMP1 (green) co-localization in WT astrocytes incubated with WT or App$^{NL\text{-}G\text{-}F}$ neuronal mito-EVs. Scale bar=20 µm; insert=3 µm. **(d)** Mander's coefficient indicating MitoTracker-LAMP1 co-localization in WT astrocytes from the indicated conditions (n=9-23 cells from 3 independent cultures). **(e)** Heatmap presents mRNA levels of mitophagy-associated genes in astrocytes from the indicated conditions. Results are normalized to WT astrocytes only conditions. Red indicates upregulation and blue represents downregulation. The housekeeping gene used was β-actin. Rotenone (10 nM) treatment was performed for 24 h (n=2-5). (**f**) Representative immunoblots of whole-cell extracts from WT or App$^{NL\text{-}G\text{-}F}$ astrocytes from the indicated conditions. Immunoblots were incubated with antibodies against autophagy

and mitophagy proteins. β3-tubulin was used as the loading control. **(g)** Expression levels of the autophagy proteins LC3I, LC3II, and p62 (n=2-3 independent cultures). **(h)** Expression levels of mitophagy proteins Parkin and pULK1 (n=2-4 independent cultures). Data presented as mean ± SEM. * $p \leq 0.05$.

In contrast, these conditions showed no alterations in mRNA levels of the genes involved in PINK1-Parkin-dependent mitophagy investigated, apart from the *App*$^{NL-G-F}$ astrocytes-WT neurons co-culture, which showed increased *Parkin* expression. We further observed that *App*$^{NL-G-F}$ astrocytes alone or co-cultured with *App*$^{NL-G-F}$ neurons presented downregulation of all mitophagy-related genes studied, compared to WT astrocytes (Figure 10e), suggesting these cells may display deficient elimination of mitochondria, corroborating mtKeima results (Figure 10b). Interestingly, when co-cultured with *App*$^{NL-G-F}$ neurons, *App*$^{NL-G-F}$ astrocytes seemed to slightly upregulate these genes, in comparison to when cultured alone (Figure 10e). Furthermore, we looked at the expression levels of proteins involved in general autophagy, but also of mitophagy specific proteins (Figure 10f). Preliminary data indicate no differences in neither LC3II/I ratio nor in p62 levels, suggesting there might be no alterations in overall autophagy (Figure 10 f,g). Accordingly with data from qPCR (Figure 10e), Parkin expression levels showed no differences in WT astrocytes co-cultured with WT or *App*$^{NL-G-F}$ neurons (Figure 10h) and its recruitment to mitochondria was also unchanged in WT astrocytes-WT PCN co-cultures, in comparison with WT astrocytes cultured alone (Figure S4a-b). On the other hand, and consistent with qPCR findings (Figure 10e), phosphorylation/activation of ULK1, which is, in its turn, an activator of receptor-mediated mitophagy proteins like FUNDC1 and AMBRA1, was increased in WT astrocytes co-cultured with WT neurons, but not in the presence of *App*$^{NL-G-F}$ neurons (Figure 10f, h). Interestingly, *App*$^{NL-G-F}$ astrocytes alone show a decrease in pULK1, which is rescued when in co-culture with *App*$^{NL-G-F}$ PCN (Figure 10f, h).

This data, although preliminary, indicates that a population of mitochondria captured by astrocytes is targeted to degradation and that receptor-mediated mitophagy mechanisms might play important roles in eliminating these organelles. However, *App*$^{NL-G-F}$ astrocytes seem to not be as effective in undergoing mitophagy, which could impair mitochondrial turnover, leading to the build-up of damaged mitochondria in AD. Nonetheless, further experiments will be needed to fully understand the dynamics between astrocytes and neurons leading to transmitophagy.

5. DISCUSSION

In this thesis, we sought out to gain insight into the mechanisms of mitochondrial exchange between astrocytes and neurons and determine how this dynamic might be affected in the *App*$^{NL-G-F}$ KI mouse model. Here, for the first time, we have provided evidence that *App*$^{NL-G-F}$ PCN and cortico-hippocampal astrocytes exhibit no bioenergetic impairments at this stage of differentiation. Despite this, deficits in mitochondrial anterograde transport were detected in *App*$^{NL-G-F}$ PCN, possibly accounting for the lower number of mitochondria in the pre-synaptic terminal at the early stages of the disease. *App*$^{NL-G-F}$ astrocytes, in turn, showed no alterations in mitochondrial movement, however, mitophagy machinery seemed to be highly compromised. Furthermore, we reported that astrocytes co-cultured with neurons change the expression of mitochondria-related genes. We also observed that PCN release healthy mitochondria to the CM, which are then captured by astrocytes through actin-dependent mechanisms. Following engulfment, mitochondria either integrate the host's astrocytic mitochondrial network or are directed to mitophagy.

Neurons are cells with high metabolic needs and largely depend on mitochondria to fulfil their energetic requirements. Therefore, adequate mitochondrial function is vital for neuronal health and survival. Mitochondrial dysfunction has been extensively reported both in AD brains and many AD models (Baloyannis, 2006). Our group has also shown that Aβ associates with and internalizes in mitochondria, possibly mediating many of these effects (Hansson Petersen et al., 2008). Surprisingly, we found that *App*$^{NL-G-F}$ PCN have no deficits in $\Delta\psi_m$ or ATP levels. In accordance with this, unpublished data from our group further shows no alterations in OCR and ECAR parameters in these neurons. Similarly, OCR and ECAR parameters remained unchanged in *App*$^{NL-G-F}$ astrocytes, unlike previously described for other AD models (Dematteis et al., 2020). This surprising absence of bioenergetic dysfunction in *App*$^{NL-G-F}$ cultures might be explained, in part, by the model herein used. Indeed, many AD studies reporting mitochondrial dysfunction so far have been performed in *APP* overexpressing AD models or after acute Aβ incubation. In these models, APP and, consequently, Aβ are not present at physiological levels, which may account for some of the pathological changes described (Saito et al., 2016). Since the *App*$^{NL-G-F}$ model only expresses APP at physiological levels, Aβ-mediated deleterious effects on mitochondria could be less pronounced, hence explaining our findings. Additionally, our group has performed a longitudinal transcriptomic, functional, and image-based study of neuronal mitochondria from adult *App*$^{NL-G-F}$ mice. We observed that at pre-symptomatic stages of the disease, this AD model shows upregulated mitochondrial function, which deteriorates with age and pathology progression (unpublished). In line with this, additional data from our group

shows upregulation in all OCR parameters in primary neurons isolated from *App*$^{NL-F}$ mice (Dentoni, 2021), a milder AD model that develops the neuropathology later than *App*$^{NL-G-F}$ mice. Therefore, we hypothesize a transitory phase may exist at early symptomatic stages when no changes of mitochondrial function are observed. Upregulation of mitochondrial genes have also been observed in MCI but not in AD patients (Mastroeni et al., 2017), suggesting that App KI models resemble some metabolic changes observed in these patients.

Neuronal bioenergetics, however, go beyond simply producing the necessary ATP as these cells must also ensure energy production occurs at regions with higher metabolic needs, like the synapse. Neurons are long, highly polarized cells and mitochondrial biogenesis primarily occurs in the soma. Therefore, mitochondria must travel long distances along the axon, a process energetically demanding by itself, to reach synaptic terminals where these organelles control Ca^{2+} homeostasis and provide ATP to modulate synaptic transmission (Devine & Kittler, 2018). Previous studies have shown that primary neurons from Tg2576 AβPP transgenic mice and $Aβ_{25-35}$-treated mouse hippocampal neurons have reduced mitochondrial anterograde transport, while retrograde movement does not seem to be greatly affected (Calkins et al., 2011; Calkins & Reddy, 2011). $Aβ_{25-35}$ treatment further resulted in decreased velocity of movement. Also, data from our group demonstrates that *App*$^{NL-F}$ neurons have a significantly increased number of stationary mitochondria, despite increased OCR, together with downregulation of mitochondrial anterograde transport in favour of retrograde transport (Dentoni, 2021). Accordingly, we now report an overall downregulation in the number of motile mitochondria in *App*$^{NL-G-F}$ PCN, accompanied by a substantial reduction of mitochondrial anterograde transport. Furthermore, mitochondrial speed during anterograde movement was also highly reduced. In contrast, we reveal mitochondrial distribution in *App*$^{NL-G-F}$ astrocytes is not affected, thus providing one of the first reports regarding mitochondrial movement in astrocytes in AD models. Interestingly, we did not observe alterations in the levels of mitochondrial transport machinery proteins in *App*$^{NL-G-F}$ PCN nor astrocytes. Thus, we hypothesize functional mechanisms or local proteomic changes might underlie the deficits in mitochondrial trafficking found in *App*$^{NL-G-F}$ neurons. Ca^{2+} interaction with Miro EF hand domains arrests mitochondrial transport and several reports have shown increased levels of cytosolic Ca^{2+} in AD neurons (Bezprozvanny & Mattson, 2008), resulting in lower affinity of Miro with kinesin and, consequently, mitochondrial anterograde transport impairment (Xinnan Wang & Schwarz, 2009). Moreover, Mfn2-Miro1 interaction was previously described to be necessary for axonal transport (Misko et al., 2010), while a consistent downregulation of Mfn2 is observed in this model or after acute Aβ incubation (Leal et al., 2020). However,

the relevance of these processes in the *App*$^{NL-G-F}$ model remains to be explored. Inhibition of mitochondrial anterograde transport hinders mitochondria from reaching the pre-synaptic terminal, leading to synaptic dysfunction and loss (Z. H. Sheng & Cai, 2012). Here, we also observed depletion of the pre-synaptic mitochondrial pool in the brain of early symptomatic *App*$^{NL-G-F}$ mice, indicating that, even though total ATP production by mitochondria is not affected in primary *App*$^{NL-G-F}$ neurons, energy supply to the synapse might be compromised before synaptic loss occurs. Corroborating these evidence, two recently published studies established axonal terminals determine neuronal vulnerability in AD with a molecular framework selective for regulation of neurotransmitter secretion, microtubule-based movement, and autophagy (Hark et al., 2021; Roussarie et al., 2020).

Astrocytes detect variations in neuronal activity and provide neuronal support in a myriad of ways both under physiological and pathological conditions. Neuronal activity has been shown to induce mitochondrial network rearrangement and upregulation of antioxidant defence-associated genes in astrocytes (Ioannou et al., 2019a; T. L. Stephen et al., 2015). Additionally, reports of mitochondrial transfer in the CNS, involving astrocytes and neurons, emerged recently (Hayakawa et al., 2016). Therefore, and considering the deficits in mitochondrial transport and pre-synaptic mitochondria here reported, which likely affect local metabolism, we investigated whether astrocytes could regulate the expression of mitochondrial-related genes and, thus, be better equipped to support neighbouring affected neurons. We found that WT astrocytes in the presence of either WT or *App*$^{NL-G-F}$ neurons upregulate *KIF5β*, a major component of the mitochondrial transport machinery. It has been shown previously that overexpression of mitochondrial movement proteins such as Miro1 can enhance mitochondrial transfer (Babenko et al., 2018). Thus, these results suggest mechanisms of intercellular mitochondrial transfer could occur between astrocytes and neurons in these co-cultures. On the other hand, *App*$^{NL-G-F}$ astrocytes cultured alone or in the presence of *App*$^{NL-G-F}$ PCN show downregulation of the mitochondria-related genes here investigated, relatively to WT astrocytes. Consistent with this data, a recent study involving whole-genome microarray showed downregulation of mitochondrial genes in primary hippocampal astrocytes from the 3xTg AD mouse model, compared to non-transgenic mouse (Ruffinatti et al., 2018). This study further showed massive downregulation of cell-cell communication genes in 3xTg astrocytes, indicating that AD astrocytes might be less capable of interpreting and producing adequate responses to support neuronal demands and activity. Remarkably, we also found that co-culturing *App*$^{NL-G-F}$ astrocytes with WT PCN, instead of *App*$^{NL-G-F}$ PCN, increased the expression of several mitochondrial transport and biogenesis-associated genes assessed, indicating that the presence of WT neurons could potentially improve astrocytic phenotype.

Further experiments on the astrocyte-neuron mitochondrial dynamics here involved, revealed that astrocytes uptake mitochondria released by neurons. Surprisingly, *App*$^{NL-G-F}$ astrocytes have a similar ability to engulf mito-EVs as compared to WT astrocytes. Instead, deficits in the engulfment of *App*$^{NL-G-F}$-derived mito-EVs are observed regardless of the astrocytic genotype. These data suggest that neuronal genotype accounts for most of the alterations observed in mitochondrial exchange between these cells. Differential proteomics between mito-EVs released by WT and *App*$^{NL-G-F}$ could underly these differences. Indeed, EVs isolated from the brains of AD patients are highly enriched in Aβ, phosphorylated tau, and other signature proteins not found in EVs from control patients (Muraoka, DeLeo, et al., 2020; Muraoka, Jedrychowski, et al., 2020). Alterations on mito-EVs cargo were also found in brains from Down Syndrome models that overexpress *App*, including downregulation of ETC complexes (D'Acunzo et al., 2021). Therefore, *App*$^{NL-G-F}$ mito-EVs protein content could be different from WT mito-EVs and perceived as danger signals by astrocytes, leading to *App*$^{NL-G-F}$ mito-EVs accumulation in the CM. Nonetheless, full proteomic characterization of each mito-EVs phenotype would be necessary to sustain this theory. A recent study by Mochly-Rosen lab further showed that the release of fragmented and dysfunctional mitochondria into the neuronal milieu can propagate inflammatory neurodegeneration (Joshi et al., 2019), highlighting the importance of efficient elimination of extracellular mitochondria.

Different mechanisms for mito-EVs internalization have been described. In line with previous studies (Peruzzotti-Jametti et al., 2021; Sinclair et al., 2016), we found that incubating cytoD-treated astrocytes with neuronal CM blocked mito-EVs uptake by neurons as indicated by the high levels of ATP in the CM and decreased number of MitoTracker^{+} particles detected in astrocytes, thus providing evidence that neuronal mitochondria uptake by astrocytes is an actin-dependent process. Interestingly, we observed that only a small part of the engulfed mitochondria appeared to be fully integrated into the astrocytic mitochondrial network, while others seemed to be in the process of integrating the network. A recent report from Pluchino's group demonstrated that, within 6 h after treating macrophages with neural stem cells-derived mito-EVs, most exogenous mitochondria were found either attached or included in the host macrophage's mitochondrial network (Peruzzotti-Jametti et al., 2021). Importantly, this was more evident in macrophages challenged with lipopolysaccharide, which induces a reactive, pro-inflammatory phenotype in these cells, prior to treatment with mito-EVs, indicating that the rate and speed of mitochondrial engulfment and incorporation in the host's mitochondrial network might depend on cellular health and needs. The period of time these processes take to occur could also be affected by the type of cell capturing

the mitochondria, as different cell types might have different susceptibility for accepting exogenous material. Therefore, additional experiments with different time points should be carried out to assess if the population of mitochondria incorporated in the astrocyte's mitochondrial network would increase over time. Furthermore, we found yet another significant population of neuronal-derived mitochondria in astrocytes that did not appear to express TOM20 nor localize with the host's mitochondrial network, indicating these remaining mitochondria might have a different fate.

TOM20 is an integral protein of the mitochondrial TOM complex involved in protein import to mitochondria. The absence of TOM20 could hinder nuclear-encoded mitochondrial proteins from being imported into the organelle and, consequently, lead to mitochondrial impairment. Damaged mitochondria are typically targeted to degradation and recent reports have demonstrated that astrocytes contribute to neuronal homeostasis by capturing and degrading mitochondria shed by neurons to the extracellular environment (C. H. O. Davis et al., 2014). Therefore, we then asked whether a fraction of the captured mitochondria by astrocytes could be targeted for elimination. Our preliminary data shows a slight upregulation of mitophagy in WT and *App*$^{NL-G-F}$ astrocytes cultured with neurons, while a % of neuronal-derived mitochondria also co-localize with lysosomes in astrocytes. However, *App*$^{NL-G-F}$ astrocytes cultured alone showed decreased mitophagy events associated with downregulation of mitophagy-related genes. These data are in accordance with a recent work from Vilhelm Bohr lab where they show both PINK1/Parkin-mediated and receptor-mediated mitophagy are severely impaired in AD patients and both Aβ and tau models (Fang et al., 2019). Interestingly, this downregulation was partially restored in *App*$^{NL-G-F}$ astrocytes upon co-culture with *App*$^{NL-G-F}$ PCN, suggesting that, even though these astrocytes might have deficient capacity of undergoing mitophagy, they still retain some ability to respond to and support neuronal function. Upregulation of mitophagy in co-cultures seemed to be mainly receptor-mediated, as a general upregulation of *Ambra1* and *Fundc1* was observed. Accordingly, we found that phosphorylation/activation of ULK1, a kinase which, upon phosphorylation, activates AMBRA1 and FUNCD1, among other proteins, was increased in WT astrocytes in the presence of WT PCN, but rather decreased in *App*$^{NL-G-F}$ astrocytes cultured alone or in the presence of WT PCN. Altogether, these results suggest that not all mitochondria released by PCN might retain fully functional integrity, being flagged to receptor-mediated mitophagy in astrocytes, which is impaired in the *App*$^{NL-G-F}$ model. Although we have observed increased mRNA expression and immunoreactivity of proteins from the initial steps of mitophagy in astrocytes, we cannot rule out that mito-EVs could have been previously signalled to mitophagy in neurons. Indeed, a recent study reported that, in a Parkinson's disease model, damaged

mitochondria are released by neurons and undergo transmitophagy in nearby astrocytes (Morales et al., 2020). The authors further observed that mitophagy started in dopaminergic neurons (showing high Pink1, parkin and AMBRA1 immunoreactivity and development of autophagosomes) but finalized in neighbouring astrocytes where autophagolysosomes were detected. Further investigation will still be needed to determine whether the mitochondria co-localizing with the lysosomes correspond to $TOM20^-$ mitochondria and the exact mechanisms involved in the elimination of neuronal mitochondria in astrocytes.

6. CONCLUDING REMARKS AND FUTURE PERSPECTIVES

Our work provides substantial evidence of neuron to astrocyte mitochondrial transfer and that this exchange could be affected in the *App*$^{NL-G-F}$ mouse model, leading to defects in mitochondria turnover and contributing to AD pathology. However, as previously mentioned, further experiments are still lacking to fully understand the contribution of each neuronal and astrocytic phenotype to the obtained outcomes. Also, additional questions remain unanswered, such as why are neurons releasing such high amounts of mitochondria? And can the increased levels of extracellular mitochondria in *App* KI neurons co-cultured with astrocytes influence neurodegeneration? Furthermore, here we did not observe astrocyte to neuron mitochondrial transfer under our experimental setup. Indeed, *App*$^{NL-G-F}$ neurons showed deficits in mitochondrial transport to the pre-synaptic terminal and, consequently, reduced number of mitochondria at these locations, which has been shown to lead to synaptic dysfunction. Therefore, and according to previous reports that mitochondrial transfer occurs from healthy to stressed and dysfunctional cells, we expected that astrocytes could aid *App*$^{NL-G-F}$ neurons by transferring healthy mitochondria. One explanation to why we did not observe this might relate to the fact that other mechanisms of mitochondrial transfer, such as TNTs, could be involved in the process, as previously reported. Indeed, we showed WT astrocytes in co-culture with neurons upregulate mitochondrial transport-related genes. While it is true upregulation of these genes could be related to the need of integrating neuronal mitochondria in the host's mitochondrial network or transporting them towards lysosomes, as we described here, it could also be a way for the cell to get equipped with the necessary transport machinery to move mitochondria through TNTs. Therefore, further experiments and the establishment of co-cultures that allow the formation of TNTs between astrocytes and neurons should be carried out in the future to further assess mechanisms of mitochondrial exchange between these cells.

7. REFERENCES

Abounit, S., Wu, J. W., Duff, K., Victoria, G. S., & Zurzolo, C. (2016). Tunnelling nanotubes: A possible highway in the spreading of tau and other prion-like proteins in neurodegenerative diseases. *Prion*, *10*(5), 344–351. https://doi.org/10.1080/19336896.2016.1223003

Ahmad, T., Mukherjee, S., Pattnaik, B., Kumar, M., Singh, S., Rehman, R., Tiwari, B. K., Jha, K. A., Barhanpurkar, A. P., Wani, M. R., Roy, S. S., Mabalirajan, U., Ghosh, B., & Agrawal, A. (2014). Miro1 regulates intercellular mitochondrial transport & enhances mesenchymal stem cell rescue efficacy. *EMBO Journal*, *33*(9), 994–1010. https://doi.org/10.1002/embj.201386030

Alberts, B., Johnson, A., Lewis, J., Morgan, D., Raff, M., Roberts, K., & Walter, P. (2017). Molecular Biology of the Cell. In *Molecular Biology of the Cell*. https://doi.org/10.1201/9781315735368

Allaman, I., Gavillet, M., Bélanger, M., Laroche, T., Viertl, D., Lashuel, H. A., & Magistretti, P. J. (2010). Amyloid-β aggregates cause alterations of astrocytic metabolic phenotype: Impact on neuronal viability. *Journal of Neuroscience*, *30*(9), 3326–3338. https://doi.org/10.1523/JNEUROSCI.5098-09.2010

Alnaes, E., & Rahamimoff, R. (1975). On the role of mitochondria in transmitter release from motor nerve terminals. *The Journal of Physiology*, *248*(2), 285–306. https://doi.org/10.1113/jphysiol.1975.sp010974

Alvarez-Dolado, M., Pardal, R., Garcia-Verdugo, J. M., Fike, J. R., Lee, H. O., Pfeffer, K., Lois, C., Morrison, S. J., & Alvarez-Bullia, A. (2003). Fusion of bone-marrow-derived cells with Purkinje neurons, cardiomyocytes and hepatocytes. *Nature*, *425*(6961), 968–973. https://doi.org/10.1038/nature02069

Alzheimer's Association. (2020). *On the Front Lines: Primary Care Physicians and Alzheimer's Care in America*. https://www.alz.org/news/2020/primary-care-physicians-on-the-front-lines-of-diag

Alzheimer, A. (1910). *Beiträge zur Kenntnis der Pathologischen Neuroglia und ihrer Beziehungen zu den Abbauvorgängen im Nervengewebe*. G. Fischer. https://books.google.se/books?id=9z4YjwEACAAJ

Ames, A. 3rd. (2000). CNS energy metabolism as related to function. *Brain Research Reviews*, *34*(1–2), 42–68. https://doi.org/10.1016/S0165-0173(00)00038-2

Andersson, S. G. E., Karlberg, O., Canbäck, B., Kurland, C. G., Whatley, F. R., Van Der Giezen, M., Martin, W., Tielens, A. G. M., Allen, J. F., & Raven, J. A. (2003). On the origin of mitochondria: A genomics perspective. *Philosophical Transactions of the Royal Society B: Biological Sciences*, *358*(1429), 165–179. https://doi.org/10.1098/rstb.2002.1193

Angulo, M. C., Le Meur, K., Kozlov, A. S., Charpak, S., & Audinat, E. (2008). GABA, a forgotten gliotransmitter. In *Progress in Neurobiology*, 86(3), 297–303. https://doi.org/10.1016/j.pneurobio.2008.08.002

Apelt, J., Ach, K., & Schliebs, R. (2003). Aging-related down-regulation of neprilysin, a putative b-amyloid-degrading enzyme, in transgenic Tg2576 Alzheimer-like mouse brain is

accompanied by an astroglial upregulation in the vicinity of b-amyloid plaques. *Neuroscience Letters.* 339(3), 183-186 https://doi.org/10.1016/S0304-3940(03)00030-2

Area-Gomez, E., Del Carmen Lara Castillo, M., Tambini, M. D., Guardia-Laguarta, C., De Groof, A. J. C., Madra, M., Ikenouchi, J., Umeda, M., Bird, T. D., Sturley, S. L., & Schon, E. A. (2012). Upregulated function of mitochondria-associated ER membranes in Alzheimer disease. *EMBO Journal*, *31*(21), 4106–4123. https://doi.org/10.1038/emboj.2012.202

Babenko, V. A., Silachev, D. N., Popkov, V. A., Zorova, L. D., Pevzner, I. B., Plotnikov, E. Y., Sukhikh, G. T., & Zorov, D. B. (2018). Miro1 enhances mitochondria transfer from multipotent mesenchymal stem cells (MMSC) to neural cells and improves the efficacy of cell recovery. *Molecules*, *23*(3), 687. https://doi.org/10.3390/molecules23030687

Bak, L. K., Schousboe, A., & Waagepetersen, H. S. (2006). The glutamate/GABA-glutamine cycle: Aspects of transport, neurotransmitter homeostasis and ammonia transfer. In *Journal of Neurochemistry* 98(3), 641–653. https://doi.org/10.1111/j.1471-4159.2006.03913.x

Baloyannis, S. J. (2006). Mitochondrial alterations in Alzheimer's disease. *Journal of Alzheimer's Disease*, *9*(2), 119–126. https://doi.org/10.3233/JAD-2006-9204

Bejanin, A., Schonhaut, D. R., Joie, R. La, Kramer, J. H., Baker, S. L., Sosa, N., Ayakta, N., Cantwell, A., Janabi, M., Lauriola, M., O'neil, J. P., Gorno-Tempini, M. L., Miller, Z. A., Rosen, H. J., Miller, B. L., Jagust, W. J., & Rabinovici, G. D. (2017). Tau pathology and neurodegeneration contribute to cognitive impairment in Alzheimer's disease. *Brain,* 140(12), 3286-3300 https://doi.org/10.1093/brain/awx243

Bekris, L. M., Yu, C. E., Bird, T. D., & Tsuang, D. W. (2010). Genetics of Alzheimer disease. In *Journal of Geriatric Psychiatry and Neurology*, 23(4) 213–227. https://doi.org/10.1177/0891988710383571

Bezprozvanny, I., & Mattson, M. P. (2008). Neuronal calcium mishandling and the pathogenesis of Alzheimer's disease. *Trends in Neurosciences*, *31*(9), 454–463. https://doi.org/10.1016/j.tins.2008.06.005

Bi, G. Q., Morris, R. L., Liao, G., Alderton, J. M., Scholey, J. M., & Steinhardt, R. A. (1997). Kinesin- and myosin-driven steps of vesicle recruitment for Ca2+- regulated exocytosis. *Journal of Cell Biology*, *138*(5), 999–1008. https://doi.org/10.1083/jcb.138.5.999

Billups, B., & Forsythe, I. D. (2002). Presynaptic mitochondrial calcium sequestration influences transmission at mammalian central synapses. *Journal of Neuroscience*, *22*(14), 5840–5847. https://doi.org/10.1523/jneurosci.22-14-05840.2002

Boland, B., Kumar, A., Lee, S., Platt, F. M., Wegiel, J., Yu, W. H., & Nixon, R. A. (2008). Autophagy induction and autophagosome clearance in neurons: Relationship to autophagic pathology in Alzheimer's disease. *Journal of Neuroscience*, *28*(27), 6926–6937. https://doi.org/10.1523/JNEUROSCI.0800-08.2008

Brickley, K., & Stephenson, F. A. (2011). Trafficking kinesin protein (TRAK)-mediated transport of mitochondria in axons of hippocampal neurons. *Journal of Biological Chemistry*, *286*(20), 18079–18092. https://doi.org/10.1074/jbc.M111.236018

Bukoreshtliev, N. V, Wang, X., Hodneland, E., Gurke, S., Barroso, J. F. V., & Gerdes, H. H.

(2009). Selective block of tunneling nanotube (TNT) formation inhibits intercellular organelle transfer between PC12 cells. *FEBS Letters*, *583*(9), 1481–1488. https://doi.org/10.1016/j.febslet.2009.03.065

Calkins, M. J., Manczak, M., Mao, P., Shirendeb, U., & Reddy, P. H. (2011). Impaired mitochondrial biogenesis, defective axonal transport of mitochondria, abnormal mitochondrial dynamics and synaptic degeneration in a mouse model of Alzheimer's disease. *Human Molecular Genetics*, *20*(23), 4515–4529. https://doi.org/10.1093/hmg/ddr381

Calkins, M. J., & Reddy, P. H. (2011). Amyloid beta impairs mitochondrial anterograde transport and degenerates synapses in Alzheimer's disease neurons. *Biochimica et Biophysica Acta*, *1812*(4), 507–513. https://doi.org/10.1016/j.bbadis.2011.01.007

Cenini, G., & Voos, W. (2019). Mitochondria as potential targets in Alzheimer disease therapy: An update. In *Frontiers in Pharmacology*, 10(902). https://doi.org/10.3389/fphar.2019.00902

Chan, D. C. (2006). Mitochondria: Dynamic Organelles in Disease, Aging, and Development. *Cell*, *125*(7), 1241–1252. https://doi.org/10.1016/j.cell.2006.06.010

Chang, J. C., Wu, S. L., Liu, K. H., Chen, Y. H., Chuang, C. Sen, Cheng, F. C., Su, H. L., Wei, Y. H., Kuo, S. J., & Liu, C. S. (2016). Allogeneic/xenogeneic transplantation of peptide-labeled mitochondria in Parkinson's disease: Restoration of mitochondria functions and attenuation of 6-hydroxydopamine-induced neurotoxicity. *Translational Research*, *170*, 40-56.e3. https://doi.org/10.1016/j.trsl.2015.12.003

Charles, A. C., Merrill, J. E., Dirksen, E. R., & Sandersont, M. J. (1991). Intercellular signaling in glial cells: Calcium waves and oscillations in response to mechanical stimulation and glutamate. *Neuron*, *6*(6), 983–992. https://doi.org/10.1016/0896-6273(91)90238-U

Chen, H., Chomyn, A., & Chan, D. C. (2005). Disruption of fusion results in mitochondrial heterogeneity and dysfunction. *Journal of Biological Chemistry*, *280*(28), 26185–26192. https://doi.org/10.1074/jbc.M503062200

Chen, H., Detmer, S. A., Ewald, A. J., Griffin, E. E., Fraser, S. E., & Chan, D. C. (2003). Mitofusins Mfn1 and Mfn2 coordinately regulate mitochondrial fusion and are essential for embryonic development. *Journal of Cell Biology*, *160*(2), 189–200. https://doi.org/10.1083/jcb.200211046

Chen, Yanmin, & Sheng, Z. H. (2013). Kinesin-1-syntaphilin coupling mediates activity-dependent regulation of axonal mitochondrial transport. *Journal of Cell Biology*, *202*(2), 351–364. https://doi.org/10.1083/jcb.201302040

Chen, Yu, & Dorn II, G. W. (2013). PINK1-Phosphorylated Mitofusin 2 Is a Parkin Receptor for Culling Damaged Mitochondria. *Science*, *340*(6131), 471–475.

Cheng, X. Y., Biswas, S., Li, J., Mao, C. J., Chechneva, O., Chen, J., Li, K., Li, J., Zhang, J. R., Liu, C. F., & Deng, W. Bin. (2020). Human iPSCs derived astrocytes rescue rotenone-induced mitochondrial dysfunction and dopaminergic neurodegeneration in vitro by donating functional mitochondria. *Translational Neurodegeneration*, *9*(13). https://doi.org/10.1186/s40035-020-00190-6

Cho, Y. M., Kim, J. H., Kim, M., Park, S. J., Koh, S. H., Ahn, H. S., Kang, G. H., Lee, J. Bin, Park, K. S., & Lee, H. K. (2012). Mesenchymal stem cells transfer mitochondria to the cells with virtually no mitochondrial function but not with pathogenic mtDNA mutations. *PLoS ONE*, *7*(3), e32778. https://doi.org/10.1371/journal.pone.0032778

Cioni, J. M., Lin, J. Q., Holtermann, A. V., Koppers, M., Jakobs, M. A. H., Azizi, A., Turner-Bridger, B., Shigeoka, T., Franze, K., Harris, W. A., & Holt, C. E. (2019). Late Endosomes Act as mRNA Translation Platforms and Sustain Mitochondria in Axons. *Cell*, *176*(1–2), 56-72.e15. https://doi.org/10.1016/j.cell.2018.11.030

Cipolat, S., De Brito, O. M., Dal Zilio, B., & Scorrano, L. (2004). OPA1 requires mitofusin 1 to promote mitochondrial fusion. *Proceedings of the National Academy of Sciences of the United States of America*, *101*(45), 15927–15932. https://doi.org/10.1073/pnas.0407043101

Coffey, E. E., Beckel, J. M., Laties, A. M., & Mitchell, C. H. (2014). Lysosomal alkalization and dysfunction in human fibroblasts with the Alzheimer's disease-linked presenilin 1 A246E mutation can be reversed with cAMP. *Neuroscience*, *263*, 111–124. https://doi.org/10.1016/j.neuroscience.2014.01.001

Conde, C., & Cáceres, A. (2009). Microtubule assembly, organization and dynamics in axons and dendrites. In *Nature Reviews Neuroscience*, *10*(5) 319–332. https://doi.org/10.1038/nrn2631

Corder, E. H., Saunders, A. M., Strittmatter, W. J., Schmechel, D. E., Gaskell, P. C., Small, G. W., Roses, A. D., Haines, J. L., & Pericak-Vance, M. A. (1993). Gene dose of apolipoprotein E type 4 allele and the risk of Alzheimer's disease in late onset families. *Science*, *261*(5123), 921–923. https://doi.org/10.1126/science.8346443

Cornell-Bell, A. H., Finkbeiner, S. M., Cooper, M. S., & Smith, S. J. (1990). Glutamate Induces Calcium Waves in Cultured Astrocytes: Long-Range Glial Signalling. *Science*, *247*(4941), 470–473. https://doi.org/10.1126/science.1967852

D'Acunzo, P., Pérez-González, R., Kim, Y., Hargash, T., Miller, C., Alldred, M. J., Erdjument-Bromage, H., Penikalapati, S. C., Pawlik, M., Saito, M., Saito, M., Ginsberg, S. D., Neubert, T. A., Goulbourne, C. N., & Levy, E. (2021). Mitovesicles are a novel population of extracellular vesicles of mitochondrial origin altered in down syndrome. *Science Advances*, *7*(7), 5085–5097. https://doi.org/10.1126/sciadv.abe5085

Davis, A. F., & Clayton, D. A. (1996). In situ localization of mitochondrial DNA replication in intact mammalian cells. *Journal of Cell Biology*, *135*(4), 883–893. https://doi.org/10.1083/jcb.135.4.883

Davis, C. H. O., Kim, K. Y., Bushong, E. A., Mills, E. A., Boassa, D., Shih, T., Kinebuchi, M., Phan, S., Zhou, Y., Bihlmeyer, N. A., Nguyen, J. V, Jin, Y., Ellisman, M. H., & Marsh-Armstrong, N. (2014). Transcellular degradation of axonal mitochondria. *Proceedings of the National Academy of Sciences of the United States of America*, *111*(26), 9633–9638. https://doi.org/10.1073/pnas.1404651111

De Felice, F. G., Wu, D., Lambert, M. P., Fernandez, S. J., Velasco, P. T., Lacor, P. N., Bigio, E.

H., Jerecic, J., Acton, P. J., Shughrue, P. J., Chen-Dodson, E., Kinney, G. G., & Klein, W. L. (2008). Alzheimer's disease-type neuronal tau hyperphosphorylation induced by Aβ oligomers. *Neurobiology of Aging*, *29*(9), 1334–1347. https://doi.org/10.1016/j.neurobiolaging.2007.02.029

Del Prete, D., Suski, J. M., Oulès, B., Debayle, D., Gay, A. S., Lacas-Gervais, S., Bussiere, R., Bauer, C., Pinton, P., Paterlini-Bréchot, P., Wieckowski, M. R., Checler, F., & Chami, M. (2017). Localization and Processing of the Amyloid-β Protein Precursor in Mitochondria-Associated Membranes. *Journal of Alzheimer's Disease*, *55*(4), 1549–1570. https://doi.org/10.3233/JAD-160953

Dematteis, G., Vydmantaitė, G., Ruffinatti, F. A., Chahin, M., Farruggio, S., Barberis, E., Ferrari, E., Marengo, E., Distasi, C., Morkūnienė, R., Genazzani, A. A., Grilli, M., Grossini, E., Corazzari, M., Manfredi, M., Lim, D., Jekabsone, A., & Tapella, L. (2020). Proteomic analysis links alterations of bioenergetics, mitochondria-ER interactions and proteostasis in hippocampal astrocytes from 3xTg-AD mice. *Cell Death and Disease*, *11*(8), 645. https://doi.org/10.1038/s41419-020-02911-1

Dentoni, G. (2021). *Mitochondria-Endoplasmic Reticulum contacts in neuronal cells: From physiology to therapeutics*. Karolinska Institutet.

Devine, M. J., & Kittler, J. T. (2018). Mitochondria at the neuronal presynapse in health and disease. *Nature Reviews Neuroscience*, *19*(2), 63–80. https://doi.org/10.1038/nrn.2017.170

Di Bartolomeo, S., Corazzari, M., Nazio, F., Oliverio, S., Lisi, G., Antonioli, M., Pagliarini, V., Matteoni, S., Fuoco, C., Giunta, L., D'Amelio, M., Nardacci, R., Romagnoli, A., Piacentini, M., Cecconi, F., & Fimia, G. M. (2010). The dynamic interaction of AMBRA1 with the dynein motor complex regulates mammalian autophagy. *Journal of Cell Biology*, *191*(1), 155–168. https://doi.org/10.1083/jcb.201002100

Dragicevic, N., Mamcarz, M., Zhu, Y., Buzzeo, R., Tan, J., Arendash, G. W., & Bradshaw, P. C. (2010). Mitochondrial amyloid-β levels are associated with the extent of mitochondrial dysfunction in different brain regions and the degree of cognitive impairment in Alzheimer's transgenic mice. *Journal of Alzheimer's Disease*, *20*(SUPPL.2), 535–550. https://doi.org/10.3233/JAD-2010-100342

Drubin, D. G., & Kirschner, M. W. (1986). Tau Protein Function in Living Cells. *Journal of Cell Biology,* 103(6 Pt 2), 2739.2746. httsp://doi.org/10.1083/jcb.103.6.2739

Drummond, E., & Wisniewski, T. (2017). Alzheimer's disease: experimental models and reality. In *Acta Neuropathologica*,*133*(2), 155–175). https://doi.org/10.1007/s00401-016-1662-x

Du, H., Guo, L., Yan, S., Sosunov, A. A., McKhann, G. M., & Yan, S. S. Du. (2010). Early deficits in synaptic mitochondria in an Alzheimer's disease mouse model. *Proceedings of the National Academy of Sciences of the United States of America*, *107*(43), 18670–18675. https://doi.org/10.1073/pnas.1006586107

Duchen, M. R. (2000). Mitochondria and calcium: from cell signalling to cell death. *The Journal of Physiology, 529 Pt 1*(Pt 1), 57-68. https://doi.org/10.1111/j.1469-7793.2000.00057.x

Dyall, S. D., Brown, M. T., & Johnson, P. J. (2004). Ancient Invasions: From Endosymbionts to

Organelles. *Science*, *304*(5668), 253–257. https://doi.org/10.1126/science.1094884

Edison, P., Archer, H. A., Hinz, R., Hammers, A., Pavese, N., Tai, Y. F., Hotton, G., Cutler, D., Fox, N., Kennedy, A., Rossor, M., & Brooks, D. J. (2007). Amyloid, hypometabolism, and cognition in Alzheimer's disease [11C]PIB and [18F]FDG PET study. *Neurology*, *68*(7), 501–508.

English, K., Shepherd, A., Uzor, N. E., Trinh, R., Kavelaars, A., & Heijnen, C. J. (2020). Astrocytes rescue neuronal health after cisplatin treatment through mitochondrial transfer. *Acta Neuropathologica Communications*, *8*(1 https://doi.org/10.1186/s40478-020-00897-7

Fagan, A. M., Mintun, M. A., Shah, A. R., Aldea, P., Roe, C. M., Mach, R. H., Marcus, D., Morris, J. C., & Holtzman, D. M. (2009). Cerebrospinal fluid tau and ptau181 increase with cortical amyloid deposition in cognitively normal individuals: Implications for future clinical trials of Alzheimer's disease. *EMBO Molecular Medicine*, *1*(8–9), 371–380. https://doi.org/10.1002/emmm.200900048

Fang, E. F., Hou, Y., Palikaras, K., Adriaanse, B. A., Kerr, J. S., Yang, B., Lautrup, S., Mahdi Hasan-Olive, M., Caponio, D., Dan, X., Rocktäschel, P., Croteau, D. L., Akbari, M., Greig, N. H., Fladby, T., Nilsen, H., Zameel Cader, M., Mattson, M. P., Tavernarakis, N., & Bohr, V. A. Mitophagy inhibits amyloid-β and tau pathology and reverses cognitive deficits in models of Alzheimer's disease. https://doi.org/10.1038/s41593-018-0332-9

Fellin, T., Pascual, O., Gobbo, S., Pozzan, T., Haydon, P. G., & Carmignoto, G. (2004). Neuronal synchrony mediated by astrocytic glutamate through activation of extrasynaptic NMDA receptors. *Neuron*, *43*(5), 729–743. https://doi.org/10.1016/j.neuron.2004.08.011

Francis, P. T. (2005). The interplay of neurotransmitters in Alzheimer's disease. *CNS Spectrums*, *10*(11 SUPPL. 18), 6–9. https://doi.org/10.1017/s1092852900014164

Fransson, Å., Ruusala, A., & Aspenström, P. (2006). The atypical Rho GTPases Miro-1 and Miro-2 have essential roles in mitochondrial trafficking. *Biochemical and Biophysical Research Communications*, *344*(2), 500–510. https://doi.org/10.1016/j.bbrc.2006.03.163

Freya, T. G., & Mannellab, C. A. (2000). The internal structure of mitochondria. *Trends in Biochemical Sciences*, *25*(7), 319–324. https://doi.org/10.1016/S0968-0004(00)01609-1

Friedman, J. R. & Nunnari, J. (2014). Mitochondrial form and function. *Nature*, *505*(7483), 335–343. https://doi.org/10.1038/nature12985.Mitochondrial

Friedman, J. R., Lackner, L. L., West, M., DiBenedetto, J. R., Nunnari, J., & Voeltz, G. K. (2011). ER tubules mark sites of mitochondrial division. *Science*, *334*(6054), 358–362. https://doi.org/10.1126/science.1207385

Gabaldón, T., & Huynen, M. A. (2004). Shaping the mitochondrial proteome. *Biochimica et Biophysica Acta - Bioenergetics*, *1659*(2–3), 212–220. https://doi.org/10.1016/j.bbabio.2004.07.011

Games, D., Adams, D., Alessandrini, R., Barbour, R., Borthelette, P., Blackwell, C., Carr, T., Clemens, J., Donaldson, T., Gillespie, F., Guido, T., Hagopian, S., Johnson-Wood, K., Khan, K., Lee, M., Leibowitz, P., Lieberburg, I., Little, S., Masliah, E., Zhao, J. (1995). Alzheimer-type neuropathology in transgenic mice overexpressing V717F β-amyloid precursor protein.

Nature, *373*(6514), 523–527. https://doi.org/10.1038/373523a0

Gao, J., Qin, A., Liu, D., Ruan, R., Wang, Q., Yuan, J., Cheng, T. S., Filipovska, A., Papadimitriou, J. M., Dai, K., Jiang, Q., Gao, X., Feng, J. Q., Takayanagi, H., Zhang, C., & Zheng, M. H. (2019). Endoplasmic reticulum mediates mitochondrial transfer within the osteocyte dendritic network. *Science Advances*, *5*(11), eaaw7215. https://doi.org/10.1126/sciadv.aaw7215

Geisler, S., Holmström, K. M., Skujat, D., Fiesel, F. C., Rothfuss, O. C., Kahle, P. J., & Springer, W. (2010). PINK1/Parkin-mediated mitophagy is dependent on VDAC1 and p62/SQSTM1. *Nature Cell Biology*, *12*(2), 119–131. https://doi.org/10.1038/ncb2012

Ghoshal, N., García-Sierra, F., Wuu, J., Leurgans, S., Bennett, D. A., Berry, R. W., & Binder, L. I. (2002). Tau conformational changes correspond to impairments of episodic memory in mild cognitive impairment and Alzheimer's disease. *Experimental Neurology*, *177*(2), 475–493. https://doi.org/10.1006/exnr.2002.8014

Glenner, G. G., & Wong, C. W. (1984). Alzheimer's disease: Initial report of the purification and characterization of a novel cerebrovascular amyloid protein. *Biochemical and Biophysical Research Communications*, *120*(3), 885–890. https://doi.org/10.1016/S0006-291X(84)80190-4

Green, D. R., Galluzzi, L., & Kroemer, G. (2011). Mitochondria and the Autophagy-Inflammation-Cell Death Axis in the Organismal Aging. *Science*, *333*(6046), 1109–1112. https://doi.org/10.1093/eurheartj/ehr406

Griffin, E. E., Graumann, J., & Chan, D. C. (2005). The WD40 protein Caf4p is a component of the mitochondrial fission machinery and recruits Dnm1p to mitochondria. *Journal of Cell Biology*, *170*(2), 237–248. https://doi.org/10.1083/jcb.200503148

Grundke-Iqbal, I., Iqbal, K., & Tung, Y. C. (1986). Abnormal phosphorylation of the microtubule-associated protein τ (tau) in Alzheimer cytoskeletal pathology. *Proceedings of the National Academy of Sciences of the United States of America*, *83*(13), 44913–44917. https://doi.org/10.1097/00002093-198701030-00020

Guescini, M., Genedani, S., Stocchi, V., & Agnati, L. F. (2010). Astrocytes and Glioblastoma cells release exosomes carrying mtDNA. *Journal of Neural Transmission*, *117*(1). https://doi.org/10.1007/s00702-009-0288-8

Göbel, J., Engelhardt, E., Pelzer, P., Sakthivelu, V., Jahn, H. M., Jevtic, M., Folz-Donahue, K., Kukat, C., Schauss, A., Frese, C. K., Giavalisco, P., Ghanem, A., Conzelmann, K. K., Motori, E., & Bergami, M. (2020). Mitochondria-Endoplasmic Reticulum Contacts in Reactive Astrocytes Promote Vascular Remodeling. *Cell Metabolism*, *31*(4), 791-808.e8. https://doi.org/10.1016/j.cmet.2020.03.005

Hajnóczky, G., Csordás, G., Das, S., Garcia-Perez, C., Saotome, M., Roy, S. S., & Yi, M. (2006). Mitochondrial calcium signalling and cell death: approaches for assessing the role of mitochondrial Ca 2+ uptake in apoptosis Mitochondrial Ca 2+ transport mechanisms. *Cell Calcium*, *40*(5–6), 553–560. https://doi.org/10.1016/j.ceca.2006.08.016

Hall, A. M., & Roberson, E. D. (2012). Mouse models of Alzheimer's disease. *Brain Research*

Bulletin, *88*(1), 3–12. https://doi.org/10.1016/j.brainresbull.2011.11.017

Hamacher-Brady, A., & Brady, N. R. (2016). Mitophagy programs: Mechanisms and physiological implications of mitochondrial targeting by autophagy. *Cellular and Molecular Life Sciences*, *73*(4), 775–795. https://doi.org/10.1007/s00018-015-2087-8

Hansson Petersen, C. A., Alikhani, N., Behbahani, H., Wiehager, B., Pavlov, P. F., Alafuzoff, I., Leinonen, V., Ito, A., Winblad, B., Glaser, E., & Ankarcrona, M. (2008). The amyloid β-peptide is imported into mitochondria via the TOM import machinery and localized to mitochondrial cristae. *Proceedings of the National Academy of Sciences of the United States of America*, *105*(35), 13145–13150. https://doi.org/10.1073/pnas.0806192105

Hark, T. J., Rao, N. R., Castillon, C., Basta, T., Smukowski, S., Bao, H., Upadhyay, A., Bomba-Warczak, E., Nomura, T., O'Toole, E. T., Morgan, G. P., Ali, L., Saito, T., Guillermier, C., Saido, T. C., Steinhauser, M. L., Stowell, M. H. B., Chapman, E. R., Contractor, A., & Savas, J. N. (2021). Pulse-Chase Proteomics of the App Knockin Mouse Models of Alzheimer's Disease Reveals that Synaptic Dysfunction Originates in Presynaptic Terminals. *Cell Systems*, *12*(2), 141-158.e9. https://doi.org/10.1016/j.cels.2020.11.007

Hauptmann, S., Scherping, I., Dröse, S., Brandt, U., Schulz, K. L., Jendrach, M., Leuner, K., Eckert, A., & Müller, W. E. (2009). Mitochondrial dysfunction: An early event in Alzheimer pathology accumulates with age in AD transgenic mice. *Neurobiology of Aging*, *30*(10), 1574–1586. https://doi.org/10.1016/j.neurobiolaging.2007.12.005

Hayakawa, K., Esposito, E., Wang, X., Terasaki, Y., Liu, Y., Xing, C., Ji, X., & Lo, E. H. (2016). Transfer of mitochondria from astrocytes to neurons after stroke. *Nature*, *535*(7613), 551–555. https://doi.org/10.1038/nature18928

Head, E., Powell, D., Gold, B. T., & Schmitt, F. A. (2012). Alzheimer's Disease in Down Syndrome. *European Journal of Neurodegenerative Diseases*, *1*(3), 353–364.

Hecimovic, S., Wang, J., Dolios, G., Martinez, M., Wang, R., & Goate, A. M. (2004). Mutations in APP have independent effects on Aβ and CTFγ generation. *Neurobiology of Disease*, *17*(2), 205–218. https://doi.org/10.1016/j.nbd.2004.04.018

Hedskog, L., Pinho, C. M., Filadi, R., Rönnbäck, A., Hertwig, L., Wiehager, B., Larssen, P., Gellhaar, S., Sandebring, A., Westerlund, M., Graff, C., Winblad, B., Galter, D., Behbahani, H., Pizzo, P., Glaser, E., & Ankarcrona, M. (2013). Modulation of the endoplasmic reticulum-mitochondria interface in Alzheimer's disease and related models. *Proceedings of the National Academy of Sciences of the United States of America*, *110*(19), 7916–7921. https://doi.org/10.1073/pnas.1300677110

Heneka, M. T., Sastre, M., Dumitrescu-Ozimek, L., Dewachter, I., Walter, J., Klockgether, T., & Van Leuven, F. (2005). Focal glial activation coincides with increased BACE1 activation and precedes amyloid plaque deposition in APP[V717I] transgenic mice. *Journal of Neuroinflammation*, *2*(22). https://doi.org/10.1186/1742-2094-2-22

Hirokawa, N., Sato-Yoshitake, R., Yoshida, T., & Kawashima, T. (1990). Brain dynein (MAP1C) localizes on both anterogradely and retrogradely transported membranous organelles in vivo. *Journal of Cell Biology*, *111*(3), 1027–1037. https://doi.org/10.1083/jcb.111.3.1027

Hirokawa, Nobutaka, Niwa, S., & Tanaka, Y. (2010). Molecular motors in neurons: Transport mechanisms and roles in brain function, development, and disease. *Neuron*, *68*(4), 610–638. https://doi.org/10.1016/j.neuron.2010.09.039

Hsiao, K., Chapman, P., Nilsen, S., Eckman, C., Harigaya, Y., Younkin, S., Yang, F., & Cole, G. (1996). Correlative Memory Deficits, AP3 Elevation, and Amyloid Plaques in Transgenic Mice. *Science, 274*(5284),

Hubley, M. J., Locke, B. R., & Moerland, T. S. (1996). The effects of temperature, pH, and magnesium on the diffusion coefficient of ATP in solutions of physiological ionic strength. *Biochimica et Biophysica Acta - General Subjects*, *1291*(2), 115–121. https://doi.org/10.1016/0304-4165(96)00053-0

Iadecola, C., & Nedergaard, M. (2007). Glial regulation of the cerebral microvasculature. In *Nature Neuroscience,* 10(11), 1369–1376. https://doi.org/10.1038/nn2003

Ioannou, M. S., Jackson, J., Sheu, S. H., Chang, C. L., Weigel, A. V., Liu, H., Pasolli, H. A., Xu, C. S., Pang, S., Matthies, D., Hess, H. F., Lippincott-Schwartz, J., & Liu, Z. (2019a). Neuron-Astrocyte Metabolic Coupling Protects against Activity-Induced Fatty Acid Toxicity. *Cell*, *177*(6), 1522-1535.e14. https://doi.org/10.1016/j.cell.2019.04.001

Ioannou, M. S., Jackson, J., Sheu, S. H., Chang, C. L., Weigel, A. V, Liu, H., Pasolli, H. A., Xu, C. S., Pang, S., Matthies, D., Hess, H. F., Lippincott-Schwartz, J., & Liu, Z. (2019b). Neuron-Astrocyte Metabolic Coupling Protects against Activity-Induced Fatty Acid Toxicity. *Cell*, *177*(6), 1522-1535.e14. https://doi.org/10.1016/j.cell.2019.04.001

Islam, M. N., Das, S. R., Emin, M. T., Wei, M., Sun, L., Westphalen, K., Rowlands, D. J., Quadri, S. K., Bhattacharya, S., & Bahttacharya, J. (2012). Mitochondrial transfer from bone marrow-derived stromal cells to pulmonary alveoli protects against lung injury. *Nature Medicine*, *18*(15), 759–765. https://doi.org/10.1038/nm.2736.Mitochondrial

Jahn, R., & Fasshauer, D. (2012). Molecular machines governing exocytosis of synaptic vesicles. *Nature, 490*(7419), 201–207. https://doi.org/10.1038/nature11320

Jiao, H., Jiang, D., Hu, X., Du, W., Ji, L., Yang, Y., Li, X., Sho, T., Wang, X., Li, Y., Wu, Y.-T., Wei, Y.-H., Hu, X., & Yu, L. (2021). Mitocytosis, a migrasome-mediated mitochondrial quality-control process. *Cell*, *184*(11), 2896-2910.e13. https://doi.org/10.1016/j.cell.2021.04.027

Jin, M., Shepardson, N., Yang, T., Chen, G., Walsh, D., & Selkoe, D. J. (2011). Soluble amyloid β-protein dimers isolated from Alzheimer cortex directly induce Tau hyperphosphorylation and neuritic degeneration. *Proceedings of the National Academy of Sciences of the United States of America*, *108*(14), 5819–5824. https://doi.org/10.1073/pnas.1017033108

Jin, S. M., Lazarou, M., Wang, C., Kane, L. A., Narendra, D. P., & Youle, R. J. (2010). Mitochondrial membrane potential regulates PINK1 import and proteolytic destabilization by PARL. *Journal of Cell Biology*, *191*(5), 933–942. https://doi.org/10.1083/jcb.201008084

Jo, S., Yarishkin, O., Hwang, Y. J., Chun, Y. E., Park, M., Woo, D. H., Bae, J. Y., Kim, T., Lee, J., Chun, H., Park, H. J., Lee, D. Y., Hong, J., Kim, H. Y., Oh, S. J., Park, S. J., Lee, H., Yoon, B. E., Kim, Y., … Lee, C. J. (2014). GABA from reactive astrocytes impairs memory in mouse

models of Alzheimer's disease. *Nature Medicine*, *20*(8), 886–896. https://doi.org/10.1038/nm.3639

Johnson, E. C. B., Dammer, E. B., Duong, D. M., Ping, L., Zhou, M., Yin, L., Higginbotham, L. A., Guajardo, A., White, B., Troncoso, J. C., Thambisetty, M., Montine, T. J., Lee, E. B., Trojanowski, J. Q., Beach, T. G., Reiman, E. M., Haroutunian, V., Wang, M., Schadt, E., … Seyfried, N. T. (2020). Large-scale proteomic analysis of Alzheimer's disease brain and cerebrospinal fluid reveals early changes in energy metabolism associated with microglia and astrocyte activation. *Nature Medicine*, *26*(5), 769–780. https://doi.org/10.1038/s41591-020-0815-6

Jonsson, T., Atwal, J. K., Steinberg, S., Snaedal, J., Jonsson, P. V., Bjornsson, S., Stefansson, H., Sulem, P., Gudbjartsson, D., Maloney, J., Hoyte, K., Gustafson, A., Liu, Y., Lu, Y., Bhangale, T., Graham, R. R., Huttenlocher, J., Bjornsdottir, G., Andreassen, O. A., Stefansson, K. (2012). A mutation in APP protects against Alzheimer's disease and age-related cognitive decline. *Nature*, *488*(7409), 96. https://doi.org/10.1038/nature11283

Joshi, A. U., Minhas, P. S., Liddelow, S. A., Haileselassie, B., Andreasson, K. I., Dorn, G. W., & Mochly-Rosen, D. (2019). Fragmented mitochondria released from microglia trigger A1 astrocytic response and propagate inflammatory neurodegeneration. *Nature Neuroscience*, *22*(10), 1635–1648. https://doi.org/10.1038/s41593-019-0486-0

Jourdain, P., Bergersen, L. H., Bhaukaurally, K., Bezzi, P., Santello, M., Domercq, M., Matute, C., Tonello, F., Gundersen, V., & Volterra, A. (2007). Glutamate exocytosis from astrocytes controls synaptic strength. *Nature Neuroscience*, *10*(3), 331–339. https://doi.org/10.1038/nn1849

Kamenetz, F., Tomita, T., Hsieh, H., Seabrook, G., Borchelt, D., Iwatsubo, T., Sisodia, S., & Malinow, R. (2003). APP Processing and Synaptic Function. *Neuron*, *37*(6), 925–937. https://doi.org/10.1016/S0896-6273(03)00124-7

Kametani, F., & Hasegawa, M. (2018). Reconsideration of amyloid hypothesis and tau hypothesis in Alzheimer's disease. *Frontiers in Neuroscience, 12*(25). https://doi.org/10.3389/fnins.2018.00025

Kanai, Y., Okada, Y., Tanaka, Y., Harada, A., Terada, S., & Hirokawa, N. (2000). KIF5C, a novel neuronal kinesin enriched in motor neurons. *Journal of Neuroscience*, *20*(17), 6374–6384. https://doi.org/10.1523/jneurosci.20-17-06374.2000

Kane, L. A., Lazarou, M., Fogel, A. I., Li, Y., Yamano, K., Sarraf, S. A., Banerjee, S., & Youle, R. J. (2014). PINK1 phosphorylates ubiquitin to activate parkin E3 ubiquitin ligase activity. *Journal of Cell Biology*, *205*(2), 143–153. https://doi.org/10.1083/jcb.201402104

Kang, J. S., Tian, J. H., Pan, P. Y., Zald, P., Li, C., Deng, C., & Sheng, Z. H. (2008). Docking of Axonal Mitochondria by Syntaphilin Controls Their Mobility and Affects Short-Term Facilitation. *Cell*, *132*(1), 137–148. https://doi.org/10.1016/j.cell.2007.11.024

Kitay, B. M., McCormack, R., Wang, Y., Tsoulfas, P., & Zhai, R. G. (2013). Mislocalization of neuronal mitochondria reveals regulation of wallerian degeneration and NMNAT/ WLDS-mediated axon protection independent of axonal mitochondria. *Human Molecular Genetics*,

22(8), 1601–1614. https://doi.org/10.1093/hmg/ddt009

Koehler, R. C., Roman, R. J., & Harder, D. R. (2009). Astrocytes and the regulation of cerebral blood flow. *Trends in Neurosciences*, *32*(3), 160–169. https://doi.org/10.1016/j.tins.2008.11.005

Kofuji, P., & Newman, E. A. (2004). Potassium buffering in the central nervous system. *Neuroscience*, *129*(4), 1043–1054. https://doi.org/10.1016/j.neuroscience.2004.06.008

Koistinaho, M., Lin, S., Wu, X., Esterman, M., Koger, D., Hanson, J., Higgs, R., Liu, F., Malkani, S., Bales, K. R., & Paul, S. M. (2004). Apolipoprotein E promotes astrocyte colocalization and degradation of deposited amyloid-β peptides. *Nature Medicine*, *10*(7), 719–726. https://doi.org/10.1038/nm1058

Kolarova, M., García-Sierra, F., Bartos, A., Ricny, J., & Ripova, D. (2012). Structure and pathology of tau protein in Alzheimer disease. *International Journal of Alzheimer's Disease*, *2012*. https://doi.org/10.1155/2012/731526

Kopeikina, K. J., Carlson, G. A., Pitstick, R., Ludvigson, A. E., Peters, A., Luebke, J. I., Koffie, R. M., Frosch, M. P., Hyman, B. T., & Spires-Jones, T. L. (2011). Tau accumulation causes mitochondrial distribution deficits in neurons in a mouse model of tauopathy and in human Alzheimer's disease brain. *American Journal of Pathology*, *179*(4), 2071–2082. https://doi.org/10.1016/j.ajpath.2011.07.004

Kosik, K. S., Joachim, C. L., & Selkoe, D. J. (1986). Microtubule-associated protein tau (T) is a major antigenic component of paired helical filaments in Alzheimer disease. *Proceedings of the National Academy of Sciences of the United States of America, 83*(11), 4044-4048. https://doi.org/10.1073/pnas.83.11.4044

Kumar-Singh, S., Theuns, J., Van Broeck, B., Pirici, D., Vennekens, K., Corsmit, E., Cruts, M., Dermaut, B., Wang, R., & Van Broeckhoven, C. (2006). Mean Age-of-Onset of Familial Alzheimer Disease Caused by Presilin Mutation Correlates With Both Increased Aβ42 and Decreased Aβ40. *Human Mutation*, *27*(7), 686–695. https://doi.org/10.1002/humu

Kumar, A., Singh, A., & Ekavali. (2015). A review on Alzheimer's disease pathophysiology and its management: An update. *Pharmacological Reports*, *67*(2), 195–203. https://doi.org/10.1016/j.pharep.2014.09.004

Kuzniewska, B., Cysewski, D., Wasilewski, M., Sakowska, P., Milek, J., Kulinski, T. M., Winiarski, M., Kozielewicz, P., Knapska, E., Dadlez, M., Chacinska, A., Dziembowski, A., & Dziembowska, M. (2020). Mitochondrial protein biogenesis in the synapse is supported by local translation. *EMBO Reports*, *21*(8), e48882. https://doi.org/10.15252/embr.201948882

LaPointe, N. E., Morfini, G., Pigino, G., Gaisina, I. N., Kozikowski, A. P., Binder, L. I., & Brady, S. T. (2009). The amino terminus of tau inhibits kinesin-dependent axonal transport: Implications for filament toxicity. *Journal of Neuroscience Research*, *87*(2), 440–451. https://doi.org/10.1002/jnr.21850

Leal, N. S., Dentoni, G., Schreiner, B., Naia, L., Piras, A., Gra, C., Cattaneo, A., Meli, G., Hamasaki, M., Nilsson, P., & Ankarcrona, M. (2020). Amyloid B-Peptide Increases Mitochondria-Endoplasmic Reticulum Contacts Altering Mitochondrial Function and

Autophagosome Formation in Alzheimer's Disease-Related Models. *Cells*, *9*(2552), 1–21.

Leal, N. S., Schreiner, B., Pinho, C. M., Filadi, R., Wiehager, B., Karlström, H., Pizzo, P., & Ankarcrona, M. (2016). Mitofusin-2 knockdown increases ER–mitochondria contact and decreases amyloid β-peptide production. *Journal of Cellular and Molecular Medicine*, *20*(9), 1686–1695. https://doi.org/10.1111/jcmm.12863

Lee, L., Kosuri, P., & Arancio, O. (2014). Picomolar amyloid-β peptides enhance spontaneous astrocyte calcium transients. *Journal of Alzheimer's Disease*, *38*(1), 49–62. https://doi.org/10.3233/JAD-130740

Lennie, P. (2003). The Cost of Cortical Computation. *Current Biology*, *13*(6), 493–497. https://doi.org/10.1016/S

Lewis, T. L., Turi, G. F., Kwon, S. K., Losonczy, A., & Polleux, F. (2016). Progressive Decrease of Mitochondrial Motility during Maturation of Cortical Axons In Vitro and In Vivo. *Current Biology*, *26*(19), 2602–2608. https://doi.org/10.1016/j.cub.2016.07.064

Li, Y., Rinne, J. O., Mosconi, L., Pirraglia, E., Rusinek, H., Desanti, S., Kemppainen, N., Någren, K., Kim, B. C., Tsui, W., & De Leon, M. J. (2008). Regional analysis of FDG and PIB-PET images in normal aging, mild cognitive impairment, and Alzheimer's disease. *European Journal of Nuclear Medicine and Molecular Imaging*, *35*(12), 2169–2181. https://doi.org/10.1007/s00259-008-0833-y

Liddelow, S. A., & Barres, B. A. (2017). Reactive Astrocytes: Production, Function, and Therapeutic Potential. *Immunity*, *46*(6), 957–967. https://doi.org/10.1016/j.immuni.2017.06.006

Liu, K., Ji, K., Guo, L., Wu, W., Lu, H., Shan, P., & Yan, C. (2014). Mesenchymal stem cells rescue injured endothelial cells in an in vitro ischemia-reperfusion model via tunneling nanotube like structure-mediated mitochondrial transfer. *Microvascular Research*, *92*, 10–18. https://doi.org/10.1016/j.mvr.2014.01.008

Llorente-Folch, I., Rueda, C. B., Pardo, B., Szabadkai, G., Duchen, M. R., & Satrustegui, J. (2015). The regulation of neuronal mitochondrial metabolism by calcium. *Journal of Physiology*, *593*(16), 3447–3462. https://doi.org/10.1113/JP270254

López-Doménech, G., Covill-Cooke, C., Ivankovic, D., Halff, E. F., Sheehan, D. F., Norkett, R., Birsa, N., & Kittler, J. T. (2018). Miro proteins coordinate microtubule- and actin-dependent mitochondrial transport and distribution. *The EMBO Journal*, *37*(3), 321–336. https://doi.org/10.15252/embj.201696380

MacAskill, A. F., Brickley, K., Stephenson, F. A., & Kittler, J. T. (2009). GTPase dependent recruitment of Grif-1 by Miro1 regulates mitochondrial trafficking in hippocampal neurons. *Molecular and Cellular Neuroscience*, *40*(3), 301–312. https://doi.org/10.1016/j.mcn.2008.10.016

MacAskill, A. F., Rinholm, J. E., Twelvetrees, A. E., Arancibia-Carcamo, I. L., Muir, J., Fransson, A., Aspenstrom, P., Attwell, D., & Kittler, J. T. (2009). Miro1 Is a Calcium Sensor for Glutamate Receptor-Dependent Localization of Mitochondria at Synapses. *Neuron*, *61*(4), 541–555. https://doi.org/10.1016/j.neuron.2009.01.030

MacLean-Fletcher, S., & Pollard, T. D. (1980). Mechanism of action of cytochalasin B on actin. *Cell*, *20*(2), 329–341. https://doi.org/10.1016/0092-8674(80)90619-4

Magistretti, P. J. (2006). Neuron-glia metabolic coupling and plasticity. *Journal of Experimental Biology*, *209*(12) 2304–2311. https://doi.org/10.1242/jeb.02208

Mahley, R. W. (2016). Central Nervous System Lipoproteins: ApoE and Regulation of Cholesterol Metabolism. *Arteriosclerosis, Thrombosis, and Vascular Biology*, *36*(7), 1305–1315. https://doi.org/10.1201/9781315164533

Manczak, M., Anekonda, T. S., Henson, E., Park, B. S., Quinn, J., & Reddy, P. H. (2006). Mitochondria are a direct site of Aβ accumulation in Alzheimer's disease neurons: Implications for free radical generation and oxidative damage in disease progression. *Human Molecular Genetics*, *15*(9), 1437–1449. https://doi.org/10.1093/hmg/ddl066

Manczak, M., Calkins, M. J., & Reddy, P. H. (2011). Impaired mitochondrial dynamics and abnormal interaction of amyloid beta with mitochondrial protein Drp1 in neurons from patients with Alzheimer's disease: Implications for neuronal damage. *Human Molecular Genetics*, *20*(13), 2495–2509. https://doi.org/10.1093/hmg/ddr139

Manczak, M., & Reddy, P. H. (2012). Abnormal interaction between the mitochondrial fission protein Drp1 and hyperphosphorylated tau in Alzheimer's disease neurons: Implications for mitochondrial dysfunction and neuronal damage. *Human Molecular Genetics*, *21*(11), 2538–2547. https://doi.org/10.1093/hmg/dds072

Mandelkow, E. M., Biernat, J., Drewes, G., Gustke, N., Trinczek, B., & Mandelkow, E. (1995). Tau domains, phosphorylation, and interactions with microtubules. *Neurobiology of Aging*, *16*(3), 355–362. https://doi.org/10.1016/0197-4580(95)00025-A

Masters, C. L., Simms, G., Weinman, N. A., Multhaup, G., McDonald, B. L., & Beyreuther, K. (1985). Amyloid plaque core protein in Alzheimer disease and Down syndrome. *Proceedings of the National Academy of Sciences of the United States of America*, *82*(12), 4245–4249. https://doi.org/10.1073/pnas.82.12.4245

Masters, Colin L., Bateman, R., Blennow, K., Rowe, C. C., Sperling, R. A., & Cummings, J. L. (2015). Alzheimer's disease. *Nature Reviews Disease Primers*, *1*, 1–18. https://doi.org/10.1038/nrdp.2015.56

Mastroeni, D., Khdour, O. M., Delvaux, E., Nolz, J., Olsen, G., Berchtold, N., Cotman, C., Hecht, S. M., & Coleman, P. D. (2017). Nuclear but not mitochondrial-encoded oxidative phosphorylation genes are altered in aging, mild cognitive impairment, and Alzheimer's disease. *Alzheimer's Dementia*, *13*(5), 510–519. https://doi.org/10.1016/j.jalz.2016.09.003.Nuclear

Masuzawa, A., Black, K. M., Pacak, C. A., Ericsson, M., Barnett, R. J., Drumm, C., Seth, P., Bloch, D. B., Levitsky, S., Cowan, D. B., & McCully, J. D. (2013). Transplantation of autologously derived mitochondria protects the heart from ischemia-reperfusion injury. *American Journal of Physiology - Heart and Circulatory Physiology*, *304*(7), 966–982. https://doi.org/10.1152/ajpheart.00883.2012

Matsuoka, Y., Picciano, M., Maleste, B., LaFrancois, J., Zehr, C., Daeschner, J. A. M., Olschowka,

J. A., Fonseca, M. I., O'Banion, M. K., Tenner, A. J., Lemere, C. A., & Duff, K. (2001). Inflammatory responses to amyloidosis in a transgenic mouse model of Alzheimer's disease. *American Journal of Pathology*, *158*(4), 1345–1354. https://doi.org/10.1016/S0002-9440(10)64085-0

Mcmanus, M. J., Murphy, M. P., & Franklin, J. L. (2011). The mitochondria-targeted antioxidant mitoq prevents loss of spatial memory retention and early neuropathology in a transgenic mouse model of Alzheimer's disease. *Journal of Neuroscience*, *31*(44), 15703–15715. https://doi.org/10.1523/JNEUROSCI.0552-11.2011

Merlini, M., Meyer, E. P., Ulmann-Schuler, A., & Nitsch, R. M. (2011). Vascular β-amyloid and early astrocyte alterations impair cerebrovascular function and cerebral metabolism in transgenic arcAβ mice. *Acta Neuropathologica*, *122*(3), 293–311. https://doi.org/10.1007/s00401-011-0834-y

Miller, K. E., & Sheetz, M. P. (2004). Axonal mitochondrial transport and potential are correlated. *Journal of Cell Science*, *117*(13), 2791–2804. https://doi.org/10.1242/jcs.01130

Misko, A., Jiang, S., Wegorzewska, I., Milbrandt, J., & Baloh, R. H. (2010). Mitofusin 2 is necessary for transport of axonal mitochondria and interacts with the Miro/Milton complex. *Journal of Neuroscience*, *30*(12), 4232–4240. https://doi.org/10.1523/JNEUROSCI.6248-09.2010

Mitew, S., Kirkcaldie, M. T. K., Dickson, T. C., & Vickers, J. C. (2013). Altered synapses and gliotransmission in Alzheimer's disease and AD model mice. *Neurobiology of Aging*, *34*(10), 2341–2351. https://doi.org/10.1016/j.neurobiolaging.2013.04.010

Mittler, R. (2017). ROS Are Good. *Trends in Plant Science*, *22*(1), 11–19. https://doi.org/10.1016/j.tplants.2016.08.002

Mizushima, N. (2007). Autophagy: process and function. *Genes and Development, 21*, 2861-2873. https://doi.org/10.1101/gad.1599207

Mohammadalipour, A., Dumbali, S. P., & Wenzel, P. L. (2020). Mitochondrial Transfer and Regulators of Mesenchymal Stromal Cell Function and Therapeutic Efficacy. *Frontiers in Cell and Developmental Biology*, *8*(603292). https://doi.org/10.3389/fcell.2020.603292

Morales, I., Sanchez, A., Puertas-Avendaño, R., Rodriguez-Sabate, C., Perez-Barreto, A., & Rodriguez, M. (2020). Neuroglial transmitophagy and Parkinson's disease. *Glia*, *68*(11), 2277–2299. https://doi.org/10.1002/glia.23839

Mota, S. I., Ferreira, I. L., & Rego, A. C. (2014). Dysfunctional synapse in Alzheimer's disease - A focus on NMDA receptors. *Neuropharmacology*, *76*(PART A), 16–26. https://doi.org/10.1016/j.neuropharm.2013.08.013

Mozdy, A. D., McCaffery, J. M., & Shaw, J. M. (2000). Dnm1p GTPase-mediated mitochondrial fission is a multi-step process requiring the novel integral membrane component Fis1p. *Journal of Cell Biology*, *151*(2), 367–379. https://doi.org/10.1083/jcb.151.2.367

Muraoka, S., DeLeo, A. M., Sethi, M. K., Yukawa-Takamatsu, K., Yang, Z., Ko, J., Hogan, J. D., Ruan, Z., You, Y., Wang, Y., Medalla, M., Ikezu, S., Chen, M., Xia, W., Gorantla, S., Gendelman, H. E., Issadore, D., Zaia, J., & Ikezu, T. (2020). Proteomic and biological

profiling of extracellular vesicles from Alzheimer's disease human brain tissues. *Alzheimer's and Dementia*, *16*(6), 896–907. https://doi.org/10.1002/alz.12089

Muraoka, S., Jedrychowski, M. P., Yanamandra, K., Ikezu, S., Gygi, S. P., & Ikezu, T. (2020). Proteomic Profiling of Extracellular Vesicles Derived from Cerebrospinal Fluid of Alzheimer's Disease Patients: A Pilot Study. *Cells*, *9*(9). https://doi.org/10.3390/cells9091959

Murray, L. M. A., & Krasnodembskaya, A. D. (2019). Concise Review: Intercellular Communication Via Organelle Transfer in the Biology and Therapeutic Applications of Stem Cells. *Stem Cells*, *37*(1), 14–25. https://doi.org/10.1002/stem.2922

Nagele, R. G., D'Andrea, M. R., Lee, H., Venkataraman, V., & Wang, H. Y. (2003). Astrocytes accumulate Aβ42 and give rise to astrocytic amyloid plaques in Alzheimer disease brains. *Brain Research*, *971*(2), 197–209. https://doi.org/10.1016/S0006-8993(03)02361-8

Nagelhus, E. A., Mathiisen, T. M., & Ottersen, O. P. (2004). Aquaporin-4 in the central nervous system: Cellular and subcellular distribution and coexpression with KIR4.1. *Neuroscience*, *129*(4), 905–913. https://doi.org/10.1016/j.neuroscience.2004.08.053

Naia, L., Pinho, C. M., Dentoni, G., Liu, J., Leal, N. S., Ferreira, D. M. S., Schreiner, B., Filadi, R., Fão, L., Connolly, N. M. C., Forsell, P., Nordvall, G., Shimozawa, M., Greotti, E., Basso, E., Theurey, P., Gioran, A., Joselin, A., Arsenian-Henriksson, M., Ankarcrona, M. (2021). Neuronal cell-based high-throughput screen for enhancers of mitochondrial function reveals luteolin as a modulator of mitochondria-endoplasmic reticulum coupling. *BMC Biology*, *19*(1). https://doi.org/10.1186/s12915-021-00979-5

Newmeyer, D. D., & Ferguson-Miller, S. (2003). Mitochondria: Releasing power for life and unleashing the machineries of death. *Cell*, *112*(6). https://doi.org/10.1016/S0092-8674(03)00195-8

Nilsen, L. H., Witter, M. P., & Sonnewald, U. (2014). Neuronal and astrocytic metabolism in a transgenic rat model of Alzheimer's disease. *Journal of Cerebral Blood Flow and Metabolism*, *34*(5), 906–914. https://doi.org/10.1038/jcbfm.2014.37

O'brien, R. J., & Wong, P. C. (2011). Amyloid Precursor Protein Processing and Alzheimer's Disease. *Annual Review of Neuroscience, 34*, 185-204. https://doi.org/10.1146/annurev-neuro-061010-113613

Oddo, S., Caccamo, A., Kitazawa, M., Tseng, B. P., & LaFerla, F. M. (2003). Amyloid deposition precedes tangle formation in a triple transgenic model of Alzheimer's disease. *Neurobiology of Aging*, *24*(8), 1063–1070. https://doi.org/10.1016/j.neurobiolaging.2003.08.012

Oddo, S., Caccamo, A., Shepherd, J. D., Murphy, M. P., Golde, T. E., Kayed, R., Metherate, R., Mattson, M. P., Akbari, Y., & LaFerla, F. M. (2003). Triple-transgenic model of Alzheimer's Disease with plaques and tangles: Intracellular Aβ and synaptic dysfunction. *Neuron*, *39*(3), 409–421. https://doi.org/10.1016/S0896-6273(03)00434-3

Okamura, N., & Yanai, K. (2017). Brain imaging: Applications of tau PET imaging. *Nature Review Neurology,* 13(4), 197-198. https://doi.org/10.1038/nrneurol.2017.38

Oliet, S. H. R., & Mothet, J. P. (2009). Regulation of N-methyl-d-aspartate receptors by astrocytic

d-serine. *Neuroscience, 158(*1), 275–283. https://doi.org/10.1016/j.neuroscience.2008.01.071

Oliver, D. M., & Hemachandra Reddy, P. (2019). Molecular Basis of Alzheimer's Disease: Focus on Mitochondria. *Journal of Alzheimer's Disease 72*, S95–S116. https://doi.org/10.3233/JAD-190048

Osellame, L. D., Blacker, T. S., & Duchen, M. R. (2012). Cellular and molecular mechanisms of mitochondrial function. *Best Practice and Research: Clinical Endocrinology and Metabolism*, *26*(6), 711–723. https://doi.org/10.1016/j.beem.2012.05.003

Otera, H., Ishihara, N., & Mihara, K. (2013). New insights into the function and regulation of mitochondrial fission. *Biochimica et Biophysica Acta - Molecular Cell Research*, *1833*(5), 1256–1268. https://doi.org/10.1016/j.bbamcr.2013.02.002

Palikaras, K., Lionaki, E., & Tavernarakis, N. (2018). Mechanisms of mitophagy in cellular homeostasis, physiology and pathology. *Nature Cell Biology, 20*(9) 1013–1022. https://doi.org/10.1038/s41556-018-0176-2

Pathak, D., Shields, L. Y., Mendelsohn, B. A., Haddad, D., Lin, W., Gerencser, A. A., Kim, H., Brand, M. D., Edwards, R. H., & Nakamura, K. (2015). The role of mitochondrially derived ATP in synaptic vesicle recycling. *Journal of Biological Chemistry*, *290*(37), 22325–22336. https://doi.org/10.1074/jbc.M115.656405

Pavlov, P. F., Wiehager, B., Sakai, J., Frykman, S., Behbahani, H., Winblad, B., & Ankarcrona, M. (2011). Mitochondrial γ-secretase participates in the metabolism of mitochondria-associated amyloid precursor protein. *The FASEB Journal*, *25*(1), 78–88. https://doi.org/10.1096/fj.10-157230

Pearson, H. A., & Peers, C. (2006). Physiological roles for amyloid β peptides. *Journal of Physiology*, *575*(1), 5–10. https://doi.org/10.1113/jphysiol.2006.111203

Perea, G., Navarrete, M., & Araque, A. (2009). Tripartite synapses: astrocytes process and control synaptic information. *Trends in Neurosciences*, *32*(8), 421–431. https://doi.org/10.1016/j.tins.2009.05.001

Perez Ortiz, J. M., & Swerdlow, R. H. (2019). Mitochondrial dysfunction in Alzheimer's disease: Role in pathogenesis and novel therapeutic opportunities. *British Journal of Pharmacology*, *176*(18), 3489–3507. https://doi.org/10.1111/bph.14585

Peruzzotti-Jametti, L., Bernstock, J. D., Willis, C. M., Manferrari, G., Rogall, R., Fernandez-Vizarra, E., Williamson, J. C., Braga, A., van den Bosch, A., Leonardi, T., Krzak, G., Kittel, Á., Benincá, C., Vicario, N., Tan, S., Bastos, C., Bicci, I., Iraci, N., Smith, J. A., Pluchino, S. (2021). Neural stem cells traffic functional mitochondria via extracellular vesicles. *PLoS Biology*, *19*(4), e3001166. https://doi.org/10.1371/journal.pbio.3001166

Phelps, C. H. (1972). Barbiturate-induced glycogen accumulation in brain. An electron microscopic study. *Brain Research*, *39*(1), 225–234. https://doi.org/10.1016/0006-8993(72)90797-4

Phinney, D. G., Di Giuseppe, M., Njah, J., Sala, E., Shiva, S., St Croix, C. M., Stolz, D. B., Watkins, S. C., Di, Y. P., Leikauf, G. D., Kolls, J., Riches, D. W. H., Deiuliis, G., Kaminski, N.,

Boregowda, S. V, McKenna, D. H., & Ortiz, L. A. (2015). Mesenchymal stem cells use extracellular vesicles to outsource mitophagy and shuttle microRNAs. *Nature Communications*, *6*, 1–15. https://doi.org/10.1038/ncomms9472

Pilling, A. D., Horiuchi, D., Lively, C. M., & Saxton, W. M. (2006). Kinesin-1 and dynein are the primary motors for fast transport of mitochondria in Drosophila motor axons. *Molecular Biology of the Cell*, *17*(4), 2057–2068. https://doi.org/10.1091/mbc.E05-06-0526

Price, J. L., McKeel, D. W., Buckles, V. D., Roe, C. M., Xiong, C., Grundman, M., Hansen, L. A., Petersen, R. C., Parisi, J. E., Dickson, D. W., Smith, C. D., Davis, D. G., Schmitt, F. A., Markesbery, W. R., Kaye, J., Kurlan, R., Hulette, C., Kurland, B. F., Higdon, R., Morris, J. C. (2009). Neuropathology of nondemented aging: Presumptive evidence for preclinical Alzheimer disease. *Neurobiology of Aging*, *30*(7), 1026–1036. https://doi.org/10.1016/j.neurobiolaging.2009.04.002

Qi, G., Mi, Y., Shi, X., Gu, H., Brinton, R. D., & Yin, F. (2021). ApoE4 Impairs Neuron-Astrocyte Coupling of Fatty Acid Metabolism. *Cell Reports*, *34*(1), 108572. https://doi.org/10.1016/j.celrep.2020.108572

Qin, W., Haroutunian, V., Katsel, P., Cardozo, C. P., Ho, L., Buxbaum, J. D., & Pasinetti, G. M. (2009). PGC-1α expression decreases in the Alzheimer disease brain as a function of dementia. *Archives of Neurology*, *66*(3), 352–361. https://doi.org/10.1001/archneurol.2008.588

Querfurth, H. W., & Laferla, F. M. (2010). *Alzheimer's Disease*. *9*, 329–344.

Rangaraju, V., Calloway, N., & Ryan, T. A. (2014). Activity-driven local ATP synthesis is required for synaptic function. *Cell*, *156*(4), 825–835. https://doi.org/10.1016/j.cell.2013.12.042

Rangaraju, V., Lewis, T. L., Hirabayashi, Y., Bergami, M., Motori, E., Cartoni, R., Kwon, S. K., & Courchet, J. (2019). Pleiotropic Mitochondria: The Influence of Mitochondria on Neuronal Development and Disease. *The Journal of Neuroscience : The Official Journal of the Society for Neuroscience*, *39*(42), 8200–8208. https://doi.org/10.1523/JNEUROSCI.1157-19.2019

Reddy, P. H., Tripathi, R., Troung, Q., Tirumala, K., Reddy, T. P., Anekonda, V., Shirendeb, U. P., Calkins, M. J., Reddy, A. P., Mao, P., & Manczak, M. (2012). Abnormal mitochondrial dynamics and synaptic degeneration as early events in Alzheimer's disease: Implications to mitochondria-targeted antioxidant therapeutics. *Biochimica et Biophysica Acta - Molecular Basis of Disease*, *1822*(5), 639–649. https://doi.org/10.1016/j.bbadis.2011.10.011

Rizzuto, R., Pinton, P., Carrington, W., Fay, F. S., Fogarty, K. E., Lifshitz, L. M., Tuft, R. A., & Pozzan, T. (1998). Close contacts with the endoplasmic reticulum as determinants of mitochondrial Ca2+ responses. *Science*, *280*(5370), 1763–1766. https://doi.org/10.1126/science.280.5370.1763

Robinson, S. R. (2000). Neuronal expression of glutamine synthetase in Alzheimer's disease indicates a profound impairment of metabolic interactions with astrocytes. *Neurochemistry International*, *36*(4–5), 471–482. https://doi.org/10.1016/S0197-0186(99)00150-3

Rodríguez-Martín, T., Cuchillo-Ibáñez, I., Noble, W., Nyenya, F., Anderton, B. H., & Hanger, D. P. (2013). Tau phosphorylation affects its axonal transport and degradation. *Neurobiology*

of Aging, *34*(9), 2146–2157. https://doi.org/10.1016/j.neurobiolaging.2013.03.015

Roßner, S., Apelt, J., Schliebs, R., Perez-Polo, J. R., & Bigl, V. (2001). Neuronal and glial β-secretase (BACE) protein expression in transgenic Tg2576 mice with amyloid plaque pathology. *Journal of Neuroscience Research*, *64*(5), 437–446. https://doi.org/10.1002/jnr.10069

Roßner, Steffen, Lange-Dohna, C., Zeitschel, U., & Perez-Polo, J. R. (2005). Alzheimer's disease β-secretase BACE1 is not a neuron-specific enzyme. *Journal of Neurochemistry*, *92*(2) 226–234. https://doi.org/10.1111/j.1471-4159.2004.02857.x

Roussarie, J. P., Yao, V., Rodriguez-Rodriguez, P., Oughtred, R., Rust, J., Plautz, Z., Kasturia, S., Albornoz, C., Wang, W., Schmidt, E. F., Dannenfelser, R., Tadych, A., Brichta, L., Barnea-Cramer, A., Heintz, N., Hof, P. R., Heiman, M., Dolinski, K., Flajolet, M., Greengard, P. (2020). Selective Neuronal Vulnerability in Alzheimer's Disease: A Network-Based Analysis. *Neuron*, *107*(5), 821-835.e12. https://doi.org/10.1016/j.neuron.2020.06.010

Rowland, A. A., & Voeltz, G. K. (2012). Endoplasmic reticulum-mitochondria contacts: Function of the junction. *Nature Reviews Molecular Cell Biology*, *13*(10), 607–615. https://doi.org/10.1038/nrm3440

Ruffinatti, F., Tapella, L., Gregnanin, I., Stevano, A., Chiorino, G., Canonico, P. L., Distasi, C., Genazzani, A. A., & Lim, D. (2018). Transcriptional Remodeling in Primary Hippocampal Astrocytes from an Alzheimer's Disease Mouse Model. *Current Alzheimer Research*, *15*(11), 986–1004. https://doi.org/10.2174/1567205015666180613113924

Russo, G. J., Louie, K., Wellington, A., Macleod, G. T., Hu, F., Panchumarthi, S., & Zinsmaier, K. E. (2009). Drosophila Miro is required for both anterograde and retrograde axonal mitochondrial transport. *Journal of Neuroscience*, *29*(17), 5443–5455. https://doi.org/10.1523/JNEUROSCI.5417-08.2009

Rustom, A., Saffrich, R., Markovic, I., Walther, P., & Gerdes, H. H. (2004). Nanotubular Highways for Intercellular Organelle Transport. *Science*, *303*(5660), 1007–1010. https://doi.org/10.1126/science.1093133

Safieh, M., Korczyn, A. D., & Michaelson, D. M. (2019). ApoE4: an emerging therapeutic target for Alzheimer's disease. *BMC Medicine*, *17*(1), 64. https://doi.org/10.1186/s12916-019-1299-4

Saito, T., Matsuba, Y., Mihira, N., Takano, J., Nilsson, P., Itohara, S., Iwata, N., & Saido, T. C. (2014). Single App knock-in mouse models of Alzheimer's disease. *Nature Neuroscience*, *17*(5), 661–663. https://doi.org/10.1038/nn.3697

Saito, T., Matsuba, Y., Yamazaki, N., Hashimoto, S., & Saido, T. C. (2016). Calpain activation in Alzheimer's model mice is an artifact of APP and presenilin overexpression. *Journal of Neuroscience*, *36*(38), 9933–9936. https://doi.org/10.1523/JNEUROSCI.1907-16.2016

Saotome, M., Safiulina, D., Rgy Szabadkai, G., Das, S., Fransson, Å., Aspenstrom, P., Rizzuto, R., Rgy, G., & Czky, H. (2008). Bidirectional Ca 2-dependent control of mitochondrial dynamics by the Miro GTPase. *Proceedings of the National Academy of Sciences*, *105*(52), 20728-20733. https://doi.org/10.1073/pnas.0808953105

Saura, J., Tusell, J. M., & Serratosa, J. (2003). High-Yield Isolation of Murine Microglia by Mild Trypsinization. *GLIA*, *44*(3), 183–189. https://doi.org/10.1002/glia.10274

Schreiner, B., Hedskog, L., Wiehager, B., & Ankarcrona, M. (2015). Amyloid-β peptides are generated in mitochondria-associated endoplasmic reticulum membranes. *Journal of Alzheimer's Disease*, *43*(2), 369–374. https://doi.org/10.3233/JAD-132543

Schubert, D., Soucek, T., & Blouw, B. (2009). The induction of HIF-1 reduces astrocyte activation by amyloid beta peptide. *European Journal of Neuroscience*, *29*(7), 1323–1334. https://doi.org/10.1111/j.1460-9568.2009.06712.x

Sheng, B., Wang, X., Su, B., Lee, H. G., Casadesus, G., Perry, G., & Zhu, X. (2012). Impaired mitochondrial biogenesis contributes to mitochondrial dysfunction in Alzheimer's disease. *Journal of Neurochemistry*, *120*(3), 419–429. https://doi.org/10.1111/j.1471-4159.2011.07581.x

Sheng, Z. H. (2014). Mitochondrial trafficking and anchoring in neurons: New insight and implications. *Journal of Cell Biology,* 204(7), 1087–1098. https://doi.org/10.1083/jcb.201312123

Sheng, Z. H., & Cai, Q. (2012). Mitochondrial transport in neurons: Impact on synaptic homeostasis and neurodegeneration. *Nature Reviews Neuroscience*, *13*(2), 77–93. https://doi.org/10.1038/nrn3156

Shi, X., Zhao, M., Fu, C., & Fu, A. (2017). Intravenous administration of mitochondria for treating experimental Parkinson's disease. *Mitochondrion*, *34*, 91–100. https://doi.org/10.1016/j.mito.2017.02.005

Shiba-Fukushima, K., Imai, Y., Yoshida, S., Ishihama, Y., Kanao, T., Sato, S., & Hattori, N. (2012). PINK1-mediated phosphorylation of the Parkin ubiquitin-like domain primes mitochondrial translocation of Parkin and regulates mitophagy. *Scientific Reports*, *2*(1002), 1–8. https://doi.org/10.1038/srep01002

Simonovitch, S., Schmukler, E., Bespalko, A., Iram, T., Frenkel, D., Holtzman, D. M., Masliah, E., Michaelson, D. M., & Pinkas-Kramarski, R. (2016). Impaired Autophagy in APOE4 Astrocytes. *Journal of Alzheimer's Disease*, *51*(3), 915–927. https://doi.org/10.3233/JAD-151101

Simpson, J. E., Ince, P. G., Lace, G., Forster, G., Shaw, P. J., Matthews, F., Savva, G., Brayne, C., & Wharton, S. B. (2010). Astrocyte phenotype in relation to Alzheimer-type pathology in the ageing brain. *Neurobiology of Aging*, *31*(4), 578–590. https://doi.org/10.1016/j.neurobiolaging.2008.05.015

Sinclair, K. A., Yerkovich, S. T., Hopkins, P. M. A., & Chambers, D. C. (2016). Characterization of intercellular communication and mitochondrial donation by mesenchymal stromal cells derived from the human lung. *Stem Cell Research and Therapy*, *7*(1), 1–10. https://doi.org/10.1186/s13287-016-0354-8

Smirnova, E., Griparic, L., Shurland, D. L., & Van der Bliek, A. M. (2001). Dynamin-related protein Drp1 is required for mitochondrial division in mammalian cells. *Molecular Biology of the Cell*, *12*(8), 2245–2256. https://doi.org/10.1091/mbc.12.8.2245

Smit-Rigter, L., Rajendran, R., Silva, C. A. P., Spierenburg, L., Groeneweg, F., Ruimschotel, E. M., van Versendaal, D., van der Togt, C., Eysel, U. T., Heimel, J. A., Lohmann, C., & Levelt, C. N. (2016). Mitochondrial Dynamics in Visual Cortex Are Limited In Vivo and Not Affected by Axonal Structural Plasticity. *Current Biology*, *26*(19), 2609–2616. https://doi.org/10.1016/j.cub.2016.07.033

Sofroniew, M. V. (2015). Astrocyte barriers to neurotoxic inflammation. *Nature Reviews Neuroscience*, *16*(5), 249–263. https://doi.org/10.1038/nrn3898

Sofroniew, M. V., & Vinters, H. V. (2010). Astrocytes: Biology and pathology. *Acta Neuropathologica*, *119*(1), 7–35. https://doi.org/10.1007/s00401-009-0619-8

Soucek, T., Cumming, R., Dargusch, R., Maher, P., & Schubert, D. (2003). The regulation of glucose metabolism by HIF-1 mediates a neuroprotective response to amyloid beta peptide. *Neuron*, *39*(1), 43–56. https://doi.org/10.1016/S0896-6273(03)00367-2

Spees, J. L., Olson, S. D., Whitney, M. J., & Prockop, D. J. (2006). Mitochondrial transfer between cells can rescue aerobic respiration. *Proceedings of the National Academy of Sciences of the United States of America*, *103*(5), 1283–1288. https://doi.org/10.1073/pnas.0510511103

Stelzmann, R. A., Norman Schnitzlein, H., & Reed Murtagh, F. (1995). An english translation of alzheimer's 1907 paper, "über eine eigenartige erkankung der hirnrinde." *Clinical Anatomy*, *8*(6), 429–431. https://doi.org/10.1002/ca.980080612

Stephen, T. L., Higgs, N. F., Sheehan, D. F., Awabdh, S. Al, López-Doménech, G., Arancibia-Carcamo, I. L., & Kittler, J. T. (2015). Miro1 regulates activity-driven positioning of mitochondria within astrocytic processes apposed to synapses to regulate intracellular calcium signaling. *Journal of Neuroscience*, *35*(48), 15996–16011. https://doi.org/10.1523/JNEUROSCI.2068-15.2015

Strappazzon, F., Nazio, F., Corrado, M., Cianfanelli, V., Romagnoli, A., Fimia, G. M., Campello, S., Nardacci, R., Piacentini, M., Campanella, M., & Cecconi, F. (2015). AMBRA1 is able to induce mitophagy via LC3 binding, regardless of PARKIN and p62/SQSTM1. *Cell Death and Differentiation*, *22*(3), 419–432. https://doi.org/10.1038/cdd.2014.139

Sun, N., Malide, D., Liu, J., Rovira, I. I., Combs, C. A., & Finkel, T. (2017). A fluorescence-based imaging method to measure in vitro and in vivo mitophagy using mt-Keima. *Nature Protocols*, *12*(8), 1576–1587. https://doi.org/10.1038/nprot.2017.060

Sun, T., Qiao, H., Pan, P. Y., Chen, Y., & Sheng, Z. H. (2013). Motile axonal mitochondria contribute to the variability of presynaptic strength. *Cell Reports*, *4*(3), 413–419. https://doi.org/10.1016/j.celrep.2013.06.040

Swerdlow, R. H., & Khan, S. M. (2004). A "mitochondrial cascade hypothesis" for sporadic Alzheimer's disease. *Medical Hypotheses*, *63*(1), 8–20. https://doi.org/10.1016/j.mehy.2003.12.045

Talantova, M., Sanz-Blasco, S., Zhang, X., Akhtar, M. W., Okamoto, S., Dziewczpolski, G., Nakamura, T., Cao, G., Pratt, A. E., Kang, Y.-J., Tu, S., Molokanova, E., McKercher, S. R., Hire, S. A., Sason, H., Stouffer, D. G., Buczynski, M. W., Solomon, J. P., Michale, S., … Lipton, S. A. (2013). Aβ induces astrocytic glutamate release, extrasynaptic NMDA receptor

activation, and synaptic loss. *Proceedings of the National Academy of Sciences of the United States of America*, *110*(27), E2518–E2527. https://doi.org/10.1073/pnas.1300532110

Tanaka, Y., Kanai, Y., Okada, Y., Nonaka, S., Takeda, S., Harada, A., & Hirokawa, N. (1998). Targeted disruption of mouse conventional kinesin heavy chain, kif5B, results in abnormal perinuclear clustering of mitochondria. *Cell*, *93*(7), 1147–1158. https://doi.org/10.1016/S0092-8674(00)81459-2

Tang, M. X., Maestre, G., Tsai, W. Y., Liu, X. H., Feng, L., Chung, W. Y., Chun, M., Schofield, P., Stern, Y., Tycko, B., & Mayeux, R. (1996). Effect of age, ethnicity, and head injury on the association between APOE genotypes and Alzheimer's disease. *American Journal of Human Genetics*, *58*(3), 574–584. https://doi.org/10.1111/j.1749-6632.1996.tb32593.x

Tang, Y. G., & Zucker, R. S. (1997). Mitochondrial involvement in post-tetanic potentiation of synaptic transmission. *Neuron*, *18*(3), 483–491. https://doi.org/10.1016/S0896-6273(00)81248-9

Terry, R. D., Masliah, E., Salmon, D. P., Butters, N., DeTeresa, R., Hill, R., Hansen, L. A., & Katzman, R. (1991). Physical Basis of Cognitive Alteration in Alzheimer's Disease: Synapse Loss is the Major Correlate of Cognitive Impairment. *Annals of Neurology*, *30*(4), 572–580.

Tieu, Q., & Nunnari, J. (2000). Mdv1p is a WD repeat protein that interacts with the dynamin-related GTPase, Dnm1p, to trigger mitochondrial division. *Journal of Cell Biology*, *151*(2), 353–365. https://doi.org/10.1083/jcb.151.2.353

Tilokani, L., Nagashima, S., Paupe, V., & Prudent, J. (2018). Mitochondrial dynamics: Overview of molecular mechanisms. *Essays in Biochemistry*, *62*(3), 341–360. https://doi.org/10.1042/EBC20170104

Torralba, D., Baixauli, F., & Sánchez-Madrid, F. (2016). Mitochondria know no boundaries: Mechanisms and functions of intercellular mitochondrial transfer. In *Frontiers in Cell and Developmental Biology, 4*(107). https://doi.org/10.3389/fcell.2016.00107

van Humbeeck, C., Cornelissen, T., Hofkens, H., Mandemakers, W., Gevaert, K., de Strooper, B., & Vandenberghe, W. (2011). Parkin interacts with ambra1 to induce mitophagy. *Journal of Neuroscience*, *31*(28), 10249–10261. https://doi.org/10.1523/JNEUROSCI.1917-11.2011

van Spronsen, M., Mikhaylova, M., Lipka, J., Schlager, M. A., van den Heuvel, D. J., Kuijpers, M., Wulf, P. S., Keijzer, N., Demmers, J., Kapitein, L. C., Jaarsma, D., Gerritsen, H. C., Akhmanova, A., & Hoogenraad, C. C. (2013). TRAK/Milton Motor-Adaptor Proteins Steer Mitochondrial Trafficking to Axons and Dendrites. *Neuron*, *77*(3), 485–502. https://doi.org/10.1016/j.neuron.2012.11.027

Verstreken, P., Ly, C. V., Venken, K. J. T., Koh, T. W., Zhou, Y., & Bellen, H. J. (2005). Synaptic mitochondria are critical for mobilization of reserve pool vesicles at Drosophila neuromuscular junctions. *Neuron*, *47*(3), 365–378. https://doi.org/10.1016/j.neuron.2005.06.018

Volobouева, L. A., Suh, S. W., Swanson, R. A., & Giffard, R. G. (2007). Inhibition of mitochondrial function in astrocytes: Implications for neuroprotection. *Journal of Neurochemistry*, *102*(4),

1383–1394. https://doi.org/10.1111/j.1471-4159.2007.04634.x

Von Kleist, L., Stahlschmidt, W., Bulut, H., Gromova, K., Puchkov, D., Robertson, M. J., MacGregor, K. A., Tomlin, N., Pechstein, A., Chau, N., Chircop, M., Sakoff, J., Von Kries, J. P., Saenger, W., Kräusslich, H. G., Shupliakov, O., Robinson, P. J., McCluskey, A., & Haucke, V. (2011). Role of the clathrin terminal domain in regulating coated pit dynamics revealed by small molecule inhibition. *Cell*, *146*(3), 471–484. https://doi.org/10.1016/j.cell.2011.06.025

Wang, X., & Gerdes, H. H. (2015). Transfer of mitochondria via tunneling nanotubes rescues apoptotic PC12 cells. *Cell Death and Differentiation*, *22*(7), 1181–1191. https://doi.org/10.1038/cdd.2014.211

Wang, Xiang, Bukoreshtliev, N. V., & Gerdes, H. H. (2012). Developing Neurons Form Transient Nanotubes Facilitating Electrical Coupling and Calcium Signaling with Distant Astrocytes. *PLoS ONE*, *7*(10), e47429. https://doi.org/10.1371/journal.pone.0047429

Wang, Xinglong, Su, B., Lee, H. G., Li, X., Perry, G., Smith, M. A., & Zhu, X. (2009). Impaired balance of mitochondrial fission and fusion in Alzheimer's disease. *Journal of Neuroscience*, *29*(28), 9090–9103. https://doi.org/10.1523/JNEUROSCI.1357-09.2009

Wang, Xinglong, Su, B., Siedlak, S. L., Moreira, P. I., Fujioka, H., Wang, Y., Casadesus, G., & Zhu, X. (2008). Amyloid-β overproduction causes abnormal mitochondrial dynamics via differential modulation of mitochondrial fission/fusion proteins. *Proceedings of the National Academy of Sciences of the United States of America*, *105*(49), 19318–19323. https://doi.org/10.1073/pnas.0804871105

Wang, Xinnan, & Schwarz, T. L. (2009). The Mechanism of Ca2+-Dependent Regulation of Kinesin-Mediated Mitochondrial Motility. *Cell*, *136*(1), 163–174. https://doi.org/10.1016/j.cell.2008.11.046

Wang, Y., Cui, J., Sun, X., & Zhang, Y. (2011). Tunneling-nanotube development in astrocytes depends on p53 activation. *Cell Death and Differentiation*, *18*(4), 732–742. https://doi.org/10.1038/cdd.2010.147

Wani, W. Y., Boyer-Guittaut, M., Dodson, M., Chatham, J., Darley-Usmar, V., & Zhang, J. (2015). Regulation of autophagy by protein post-translational modification. *Laboratory Investigation*, *95*(1), 14–25. https://doi.org/10.1038/labinvest.2014.131

Weidberg, H., Shvets, E., Shpilka, T., Shimron, F., Shinder, V., & Elazar, Z. (2010). LC3 and GATE-16/GABARAP subfamilies are both essential yet act differently in autophagosome biogenesis. *EMBO Journal*, *29*(11), 1792–1802. https://doi.org/10.1038/emboj.2010.74

Wenk, G. L. (2003). Neuropathologic changes in Alzheimer's disease. *Journal of Clinical Psychiatry*, *64*(SUPPL. 9), 7–10.

Wilkins, H. M., Harris, J. L., Carl, S. M., E, L., Lu, J., Eva Selfridge, J., Roy, N., Hutfles, L., Koppel, S., Morris, J., Burns, J. M., Michaelis, M. L., Michaelis, E. K., Brooks, W. M., & Swerdlow, R. H. (2014). Oxaloacetate activates brain mitochondrial biogenesis, enhances the insulin pathway, reduces inflammation and stimulates neurogenesis. *Human Molecular Genetics*, *23*(24), 6528–6541. https://doi.org/10.1093/hmg/ddu371

Wisniewski, K. E., Wisniewski, H. M., & Wen, G. Y. (1985). Occurrence of neuropathological changes and dementia of Alzheimer's disease in Down's syndrome. *Annals of Neurology*, *17*(3), 278–282. https://doi.org/10.1002/ana.410170310

Wong, Y. C., & Holzbaur, E. L. F. (2014). Optineurin is an autophagy receptor for damaged mitochondria in parkin-mediated mitophagy that is disrupted by an ALS-linked mutation. *Proceedings of the National Academy of Sciences of the United States of America*, *111*(42), E4439–E4448. https://doi.org/10.1073/pnas.1405752111

Wu, W., Tian, W., Hu, Z., Chen, G., Huang, L., Li, W., Zhang, X., Xue, P., Zhou, C., Liu, L., Zhu, Y., Zhang, X., Li, L., Zhang, L., Sui, S., Zhao, B., & Feng, D. (2014). ULK1 translocates to mitochondria and phosphorylates FUNDC1 to regulate mitophagy. *EMBO Reports*, *15*(5), 566–575. https://doi.org/10.1002/embr.201438501

Yang, C. H., Lee, K. H., Ho, W. K., & Lee, S. H. (2021). Inter-spike mitochondrial Ca2+ release enhances high frequency synaptic transmission. *Journal of Physiology*, *599*(5), 1567–1594. https://doi.org/10.1113/JP280351

Yao, Jia; Irwin, Ronald W.; Zhao, Liquin; Nilsen, Jon; Hamilton, Ryan T.; Brinton, R. D. (2009). Mitochondrial bioenergetic deficit precedes Alzheimer's pathology in female mouse model of Alzheimer's diseas. *Proceedings of the National Academy of Sciences of the United States of America*, *106*(34), 14670–14675.

Yin, K. J., Cirrito, J. R., Yan, P., Hu, X., Xiao, Q., Pan, X., Bateman, R., Song, H., Hsu, F. F., Turk, J., Xu, J., Hsu, C. Y., Mills, J. C., Holtzman, D. M., & Lee, J. M. (2006). Matrix metalloproteinases expressed by astrocytes mediate extracellular amyloid-β peptide catabolism. *Journal of Neuroscience*, *26*(43), 10939–10948. https://doi.org/10.1523/JNEUROSCI.2085-06.2006

Zala, D., Hinckelmann, M. V., Yu, H., Lyra Da Cunha, M. M., Liot, G., Cordelières, F. P., Marco, S., & Saudou, F. (2013). Vesicular glycolysis provides on-board energy for fast axonal transport. *Cell*, *152*(3), 479–491. https://doi.org/10.1016/j.cell.2012.12.029

Zamzami, N., & Kroemer, G. (2001). The mitochondrion in apoptosis: How Pandora's box opens. *Nature Reviews Molecular Cell Biology*, *2*(1), 67–71. https://doi.org/10.1038/35048073

Zenisek, D., & Matthews, G. (2000). The role of mitochondria in presynaptic calcium handling at a ribbon synapse. *Neuron*, *25*(1), 229–237. https://doi.org/10.1016/S0896-6273(00)80885-5

Zheng, X., Boyer, L., Jin, M., Mertens, J., Kim, Y., Ma, L., Ma, L., Hamm, M., Gage, F. H., & Hunter, T. (2016). Metabolic reprogramming during neuronal differentiation from aerobic glycolysis to neuronal oxidative phosphorylation. *ELife*, *5*, 1–25. https://doi.org/10.7554/eLife.13374

Zheng, Y., Zhang, X., Wu, X., Jiang, L., Ahsan, A., Ma, S., Xiao, Z., Han, F., Qin, Z. H., Hu, W., & Chen, Z. (2019). Somatic autophagy of axonal mitochondria in ischemic neurons. *Journal of Cell Biology*, *218*(6), 1891–1907. https://doi.org/10.1083/JCB.201804101

Zhou, B., Yu, P., Lin, M. Y., Sun, T., Chen, Y., & Sheng, Z. H. (2016). Facilitation of axon regeneration by enhancing mitochondrial transport and rescuing energy deficits. *Journal of*

Cell Biology, *214*(1), 103–119. https://doi.org/10.1083/jcb.201605101

Zhu, X. H., Qiao, H., Du, F., Xiong, Q., Liu, X., Zhang, X., Ugurbil, K., & Chen, W. (2012). Quantitative imaging of energy expenditure in human brain. *NeuroImage*, *60*(4), 2107–2117. https://doi.org/10.1016/j.neuroimage.2012.02.013

Zhu, X., Perry, G., Smith, M. A., & Wang, X. (2013). Abnormal Mitochondrial Dynamics in the Pathogenesis of Alzheimer's Disease. *Journal of Alzheimer's Disease*, *33*(01), S253–S262. https://doi.org/10.3233/JAD-2012-129005.Abnormal

ATTACHMENTS

1. Authorization for use of Figure 4 – Mitophagy mechanisms

Thank you for your order!

Dear Ms. Maria João Pereira,
Thank you for placing your order through Copyright Clearance Center's RightsLink® service.

Order Summary

Licensee:	Ms. Maria João Pereira
Order Date:	Jun 8, 2021
Order Number:	5084290260452
Publication:	Nature Cell Biology
Title:	Mechanisms of mitophagy in cellular homeostasis, physiology and pathology
Type of Use:	Thesis/Dissertation
Order Total:	0.00 USD

View or print complete details of your order and the publisher's terms and conditions.

Sincerely,

Copyright Clearance Center

Tel: +1-855-239-3415 / +1-978-646-2777
customercare@copyright.com
https://myaccount.copyright.com

CCC RightsLink®

2. Supplementary Figure 1

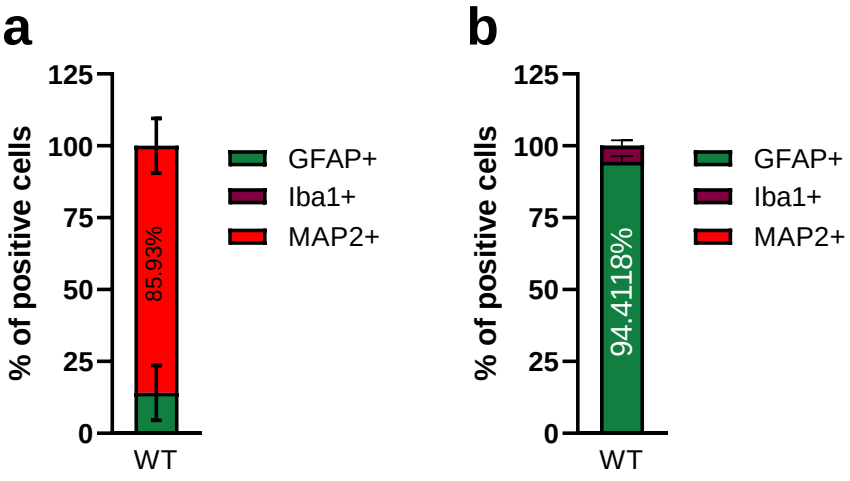

Figure 11 – Characterization of neuronal and astrocytic primary cultures. (a) The bar graph shows the percentage of neurons (MAP2+), astrocytes (GFAP+), and microglia (Iba1+) in neuronal cultures (n=3). **(b)** The bar graph shows the percentage of astrocytes (GFAP+), microglia (Iba1+), and neurons (MAP2+) in astrocytic cultures (n=3). Data presented as mean ± SEM.

3. Supplementary Figure 2

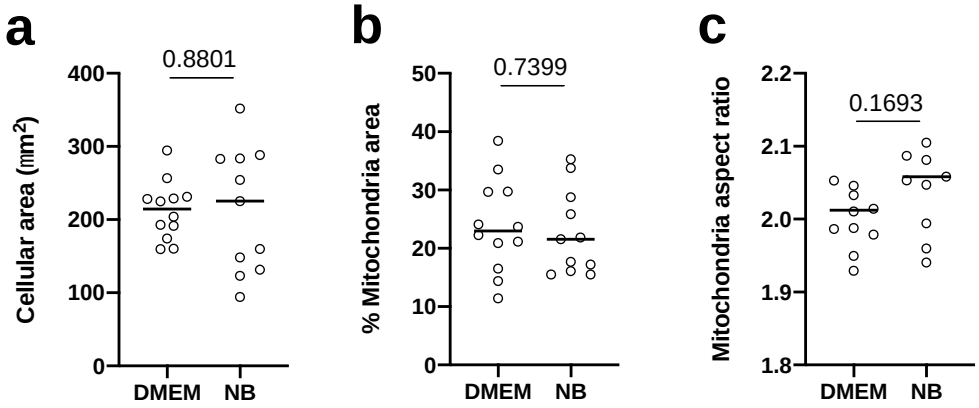

Figure 12 – Astrocytes kept in neurobasal media for 48 h do not present alterations in (a) cellular area, **(b)** cellular area occupied by mitochondria, and **(c)** mitochondrial morphology (n=12-13 from 3 independent cultures). Data presented as mean ± SEM.

4. Supplementary Figure 3

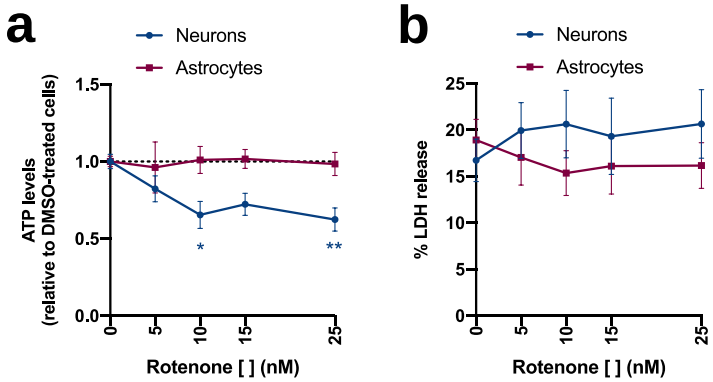

Figure 13 – Rotenone induces mitochondrial stress in neurons and astrocytes. (a) ATP and **(b)** lactate dehydrogenase (LDH) levels in neurons and astrocytes incubated with 0, 5, 10, 15 or 25 nM rotenone for 24 h (n=5 independent cultures run in triplicates). Data presented as mean ± SEM. * $p \leq 0.05$, ** $p \leq 0.01$

5. Supplementary Figure 4

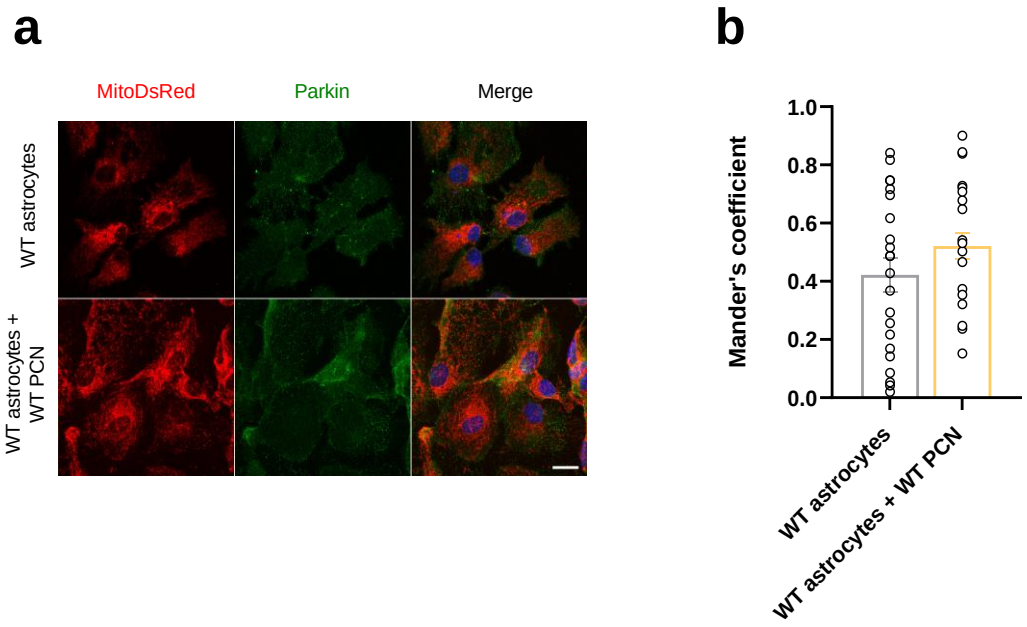

Figure 14 – Parkin recruitment to mitochondria is unchanged in WT astrocytes-WT PCN co-cultures. **(a)** Representative images showing Parkin (in green) co-localization with mitochondrial network (MitoDsred) in WT astrocytes cultured alone or in the presence of WT PCN. Scale bar= 20 mm. **(b)** Mander's coefficient indicates Parkin co-localization with mitochondria in WT astrocytes from the indicated conditions (n=21-22 cells from 2 independent experiments). Data presented as mean ± SEM.